2009

Orthogonal Pseudo-Random Sequence Enabled Cognitive and Emergency Communications

Md Jahidur Rahman
Western University

Orthogonal Pseudo-Random Sequence Enabled Cognitive and Emergency Communications

(Spine title: Orthogonal Pseudo-Random Sequence Enabled Communications)

(Thesis format: Monograph)

by

Md. Jahidur Rahman

Graduate Program
in
Engineering Science
Electrical and Computer Engineering

A thesis submitted in partial fulfillment
of the requirements for the degree of
Master of Engineering Science

School of Graduate and Postdoctoral Studies
The University of Western Ontario
London, Ontario, Canada

Abstract

With the ever-increasing demands for the broadband mobile communications, it is becoming more and more difficult to accommodate all existing and emerging wireless services and applications due to the limited communication resources particularly radio spectrum. In addition, system parameters of wireless communications often need to be adapted due to the variation of channel characteristics and user demands. Cognitive communication is emerged as an effective technique, particularly to improve the utilization rate of limited communication resources adaptively according to the change in its operating conditions and requirements. To handle these challenges efficiently and reliably in cognitive radio scenario, cyclic prefix (CP) of the OFDM system is precoded in this thesis using pseudo-random sequence. This signaling link can effectively carry transmission parameters and system adaptation information. In first part of the thesis, mutual interference minimization and transmission power adaptation enabled by the additional signaling link are also investigated.

In order to make use of this precoded cyclic prefix (PCP) signaling link, an efficient demodulation scheme is needed to reduce the implementation complexity. Therefore, a low complexity signaling demodulator along with a multipath combining technique to further improve the performance in real communication scenario like in multipath channel is proposed in the thesis.

The final aspect of this thesis is the investigation of a robust communication system using digital television (DTV) transmitter identification watermark signal which is also a modulated pseudo-random sequence. The previous study on PCP signaling is thus extended to an emergency communication system using DTV watermark. It is found that watermark based communication system is more robust than the DTV broadcasting and can reach a much wider coverage with significantly increased network reliability, which is suitable for national emergency situations.

Keywords-Pseudo-random sequence, PCP-OFDM, Cognitive radio, Power control, Signaling demodulator, DTV watermark, Emergency communications.

Acknowledgements

First and foremost, I would like to express deep gratitude to my research supervisor, Dr. Xianbin Wang, for his guidance and support during my graduate studies. Without his mentoring, the achievements in my research would have never been possible.

I would like to extend my thanks to Dr. Serguei L. Primak, Dr. Quazi Mehbubar Rahman, and Dr. Henry (Hui) Xue for being the readers of this thesis and contributing their valuable time in serving on my dissertation committee.

Many thanks to all members in my research group including Cong, Hao, Sahar, Imran for their support and helpful discussion. I truly enjoyed your accompany throughout my study period.

I am forever indebted to my family for their constant support and encouragement throughout the past years. I deeply acknowledge their understanding.

Table of Contents

List of Tables

List of Figures

Acronyms

ATSC	*Advanced Television Systems Committee*
BER	*Bit Error Rate*
CP	*Cyclic Prefix*
CR	*Cognitive Radio*
DSL	*Digital Subscriber Loops*
DTV	*Digital Television*
DVB-T	*Digital Video Broadcasting-Terrestrial*
FDM	*Frequency Division Multiplexing*
IER	*Identification Error Rate*
ICI	*Inter Carrier Interference*
ISI	*Inter Symbol Interference*
LOS	*Line of Sight*
LTE	*Long Term Evolution*
MPEG	*Moving Picture Experts group*
MRC	*Maximum Ratio Combining*
NTSC	*National Television System Committee*
OFDM	*Orthogonal Frequency Division Multiplexing*
PCP	*Precoded Cyclic Prefix*
PGC	*Programmable Gain Controller*
PSTN	*Public Switched Telephone Network*
QAM	*Quadrature Amplitude Modulation*
SER	*Symbol Error Rate*
TETRA	*TErrestrial Trunked RAdio*
TOV	*Threshold of Visibility*
TxID	*Transmitter Identification*
WLAN	*Wireless Local Area Networks*

Chapter 1
Introduction

1.1 Motivation

In recent years, wireless communication has become an integrated part of modern society and more importantly our day-to-day life vastly depends on various communication services. From house-hold to socio-economic applications, communication services exist everywhere, prevailing human life in a stringent manner than ever. Due to these overwhelming demands for wireless applications, precious communication resources particularly radio spectrum have become scarcer and more expensive. However, very often licensed users who have exclusive access right to the spectrum are not using it efficiently. As a result, there is a vast portion of the spectrum are left unused depending on time, geographical location etc.

The extremely low spectrum utilization rate leads to studies on how to allocate spectrums more efficiently so that some opportunistic access for the unlicensed user can be accommodated. The unlicensed users with the capability to access these opportunistic spectrums is usually referred as cognitive radio (CR) and the communication process is termed as cognitive communication [1].

Cognitive radio has the capability of adapting its operation according to change in environment and the users' requirements. But due to the opportunistic access requirement, i.e., spectrum sharing between licensed and unlicensed user, new dilemmas are in the frame, in terms of spectrum access mechanism, power control, interference management among primary and secondary etc. These dilemmas open up newfangled research problems for cognitive communication systems which are substantially different from conventional wireless communication systems. It should be noted that secondary users need to communicate in a way such that it does not hamper effective communication for primary or licensed users.

Along with these challenging problems, the fast changing communication channel makes the CR design even more complicated. To cope up with the variable users' requirements and change of channel characteristics, it is therefore essential to adjust the system parameters of the CR accordingly to make the communication process more effective and reliable. This process requires some sorts of negotiations or handshaking capability between the users so that they can adjust their parameters according to the changes in the environment. However, in the present situation, it is challenging to find spectrum for CR users' communication, let alone a dedicated signaling link to adjust the system parameters among the users. To have an effective cognitive communication between users, as well to adjust the system parameters according to the user demands, channel characteristics, quality of service (QoS) requirements, it is outmost necessary to establish spectrum efficient signaling link among the CR users. Therefore the first part of this thesis is motivated by these requirements and devoted to enable an efficient signaling link so that CR users can adjust the system parameters according to their requirements. It should be mentioned here that orthogonal frequency division multiplexing (OFDM) is the best candidate for cognitive radio system due to its sensing and spectrum shaping capabilities together with flexibility and adaptability [2]. Therefore the signaling link presented in this thesis is derived by precoding the cyclic prefix (CP) of OFDM symbol that can be effectively applicable for cognitive communication systems such as for power control and interference minimization purposes.

Once the cyclic prefix is precoded according to the change in system parameters using pseudo-random sequence and to be able to get this system parameters at the other users, an efficient demodulator is needed to decode this information. So the second task of the thesis is to develop a low complexity precoded cyclic prefix (PCP) signaling demodulator for this adaptive PCP-OFDM system. Since the overall complexity of the PCP-OFDM system is a major concern, it is necessary to have an efficient and low complexity demodulator for PCP signaling demodulator.

The last part of this thesis deals with a robust communication system using DTV watermark signal suitable for emergency situations. One interesting feature of Advanced Television Systems Committee (ATSC) system is that it uses pseudo-random sequence i.e., large set Kasami sequence embedded into DTV signal for identification of each transmitter in broadcasting scenarios [3]. This transmitter identification (TxID) watermark signal is more robust than the DTV signal due to large

autocorrelation peak and can reach over a wider coverage area. Therefore TxID signal can be used to make people aware more effectively with greater reliability during emergency situations.

The emergency communications bring several challenging requirements such as greater coverage area, coexistence among different communication systems, robust transmission in harsh communication environment, reliability, fast responding etc. [4]. These technical requirements reveal the fact that the establishment of emergency communication infrastructure is very challenging and rigoroùs attention is needed on important factors which depend on possible scenarios and warning systems. However, presently deployed various emergency communication systems using different platforms are not able to communicate with each other i.e., the problem lies in the sense of interoperability among these platforms [5]. On the other hand, interoperability also raises the question of reliability of the whole network because different platforms are having different reliabilities. That's why, even if the interoperability is achieved among different platforms which still necessities a substantial amount of research, the reliability of the thereafter network would be a major concern.

1.2 Research Objective

Power control is a major issue for cognitive radio networks due to the unplanned transmission coverage from unlicensed users. The unlicensed or CR users, by no means, are allowed to create unacceptable interference to primary or licensed user due to unnecessary transmission power. However, in practice, the primary users receives interference from secondary user due to this not well-controlled transmission power. One reason behind this problem is that the secondary users do not have the proper idea about how much power should be radiated to guarantee a certain performance threshold for any particular communication. The other reason is the reliability and accuracy of the spectrum sensing decision made by the secondary users.

Another major challenge in the OFDM based CR design is the subcarrier power allocation. Due to the time varying nature of channel and requirements from users, it is necessary to change the subcarrier power allocation from time to time for optimal system performance. The CR receiver can only operate properly when this subcarrier power allocation information is retrieved.

Therefore it is obvious that a signaling link is required to send these transmission power and subcarrier power information to the corresponding CR receiver, which is very difficult to set up in CR environment where even the access for secondary users is not guaranteed. Again, with the application of OFDM to cognitive radio brings new aspects to the system design. To address the challenge in this thesis, the notion of PCP-OFDM system is exploited where CP is precoded to carry different system parameters. The first objective of this thesis is to develop a transmission power control and subcarrier power allocation scheme using this PCP-OFDM system for cognitive radio networks. In this case, PCP will have real and imaginary parts where real part will be precoded to carry transmission power control information and imaginary part will be precoded to carry subcarrier power allocation information. As a result of this power control, it is possible to minimize the mutual interference to the primary and other CR users through this technique.

As the CP is precoded using Kasami sequence which provides a very large code space, we need an efficient demodulator to retrieve the information carried by PCP. The conventional approach to demodulate a PCP is to use optimal matched filtering approach. However, the implementation of this approach is very complex and it also increases the overall complexity of the PCP-OFDM receiver. Therefore effort is also given to derive an efficient technique to demodulate PCP signaling while keeping the same identification error rate performance at reduced implementation complexity.

The final topic of thesis is aimed to develop a robust communication system for emergency situations using TxID watermark signal. Due to the robustness of TxID signal, it can cover a much wider service area than the DTV signal with very low error rate. Therefore, TxID signal is employed in the proposed communication system which can be used effectively during national emergency situations.

1.3 Contributions

The first part of this thesis presents a spectrum efficient technique to manage transmission power and subcarrier power allocation for CR systems. Transmission power of cognitive radio plays a major role for mutual interference to primary users and other secondary user as well. On the other hand, with the change of channel characteristics and user demands, it is essential to re-allocate the subcarrier power to have an efficient and effective communication system. Therefore in the first part of the thesis,

an effective power control and subcarrier power allocation scheme is proposed using PCP-OFDM system for CR networks. The system parameters such as transmission power control and subcarrier power allocation information are precoded using pseudo-random sequence and send to the CR transmitter side. Then the transmitter adapts its operation based on this information for the forthcoming communications among the users. Therefore this approach enables an effective communication technique tailored for cognitive radio system where secondary user does not hamper primary users' communications. The other obvious benefit of this technique enables to avoid potential mutual interference to the primary user. This observation is verified using probability density function (PDF) of the mutual interference and interference perceived to primary user.

The second major contribution of this thesis is the proposal of a low complexity PCP signaling demodulator. The proposed signaling demodulator provides much lower complexity than other approaches but maintains the same identification performance. As the PCP is basically precoded using Kasami sequence, the key idea here is to develop a demodulation scheme following the same procedure of Kasami sequence generation. It helps us to substantially reduce the overall complexity of PCP-OFDM receiver for CR radio systems. Complexity of this signaling demodulator is compared in terms of number multipliers required. To further improve the performance in a multipath channel, a multipath combiner based on maximum ratio combining (MRC) considering unequal noise component for each multipath signal is proposed. It is found that performance of the proposed signaling demodulator can be improved to a great extent using this multipath combiner.

The final contribution of this thesis is the investigation of a robust communication system using DTV TxID watermark signal. It is found that TxID signal is more robust than DTV signal and can be reached over a wider area with very low error rate. This observation has led to develop a robust communication system which can be used during national emergency situations. A few areas in London, ON, Canada are studied and shown that watermark enabled communication system is more robust in terms of coverage, reliability, number of the nodes/stations required etc.

1.4 Thesis Outline

The rest of thesis is organized as follows. Chapter 2 describes the overall technical backgrounds those are needed to understand the subsequent chapters of this thesis. In the first section, a brief description of OFDM system, including its advantages and disadvantages and role of cyclic prefix are presented. After a brief introduction to PCP-OFDM system, generation of Kasami sequence is discussed for the precoding of transmission parameters of cognitive radio, followed by precoding technique for signaling information. Demodulation of the OFDM data signal and PCP signaling is illustrated afterwards. A discussion on power allocation technique i.e., both the transmission power control and subcarrier power allocation is presented for cognitive radio system. Finally, ATSC DTV broadcasting model including some features of this technology are discussed.

In Chapter 3, investigation on PCP enabled transmission power control and subcarrier power allocation for cognitive radio communication is discussed in details. The corresponding transmitter and receiver structures for PCP-OFDM system are shown and discussed. Probabilistic analysis for mutual interference is presented for the proposed technique, followed by simulation results for this study.

In Chapter 4, a low complexity PCP signaling demodulator is depicted and discussed in details. Also the comparison with other approaches is carried out in terms of implementation complexity of demodulators. Later in this chapter, analysis on identification error rate and a multipath combiner based on MRC is discussed followed by the simulation results for the evaluation of the performance of the proposed demodulator in different channel scenarios.

In Chapter 5, a robust communication technique is proposed using DTV TxID watermark signal. The performance of this communication system is analyzed in terms of demodulation error rate. Then the coverage for this communication technique is predicted for few DTV stations in London, ON, Canada area. In addition, coverage analysis and reliability of this communication technique is compared with other emergency communication systems.

Finally, in Chapter 6, several conclusions are drawn based on the presented studies of this thesis and some important future works are discussed at the end.

Chapter 2
Theoretical Background

Three major research topics with quite different background have been investigated in the thesis. In this chapter, the related technical information needed to better understand the thesis are discussed. Topics covered in this chapter includes the basics of OFDM system, precoded cyclic prefix(PCP)-OFDM, generation of precoded cyclic prefix, demodulation of PCP. Some background on power allocation problem in cognitive radio and basics of ATSC DTV broadcasting system are also introduced.

2.1 Orthogonal Frequency Division Multiplexing (OFDM) System

Orthogonal frequency division multiplexing (OFDM) has shown to be a very effective technique to combat multipath fading in wireless communications. Over the last two decades, OFDM has gained immense popularity in many communication applications such as digital subscriber loops (DSL), wireless local area networks (WLAN), digital video broadcasting- terrestrial (DVB-T) etc. [2]. OFDM is also considered as the primary transmission technology for the upcoming fourth generation cellular and mobile radio system such as in long term evolution (LTE) [6].

With the increase of data-rate for broadband transmissions, the corresponding symbol duration of modulated signal decreases. Traditional communication systems using single carrier modulation suffers from inter symbol interference (ISI) which is caused by the dispersive nature of wireless channels, thereby needing more complex equalization. OFDM transmits data in parallel by modulating set of orthogonal subcarriers. With this process, entire frequency selective fading channel is divided into many narrow band subchannels where the fading essentially can be considered as flat. Since the high-bit-rate are transmitted in parallel with longer symbol duration and due to use of cyclic prefix (CP), ISI problem is mitigated. As a result, the channel

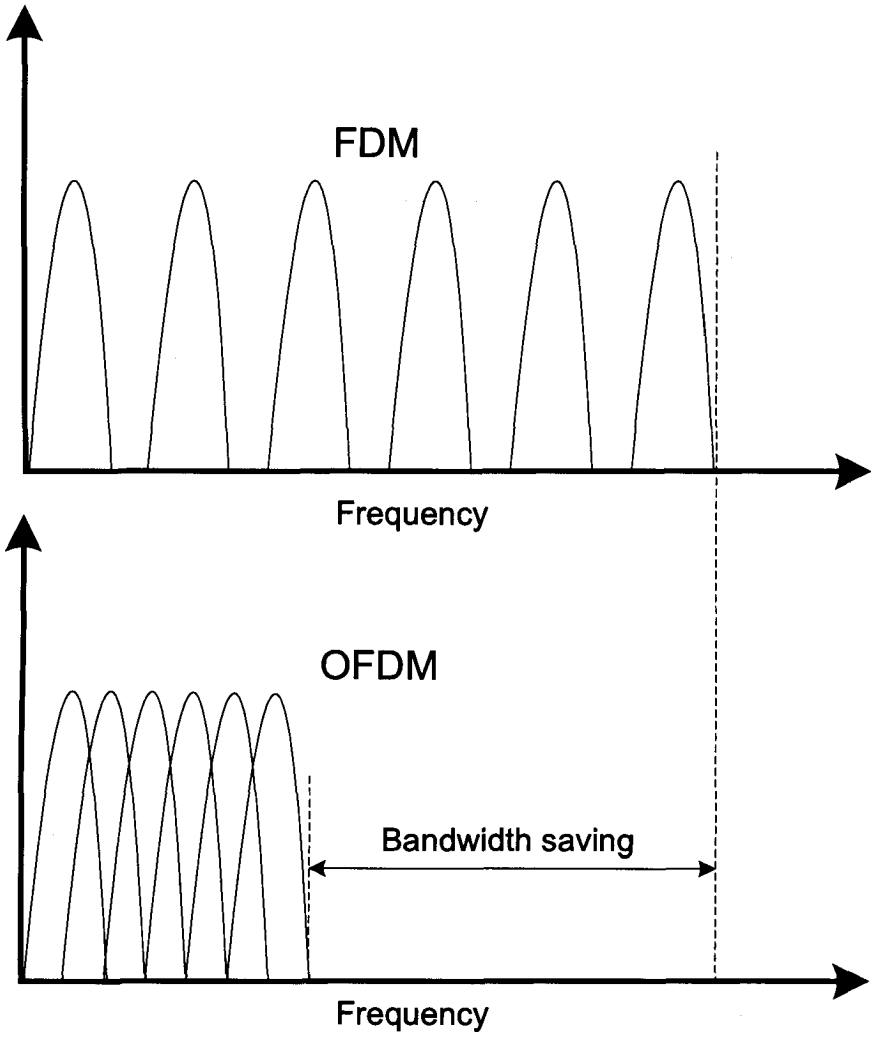

Figure 2.1: Spectrum efficiency of OFDM system.

effect for each subcarrier can be simply modeled as a complex gain and a one tap frequency domain equalizer with reduced complexity can be used.

Unlike the frequency division multiplexing (FDM) technique, OFDM also provides high spectrum efficiency due to closely-spaced orthogonal sub-carriers as shown in Fig. 2.1. In addition, motivated by the water-pouring capacity of a frequency selective channel, adaptive transmission techniques i.e., different modulation scheme and transmission power for each subcarrier can be used to increase the overall bandwidth efficiency of the system. In a nutshell, OFDM system provides the following major advantages for wireless communications:

- As the subcarriers are allowed to overlap each other, it makes efficient use of the available spectrum.
- OFDM divides the channel into narrow band subchannels where the fading is flat, therefore it is more resistant to frequency selective fading.
- Due to the use of cyclic prefix, it eliminates ISI and inter carrier interference (ICI) in wireless dispersive channel.
- In OFDM system, channel equalization is much simpler comparing to adaptive equalization techniques for single carrier systems.
- It is possible to use maximum likelihood decoding with reasonable complexity.
- Modulation and demodulation of OFDM system is computationally efficient due to widely used FFT techniques.
- It is comparatively less sensitive to sample timing offsets than single carrier systems.

However the advantages of OFDM system, as mentioned above, come at the expense of the following major disadvantages:

- The OFDM signal has a noise like amplitude with a very large dynamic range, therefore it requires RF power amplifiers with a high peak to average power ratio.
- It is more sensitive to carrier frequency offset and drift than single carrier systems.

2.1.1 Mathematical Representation

Let us consider that each OFDM symbol is specified by an N-point time-domain vector x, obtained via an IFFT of the complex data vector X of size N. Then at the transmitter side, each OFDM symbol in the time domain can be expressed in vector form as

$$x = F_N^{\mathrm{H}} X, \tag{2.1}$$

where $F_N^{\mathrm{H}} = F_N^{-1}$ is the inverse Fourier transform matrix with its (n,k)th entry which is given as $\left(\exp\{j2\pi nk/N\}/\sqrt{N}\right)$, and $(\cdot)^{\mathrm{H}}$ denotes conjugate matrix transposition.

At the receiver side, data are recovered by performing FFT with the same size N on the received signal as follows

$$X = F_N x, \tag{2.2}$$

With its (n,k)th entry given as $\left(\exp\{-j2\pi nk/N\}/\sqrt{N}\right)$.

2.1.2 Cyclic Prefix

The cyclic prefix is a crucial feature of OFDM which combats with the effects of real communication scenario like multipath. In OFDM system, ISI and ICI are avoided by introducing a guard interval at the beginning of an OFDM symbol, which is basically a duplicated copy of the last part of that same OFDM symbol [2]. The cyclic prefix still occupies the same time interval as guard period in frequency division multiplexing (FDM) system, but it ensures that the delayed replicas of the OFDM symbols will always have a complete symbol within the FFT window. As shown in Fig. 2.2, it makes the transmitted signal periodic in nature. The idea behind this is to convert the linear convolution between signal and channel response into a circular convolution. This makes the FFT of the circular convolution of signal and channel response equivalent to the their multiplication in the frequency domain.

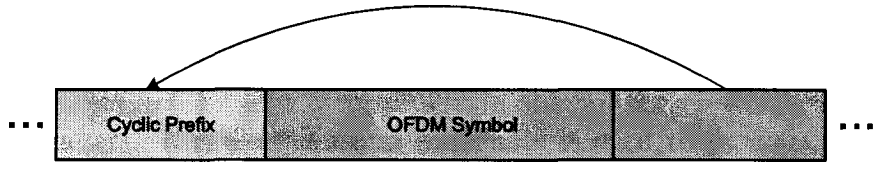

Figure 2.2: An OFDM symbol with cyclic prefix.

In order to preserve the orthogonality property, the maximum channel length should not exceed the duration of the guard interval time. There will be no ISI since the previous symbol will only have effect over samples within its CP. By doing this, orthogonality among the subcarriers is guaranteed, so there will be no ICI as well. Therefore, CP provides two important advantages, first by occupying the guard interval, it removes the effect of ISI, and by maintaining orthogonality it completely

removes the ICI. The use of OFDM in modern wireless communication systems is basically motivated by these advantages.

2.2 Precoded Cyclic Prefix(PCP)-OFDM

The precoded cyclic prefix(PCP)-OFDM symbol is basically the same as that of traditional OFDM system, except that the cyclic prefix is now replaced by a precoded pseudo-random sequence [7]. Consequently, each OFDM symbol is protected by two identical neighboring PCPs when there is no change of system parameters. In addition, the duration of each PCP-OFDM symbol becomes $N + P$ samples, where N is the size of the FFT and P is the duration of the cyclic prefix, respectively. As a result, it creates a series of OFDM symbols of $N + P$ samples protected by cyclic prefix similar to that of conventional OFDM system. The idea of the PCP-OFDM symbol is illustrated in Fig. 2.3.

Figure 2.3: Precoding the cyclic prefix of an OFDM symbol.

In PCP-OFDM, the new cyclic prefix is combined from two Kasami sequences [7], consisting of real and imaginary parts. These real and imaginary parts will be precoded to send the system parameters such as power control information, subcarrier power profile information, modulation and coding schemes etc. as well as the identification of the transmitter. Note that the same PCP is used as the cyclic prefix for all the forthcoming OFDM symbols unless there is a change in the transmission system parameters. Large set Kasami sequences is used to precode the CP in this thesis. The reason to choose large set Kasami sequence is that it has a large code space compared to other available bounded code set such as Gold code, small set of kasami sequence etc. Due to this large code space, it can represent a wide variation of system parameters for CR.

Precoded CP is inserted before the original data carrying OFDM signal and transmitted as follows

$$\mathbf{x}' = [c_P(0), c_P(1), \cdots, c_P(P-1), x(0), x(1), \cdots x(N-1)]^T. \tag{2.3}$$

However, in order to demodulate the information carried by PCP, a PCP signaling demodulator is needed in the PCP-OFDM receiver. Also, the complexity of the PCP signaling demodulator should be low enough so that the overall PCP-OFDM receiver complexity can be kept at minimal level.

2.3 PCP-OFDM in Cognitive Radio

Radio resource like wireless spectrum is looming a great challenge for future wireless communication system. Spectrum is traditionally assigned by governmental agencies to the licensed users on a long term basis. Although the fixed spectrum assignment policy generally served well in the past, the dramatic increase in demands for wireless communications in recent years poses a sheer challenge due to spectrum overcrowding [8, 9]. In the meantime, recent studies reveal that conventional spectrum allocation approach is very inflexible and utilization rate can be as low as 10% [10] depending on time and space variation. Therefore, improving spectrum utilization rate is essential to support future overwhelming wireless demands.

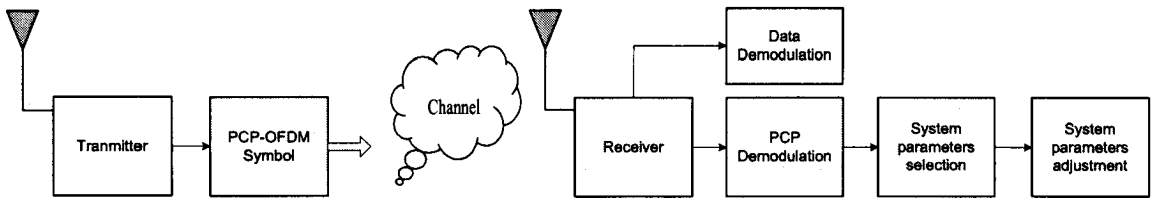

Figure 2.4: Simplified block diagram for PCP-OFDM in CR system.

The ever-increasing demand for precious radio spectrum along with the inefficient usage of licensed band has led to the advent of the cognitive radio (CR) technology, which aims to provide opportunistic spectrum usage to unlicensed users and thus lead to the co-existence and interference control problem among heterogeneous systems. Cognitive radio is a revolutionary technology enabling flexible and efficient usage of spectrum by providing opportunistic access to unlicensed users (often referred to as secondary or CR user). This technology is aiming to increase the spectrum efficiency by exploiting unused spectrum (often referred to as spectrum hole or white space) that is licensed to primary users [1, 11]. A cognitive radio is aware of the surrounding environment through spectrum sensing and measurements. It also

uses its previous experience to plan future actions and adapts itself to improve the overall communication quality and responds to user's variable needs. To achieve this, physical layer of a cognitive radio needs to be highly flexible and adaptable as well.

OFDM is one of the most widely used technologies in current wireless communication systems which has a great potential in cognitive radio communications. It is understood that OFDM will play an important role in realizing cognitive radio concept by providing a scalable, and adaptive modulated air interface. Also OFDM offers a great flexibility in this regard as it has a large number of parameters for adaption. The transmission parameters those can be changed according to the change in the characteristics of environment include bandwidth, FFT size, modulation, transmit power, subcarrier power allocation, and number of subcarriers etc. used for any particular communication. Although OFDM has the potential to meet the above requirements for CR, it needs a dedicated signaling link for negotiation between transmitter and receiver to achieve the real-time adaptation. To address this challenge, PCP-OFDM system was employed to provide an in-band signaling link in between CR transmitter and receiver. As it is purely a physical layer approach, it does not need to access to higher layer protocols which is very important for CR which requires fast adjustments of its parameters to follow up with the time varying communication environment.

2.4 Generation of Kasami Sequence for CP Precoding

As the system parameters of PCP-OFDM are precoded by large set Kasami sequence, generation of large set Kasami sequence is discussed briefly in this section.

Let u and u' form a preferred pair of binary m-sequence vectors of degree n with period $L = 2^n - 1$, where u is a binary maximal sequence vector and $u' = u[q]$ is a decimation of u with $q = t[n] \equiv 1 + 2^{(n+2)/2}$. In addition, for $q = s[n] \equiv 1 + 2^{n/2}$, $u'' = u[s(n)]$ forms another maximal sequence with period $L_1 = 2^{n/2} - 1$. Then we have a set of Gold sequences [12]

$$G(u, u') \equiv \{u, u', u \oplus u', u \oplus Du', u \oplus D^2u', ..., u \oplus D^{L-1}u'\}, \tag{2.4}$$

where D denotes the operator which shifts the code phase of a sequence vector cyclically by one unit, and $\oplus$ denotes the exclusive-OR operator. Furthermore, a set of

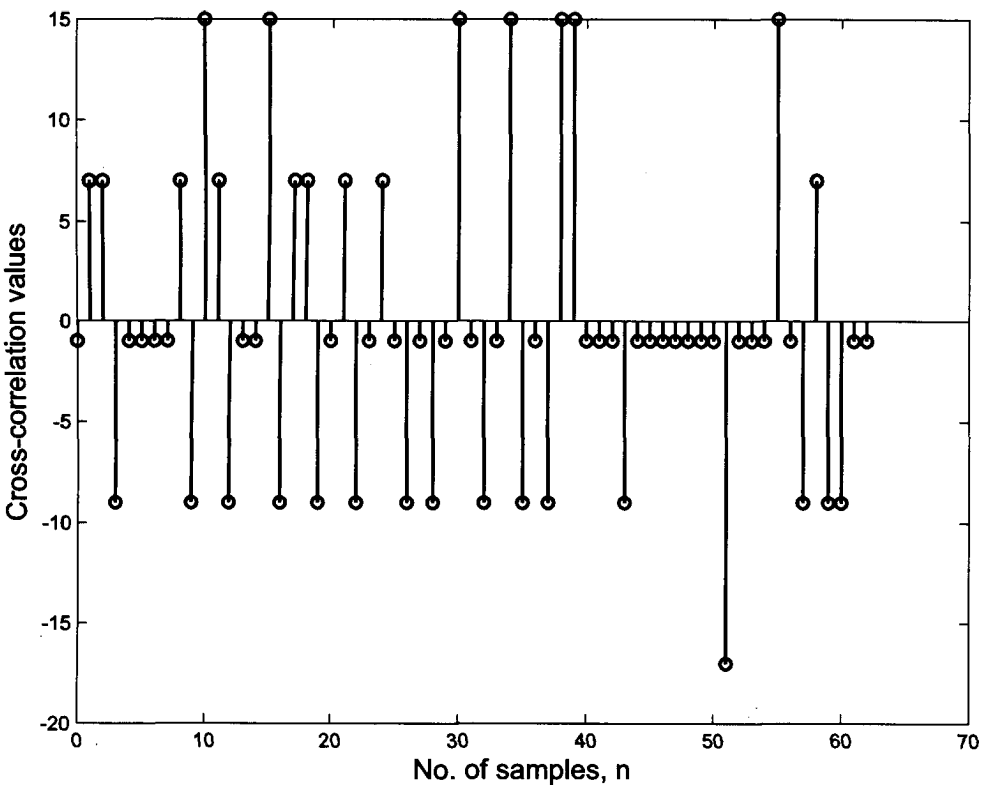

Figure 2.5: Cross-correlation values for large set kasami sequence of degree $n = 6$.

cover sequence for the shorter sequence can be defined as

$$C(u'') \equiv 0_L \bigcup [D^{j-1}c] = \{c_j, j = 0, ..., L_1\}, \tag{2.5}$$

where 0_L is an all-zero sequence with length L; $\bigcup$ denotes the union of sets; and $c = [c_0, c_1, ..., c_{L-1}]$ is the repetition of u'' by $2^{n/2} + 1$ times. Then the large set of Kasami sequence $K'(u)$, composed of sequences u, $u' = u[t(n)]$, and $u'' = u[s(n)]$, is given by

$$K'(u) = G(u, u') \bigcup \left[\bigcup_{j=1}^{L_1} \left\{ D^{j-1}c \oplus G(u, u') \right\} \right]. \tag{2.6}$$

It is noted that the code set sizes of $G(u, u')$ and $C(u'')$ are $S_G = L + 2 = 2^n + 1$ and, $S_C = L_1 + 1 = 2^{n/2}$, respectively. Hence, the code set size of complete set is

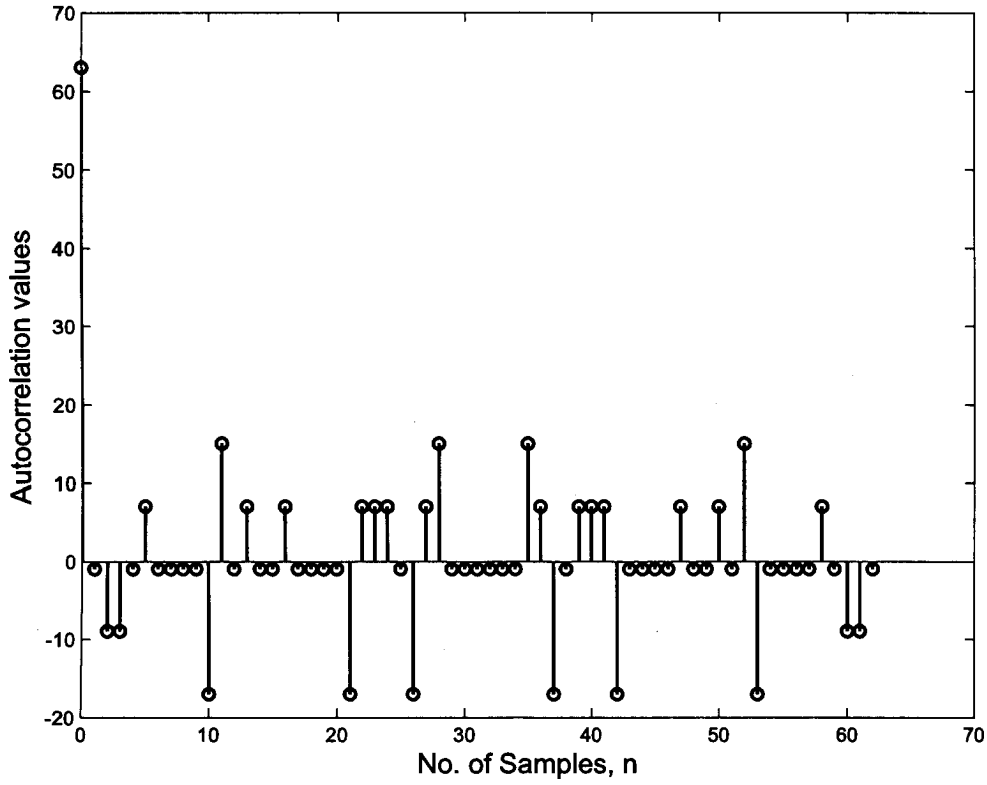

Figure 2.6: Autocorrelation value (first sample) for large set kasami sequence of degree $n = 6$.

$M' = S_C \times S_G = 2^{n/2}(2^n + 1)$.

Likewise M-CSK modulation [13], in order to modulate the CP with the large set of Kasami sequence, we need $M = 2^{3n/2}$ different input waveforms. But the code set size obtained from the Kasami set has a larger code set size. Thus we need a reduced code set size of Kasami sequence in order to modulate CP with this sequence.

To do this, Gold set obtained from u and u' can be redefined as follows,

$$\lceil G(u, u') \rceil \equiv \{u, u \oplus u', u \oplus Du', u \oplus D^2u', ..., u \oplus D^{L-1}u'\}, \tag{2.7}$$

where $\lceil G(u, u') \rceil$ is the set of Gold set reduced by one sequence. Therefore, the

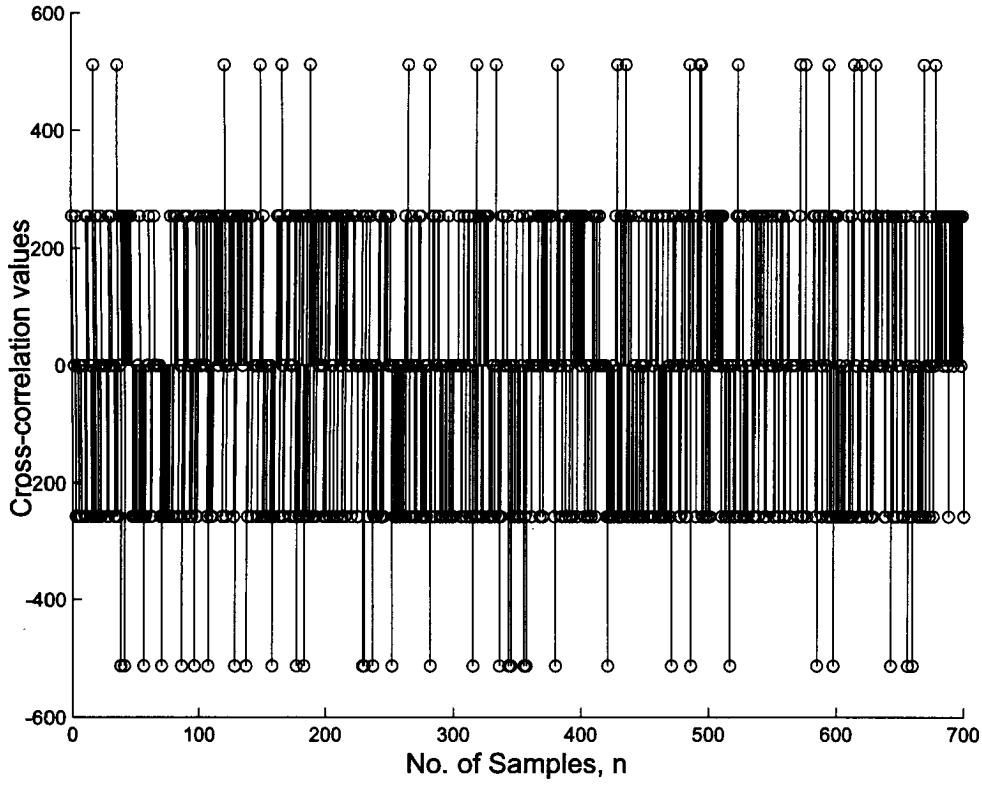

Figure 2.7: Cross-correlation values for large set kasami sequence of degree $n = 16$.

reduced set of Kasami sequence is given by,

$$K'(u) = \lceil G(u,u') \rceil \bigcup \left[\bigcup_{j=1}^{L_1} \{ D^{j-1} c \oplus \lceil G(u,u') \rceil \} \right]. \tag{2.8}$$

According to that, the code set size of the reduced Kasami set, $K(u)$ is $M = S_C \times S_G = 2^{n/2} 2^n = 2^{3n/2}$, which gives us required number of signal waveforms to modulate CP.

Fig. 2.5 shows the cross-correlation property of large set Kasami sequence for degree $n = 6$. Here cross-correlation values take on five discrete levels of {-17,-9,-1,7, 15}. Again, Fig. 2.7 shows the cross-correlation properties of a 16-bit large set Kasami sequence and the discrete levels of cross-correlation values take in the set {-513,-257,-1,255,511}.

2.4.1 Precoding of the Signaling Information

In PCP signaling link, Kasami sequence is used to modulate the cyclic prefix. One essential property of Kasami sequence is its excellent autocorrelation and cross-correlation properties [12]. In addition, Kasami sequence provides a large family of orthogonal codes that can be used to encode a large number of control information. For $\mathrm{mod}(n, 4) = 2$, where n is the degree of Kasami sequence, large set of Kasami sequences with a sequence length of $L = 2^n - 1$ has a sequence vector size of $M = 2^{n/2+1}(2^n + 1)$ [12]. Therefore precoded cyclic prefix would have M different inputs. With the M possible sequences, it is therefore possible to transmit $\log_2 M \approx 1.5n$ bits of control signaling information. This approach is similar to coded shift keying. The input data sequence can be denoted as $d = [d_0,\ d_1, \cdots,\ d_{1.5n-1}]$, where $d_i \in \{0, 1\}$. Each data sequence of control signaling information is thus associated with one unique Kasami sequence. For example, large set Kasami sequence with $n = 6$ provides 512 different options for transmitting power control and subcarrier power allocation information which is used in our analysis and simulations.

However, complexity of the detection algorithm is proportional to the size of kasami sequence code set. When the length of the CP is increased, corresponding code set size for the Kasami set is also increased which requires a more complicated detection process.

2.5 Demodulation Approach for PCP Signaling

The first step of the PCP-OFDM receiver is to recover the system parameters carried by the PCP, which will be investigated in details in the following chapters. The conventional method to demodulate a PCP sequence is to correlate the incoming PCP sequence with a set of local sequences stored in the library as shown in Fig. 2.8 [14]. Therefore, the optimum demodulator for detecting PCP sequences is optimal matched filter, which is a bank of correlators and each one is corresponding to one of the sequences in the Kasami code set. The PCP sequence is then determined based on the largest correlation peak between the incoming PCP sequence and correlator banks (local reference).

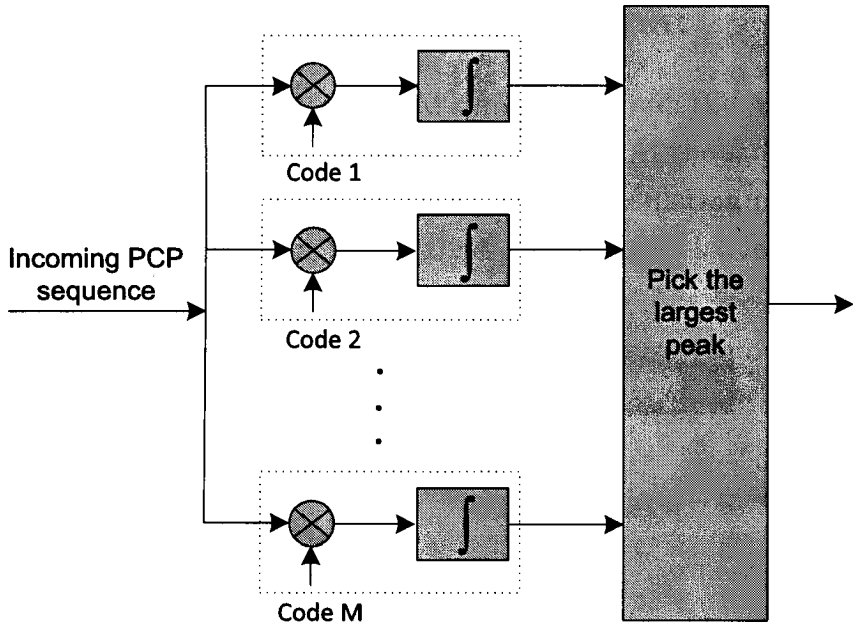

Figure 2.8: Conventional optimal matched filter based PCP sequence demodulator.

To demodulate the precoded CP, correlation based on matched filtering approach shown in Fig, 2.8 is carried as follows

$$R_m(\tau) = \frac{1}{L}\sum_{n=0}^{L-1} r(n-\tau)c_r(n), \tag{2.9}$$

where c_r is either the real or imaginary part of the reference complex CP sequence stored at the local receiver. The decision is taken based on the maximum correlation value as follows,

$$R_m = \max\{R_m(\tau)\},\ m \epsilon M,\ \tau = 1, \cdots, P, \tag{2.10}$$

where M denotes the total number of sequences. The corresponding local precoded CP leading to the maximum correlation value (R_m) will be selected to decide about the transmission system parameters.

2.6 Demodulation of OFDM Signal

In order to recover the transmitted OFDM symbol, ISI from the preceding CP needs to be computed and subtracted from the received signal. At the same time, when only N samples of the received signal are used for the demodulation process and due to the elimination of cyclic structure, ICI also needs to be canceled for proper reception as shown in Fig. 2.9.

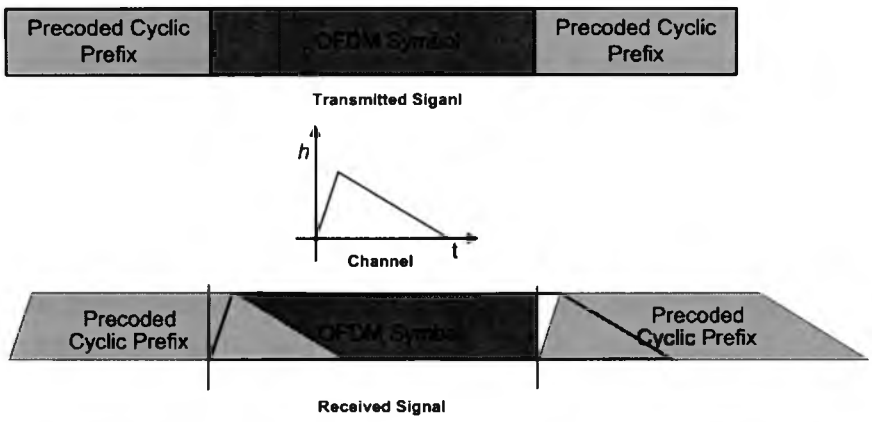

Figure 2.9: PCP-OFDM signal over a channel.

Following Fig. 2.9 the received signal can be written as

$$r = Cx + C_T c_p + w, \tag{2.11}$$

where C is the channel seen by the OFDM symbol, C_T represents the tail end of the channel impulse response, and c_p represents precoded CP sequence with L samples. It can be shown that $C + C_T = C_{cyl}$. Details of C, C_T and C_{cyl} can be found in [15]. Then substituting (2.2) into (2.11) and applying Fourier transform results

$$\mathbf{F}C_{cyl}\mathbf{F}_N^{\mathrm{H}}X = \mathbf{F}(r - C_T c_p) + \mathbf{F}C_T F_N^{\mathrm{H}}X, \tag{2.12}$$

where $C_T c_p$ is the ISI and $FC_T F_N^{\mathrm{H}}X$ is the ICI term. However, to remove the ICI, we need an iterative process because ICI also includes signal X itself. Therefore, any attempt to remove the ICI is based on the temporary decision of this signal and can be written as follows

$$\tilde{X}^{(a+1)} = \mathbf{D}^{-1}\mathbf{F}(r - C_T c_p) + \mathbf{D}^{-1}\mathbf{F}C_T F_N^{\mathrm{H}}\tilde{X}^{a}, \tag{2.13}$$

where superscript a is the iteration index and $D = FC_{cyl}F_N^{\mathrm{H}}$.

2.7 Power Allocation in Cognitive Radio

2.7.1 Transmission Power Control

Basically power control is a mechanism to select the transmit power in a communication system to achieve a performance goal constrained on various system parameters such as capacity, coverage etc. Power control is very important issue for wireless communication devices specially for hand-held devices where the power is constrained by battery life. Therefore, efficient use of power is highly sought in modern communicating system. Since both CR and primary users transmit in side by side band and their access scheme may be different from each other, unnecessary transmission power causes mutual interference which is a major limiting factor for CR communication system [16]. Therefore controlling total transmission while maintaining the required performance could greatly improve the overall performance i.e., more users can be afforded which will eventually increase the overall capacity of the network.

2.7.2 OFDM Subcarrier Power Allocation

Traditionally transmission power is allocated on each OFDM subcarrier based on channel condition for a particular communication system while maintaining constraint on total transmission power as shown in Fig. 2.10. When the channel is known through channel estimation and/or channel prediction, it is always good practice to adjust the power allocation on subcarriers for improved system performance. However, due to the mutual interference introduced by CR transmission depends on the spectral distance with respect to the primary user's spectrum [16], it is understood that power allocation on each subcarrier should also consider the quality of service (QoS) requirement for any particular communication system.

Power allocation in OFDM-based cognitive radio is emerged as an important topic for CR. To allocate subcarrier power optimally, subchannel power constraint based algorithm [17], water-filling algorithm considering mutual interference while maximizing the capacity of the secondary users [18] etc. were proposed. Beside these, QoS constrained power allocation for OFDM system is proposed in [19]. This time-variant control information needs to be sent to the other CR users. Again in

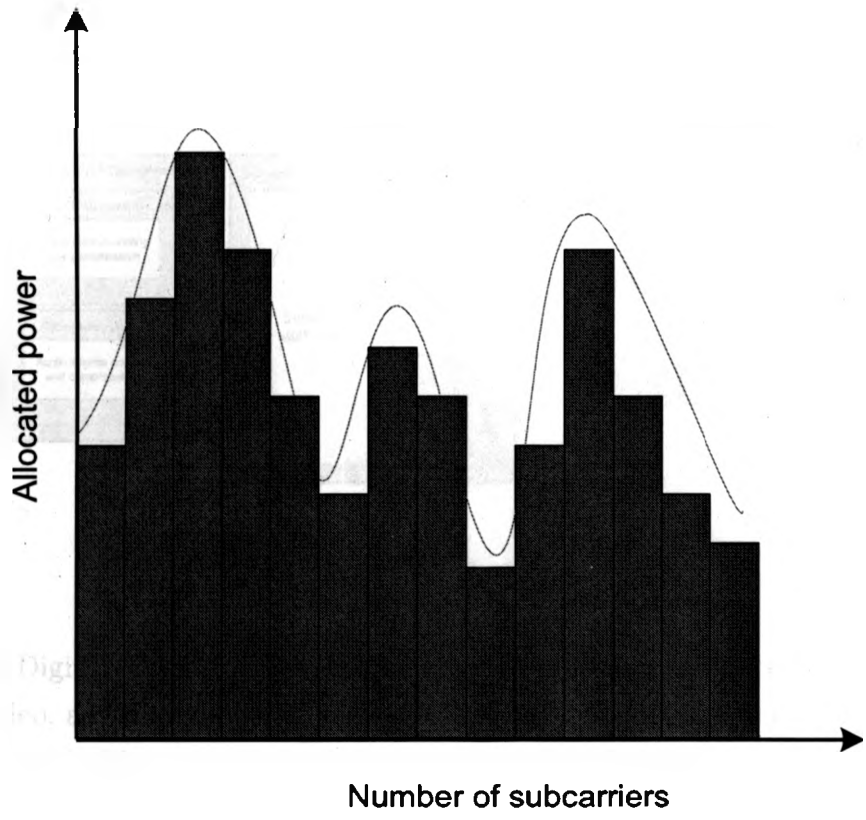

Figure 2.10: Allocated power on each subcarrier depending on channel condition.

cognitive scenario, it is not always possible to guarantee the access for the secondary users, let alone dedicated signaling link to convey this information.

2.8 ATSC DTV System Model and Its Features

As modulated pseudo-random sequence is used to enable the proposed emergency communication system using digital television (DTV) station that is presented in Chapter 5, a brief introduction of North American ATSC DTV system model and its data frame structure including watermarking technique is given in this section.

Nowadays, digital television (DTV) is gaining increasing popularity due to the exceptional transmission quality and enormous flexibility offered to both television broadcasters and consumers. In congruent with this, the U.S. TV broadcast industry

already made the digital transition [20] and that in Canada by August 31, 2011. Also few countries in Europe already made the transition. Basically, DTV networks are comprised of a plurality of transmitters, each broadcasting the same signal using either multiple frequencies or one frequency (single frequency network).

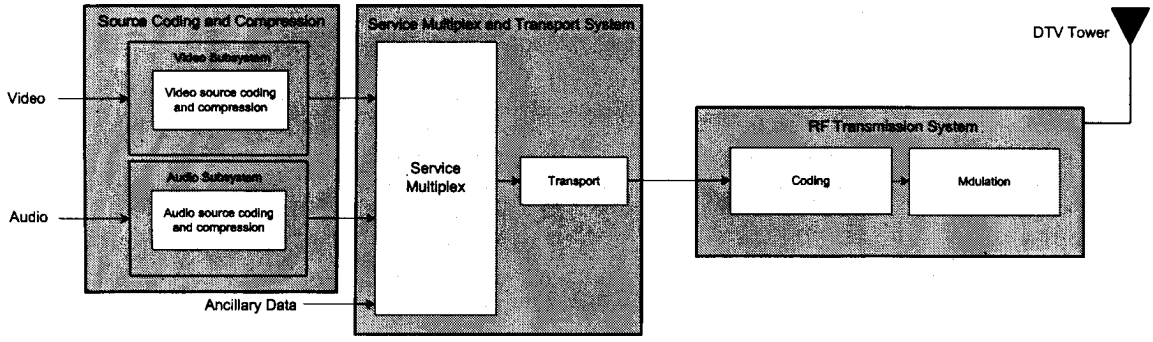

Figure 2.11: DTV broadcasting model.

The Digital Television Standard describes a system designed to transmit high quality video, audio, and ancillary data (different kinds of control data) over a single 6 MHz channel. The system can deliver reliably about 19 Mbps of throughput in a 6 MHz terrestrial broadcasting channel and about 38 Mbps of throughput in a 6 MHz cable television channel. This means that encoding a video source whose resolution can be as high as five times that of conventional television (NTSC) resolution requires a bit rate reduction by a factor of 50 or higher. To achieve this bit rate reduction, the system is designed to be efficient in utilizing available channel capacity by exploiting complex video and audio compression technology.

A DTV broadcasting model is shown in Fig. 2.11. In DTV, source coding and compression is done as a method to reduce the bit rate, which is also known as data compression, and appropriate for application to the video, audio, and ancillary digital data streams. The purpose of the source coder is to minimize the number of bits needed to represent the audio and video information. The digital television system employs the MPEG-2 video stream syntax for the coding of video and the digital audio compression (AC-3) Standard for the coding of audio [21].

The other aspect of DTV is service multiplex and transport which refers to the means of dividing the digital data stream into packets of information, the technique of uniquely identifying each packet or packet type, and the appropriate methods of

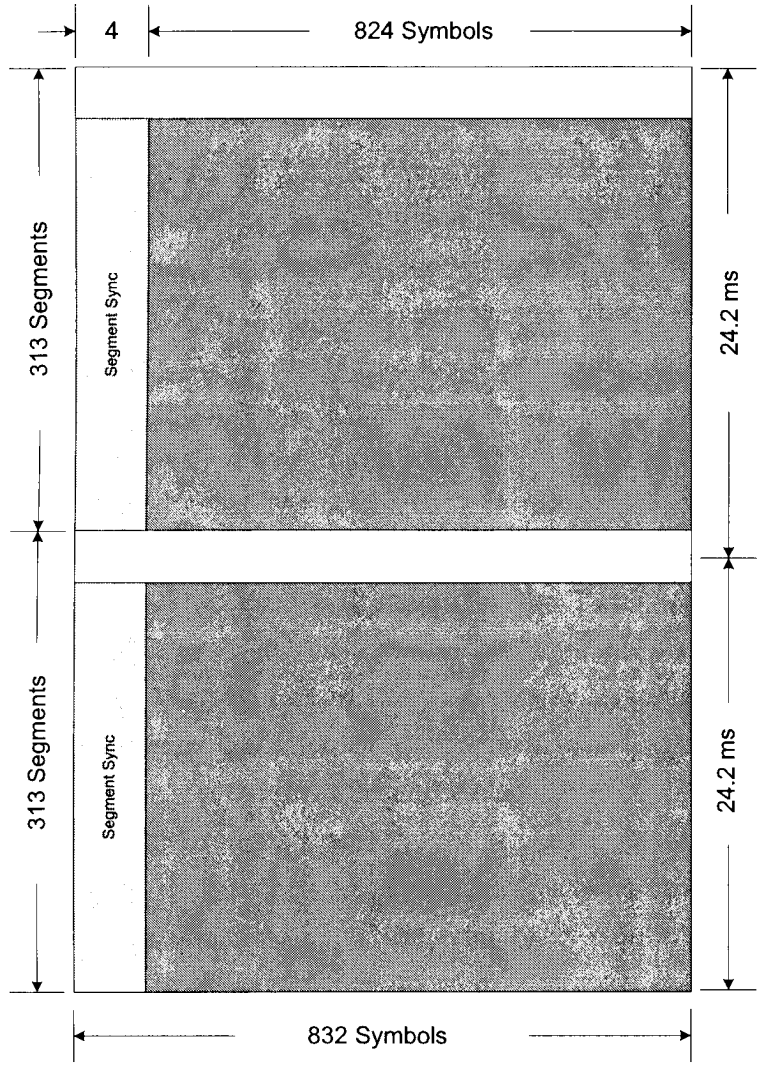

Figure 2.12: Data frame structure for ATSC DTV broadcasting system.

multiplexing video data stream packets, audio data stream packets, and ancillary data stream packets into a single data stream. In developing the transport mechanism, interoperability among digital media, such as terrestrial broadcasting, cable distribution, satellite distribution, recording media, and computer interfaces, is a prime consideration. The digital television system employs the MPEG-2 transport stream syntax for the packetization and multiplexing of video, audio, and data signals for digital broadcasting systems.

RF Transmission section does the channel coding and modulation. The channel coder takes the data bit stream and adds additional information that can be

used by the receiver to reconstruct the data from the received signal which, due to transmission impairments, may not accurately represent the transmitted signal. The modulation (or physical layer) uses the digital data stream information to modulate the transmitted signal. The modulation subsystem offers two modes: a terrestrial broadcast mode (8 VSB), and a high data rate mode (16 VSB).

Apart from the features mentioned above, transmitter identification is one of distinctive features of ATSC DTV broadcasting system which enables the broadcaster to monitor the operating status of each transmitter. More importantly, it helps the broadcaster to optimize the various adjustments of network parameters. It is inserted as a well-buried watermark to the original 8-VSB modulated DTV data signal and fitted into DTV standard according to the data frame size. The ATSC data frame is shown in Fig. 2.12. The watermark signal which is used in this case is large set Kasami sequence of degree 16. A typical requirement for the TxID sequence is the number of available orthogonal codes. This is because each sequence can only be assigned to one transmitter in the covering area of the transmitter regulating authority, may be nation-wide or region-wide. Therefore it is chosen to use large set Kasami sequence as watermark signal which provides a large code space.

It is noted that synchronous transmission of DTV signal and embedded watermark is not mandatory. However, synchronization between the DTV signal and the embedded watermark signal can reduce the amount of computation for transmitter identification. In order to achieve the synchronized transmission between the DTV signal and the embedded TxID sequence, each 16-bit Kasami sequence has to be truncated by 639 symbols such that four truncated codes can be embedded into DTV field, as indicated in Fig. 2.12. Alternatively, three full-length Kasami sequences can be used while the last sequence can be truncated by 4×639 symbols to achieve synchronous transmission.

Due to the large cross-correlation peaks of the watermark signal (Kasami sequence), it is found that embedded watermark signal is much more robust than the original DTV signal, covering a wide area. However, it is obvious that in case of demodulation of the watermark signal, dominant interference will come from in-band DTV signal which is significantly stronger than the TxID watermark signal.

2.9 Chapter Summary

In this chapter, related technical background and literatures to understand the thesis are discussed. Starting with basic OFDM system, the use of CP in OFDM, introduction to PCP-OFDM and its uses in cognitive radio are also presented. The demodulation technique for PCP signaling is then introduced. In addition, power allocation in cognitive radio and some important features of North American ATSC DTV standard is briefly discussed.

Chapter 3
Power Allocation and Interference Analysis for Cognitive Radio

3.1 Introduction

Very often unnecessary and uncontrolled transmission power from secondary user in a cognitive radio network plays decisive role in contributing mutual interference to the primary and other secondary users as well. Therefore, degradation of the primary services caused by spectrum sharing with secondary networks is mostly determined by mutual interference from secondary networks which also limits the number of active users at any given time in the CR network.

In this chapter, we have investigated an interference minimization and subcarrier power allocation technique for OFDM-based CR through precoded cyclic prefix (PCP) using complex pseudo-random sequence. The idea of this proposal is enabled by establishing a new signaling link for CR transmitter-receiver coordination based on the modulation of complex precoded CP as shown in Fig. 3.1. The real part of the PCP will be used to establish a total transmission power negotiation signaling between local transmitter and remote receiver. The local transmitter power will be determined based on the required performance of the remote receiver. The remote receiver will evaluate its error rate performance, and then convey the required transmission power adjustment information to the corresponding transmitter by precoding the CP of the OFDM symbol to be transmitted. As a result, local transmitter power will always be kept at the required level with guaranteed error rate performance for remote receiver. Consequently, mutual interference resulting from the secondary network to the primary users will be minimized.

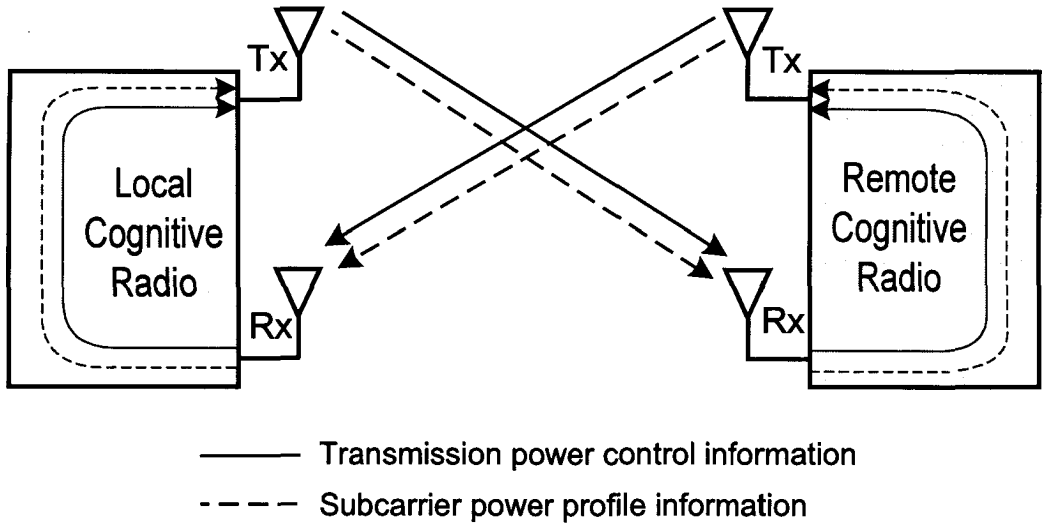

Figure 3.1: Control information transmission technique using PCP.

At the same time, imaginary part of the precoded CP will be used to carry a subcarrier power allocation profile selected from a set of predefined profiles which can serve as a suboptimal solution. Due to in-band information for the total transmission power and subcarrier power profile, unlike the conventional method, we do not need any extra signaling link to transmit these information, giving rise to improved bandwidth and power efficiency. The other inherent advantage for the proposed interference minimization technique is that the adaptation is purely at the physical layer and hence it does not incur any further delay to the network accessing higher layer that ultimately leads to a quickly adaptable CR network.

The chapter is organized as follows. PCP signaling transmitter structure and corresponding receiver structures are presented in Section 3.2 and Section 3.3, respectively. The Power control strategy i.e., total transmitter power control and subcarrier power profile allocation scheme is discussed in Section 3.4. In Section 3.5, mutual interference analysis carried out. Simulation results for this technique are presented in Section 3.6 and the chapter is summarized in Section 3.7.

3.2 Control Signaling Transmitter Structure

The PCP signaling transmitter block diagram is shown in Fig. 3.2. The difference with the conventional CP-OFDM system is that in PCP-OFDM system, precoded

CP is inserted instead of CP. The function of the programmable gain controller is to adjust the transmission power following a step-wise procedure.

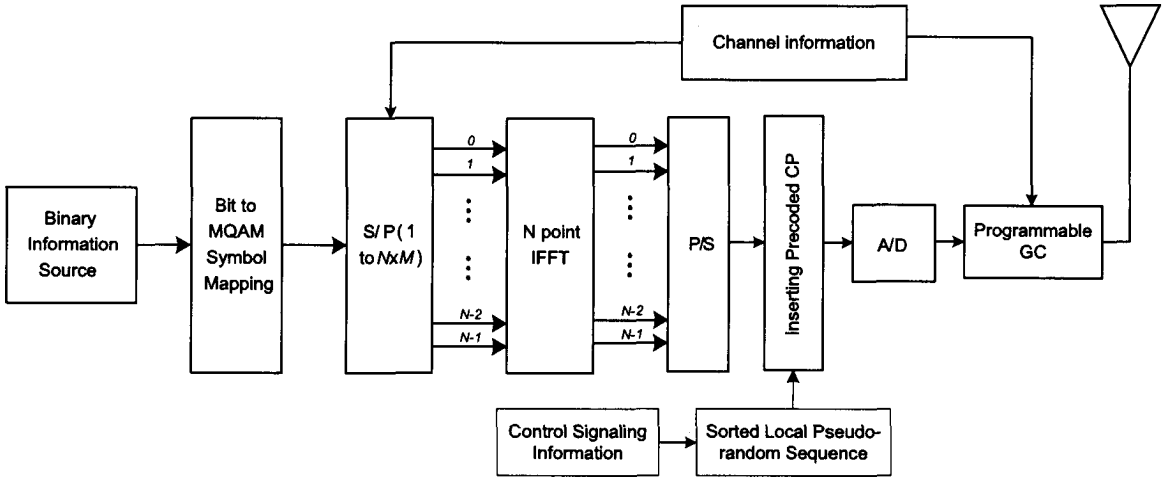

Figure 3.2: Precoded CP-OFDM based remote (or local) CR transmitter.

Let us consider each OFDM symbol at the output of Fig. 3.2 is specified by an N-point time-domain vector x, obtained via an IFFT of the complex data vector X of size N. Therefore each OFDM symbol in the time domain can be expressed in vector form as

$$x = F_N^{\mathrm{H}} X, \tag{3.1}$$

where $F_N^{\mathrm{H}} = F_N^{-1}$ is the inverse Fourier transform matrix with its (n,k)th entry given as $\left(\exp\{j2\pi nk/N\}/\sqrt{N}\right)$, and $(\cdot)^{\mathrm{H}}$ denotes conjugate matrix transposition. As discussed in Chapter 2, PCP is then inserted before OFDM signal and transmitted as follow

$$\mathbf{x}' = [c_P(0), c_P(1), \cdots, c_P(P-1), x(0), x(1), \cdots x(N-1)]^T. \tag{3.2}$$

However, due to the loss of cyclic structure, special demodulation and interference cancelation procedure for OFDM symbol is required as discussed in Section 2.6. At remote receiver, the PCP will be exploited to retrieve the system transmission parameters.

3.3 Control Signaling Receiver Structure

The task of the receiver design here which is different from conventional OFDM system, is to identify the PCP sequence used in the received signal. An efficient demodulation technique for PCP is discussed in the next chapter or simply PCP can be demodulated using optimal matched filtering approach based on correlation procedure [14]. An iterative demodulation technique as discussed in 2.6 can be used to recover the transmitted data symbol. The control signaling receiver structure is shown in Fig. 3.3.

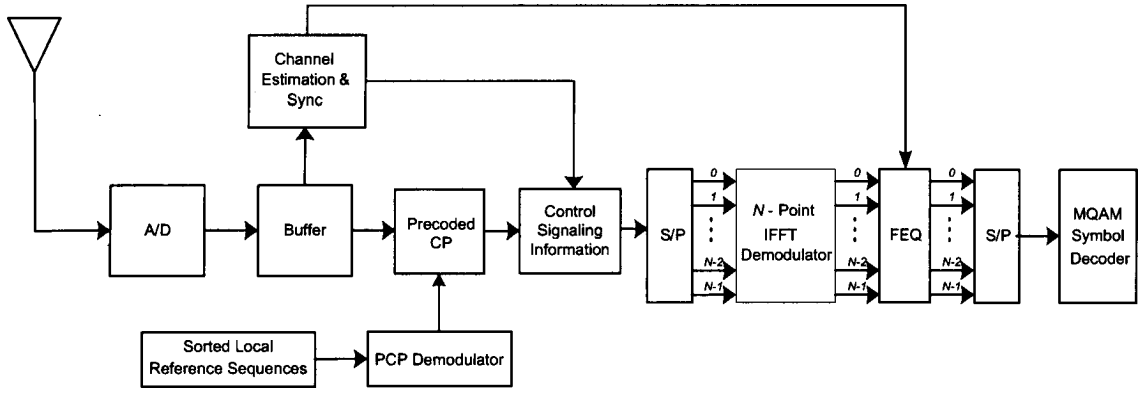

Figure 3.3: Precoded CP-OFDM based local (or remote) CR receiver.

Here we assume a slow varying channel with P taps and then the received signal vector r can be written as

$$r = H.x' + w, \tag{3.3}$$

where w is the additive white Gaussian noise (AWGN) vector with variance σ_n^2 having the same size as r, H is the channel matrix with a size of $(N + 2L - 1) \times (N + L)$ and with worst case scenario, we have $P = L$. Here L is the length of PCP.

3.4 Power Control Strategy

As the power allocation to subcarriers is dependent on total transmission power for a given transmission, they are inter-dependent to each other. Therefore power control strategy basically consists of both the two fold tasks of total transmission power control and subcarrier power allocation which are discussed in the following subsections.

3.4.1 Total Transmission Power Control

In this subsection, total transmitter power control technique will be discussed. Once the transmitted signal is received at remote CR receiver side, the performance of the current communication will be determined by evaluating signal to noise ratio (SNR) of that received signal at the demodulator output. To ensure guaranteed performance, the CR will then decide the target performance needed for particular QoS requirement and other factors related with the applications. However, the target performance can also be determined using received signal constellation based on particular modulation scheme. The next step relates the estimation of target SNR to achieve the desired performance. The necessary power adaptation information can be obtained based on the decision of the corresponding power required to achieve this target SNR. As QAM is used as our modulation scheme, the subsequent analysis will be carried out based on this modulation technique.

For widely used Λ-QAM modulation, the symbol error rate (SER) for k-th subcarrier of an OFDM signal is given by [22],

$$S_{e,k} = 2(1 - \frac{1}{\Lambda})Q\left(\sqrt{\frac{3}{(\Lambda^2 - 1)}\frac{P_k}{|H_k|^2\sigma_k^2}}\right), \tag{3.4}$$

where P_k is the average signal power and H_k indicates the channel response for subcarrier k. Therefore, the overall SER for a total of N subcarrier is followed by,

$$S_e = \frac{1}{N}\sum_{k=0}^{N-1} S_{e,k}. \tag{3.5}$$

Let us denote the target performance as $S_{e,T}$ and when it is known to the remote CR, corresponding target SNR can be determined easily as they follow one-to-one mapping relationship shown in equation (3.4). Then the target SNR ($\gamma_{T,k}$) needs to be determined to achieve the QoS constrained performance. If we take the difference between equalized output (X_k) and corresponding decision ($\tilde{X_k}$) as the noise level, the SNR for each subcarrier can be approxiated by,

$$\gamma_k = 10\log\left[\frac{|\tilde{X_k}|^2}{|X_k - \tilde{X_k}|^2}\right]. \tag{3.6}$$

Then the SNR gap to reach target performance is $\Delta\gamma_k = \gamma_{T,k} - \gamma_k$. Again, the overall SER after SNR adjustment will be verified using (3.5).

Basically, the task here is to send a gain factor, G ($P_l = \mathbf{G} \times P_l'$) through the use of PCP so that the local CR is able to adjust the required transmission power, P_l based on this signaling information.

The power adaptation information, which is equivalent to the SNR gap between the actual transmission power and target power to achieve the desired performance, will then be precoded according to the steps required to adjust the power of the local transmitter. A precoded CP is selected using a one-to-one mapping between the precoded CP and SNR gap i.e., required power to be adjusted. This power adaptation information is then sent to the local receiver through the remote transmitter as shown in Fig. 3.1. To be more precise in controlling the power adaption information, we can use 50 steps through the use of 50 pseudo-random sequences as an example. In this process, the first 25 pseudo-random sequences will be set to indicate the decrease of the power with a step of 0.1 dB. Similarly, the other 25 pseudo-random sequences will indicate the increase in power with the same step size.

Please note that the necessary increase or decrease in total transmission power can be made even in a single step adjustment. However, large variation of the transmission power within a short time is not desirable for wireless transceivers due to the use of programmable gain controller (PGC), since most PGC circuit needs some time to estimate the power of the received signal. Therefore it is essential to follow a step-wise procedure to set the transmitter power to the desired level as required by the remote receiver. Instead of adjusting the total transmission power to the desired level in one step, the procedure must follow a reasonable small step size. Again, the determination of the step size should also take into account the channel coherence time. In case of a static or slow varying wireless channel, very small step size can be used to adjust the transmission power.

3.4.2 Subcarrier Power Profile Selection

As discussed in Section 3.1, the subcarrier power profile information will be carried by the imaginary part of the complex PCP and corresponding subcarrier power profile will then be chosen from a set of predefined profiles. In this process, to determine

the optimal power allocation constrained on the system SER performance ($S_{e,k}$) corresponding power allocation problem can be formulated as follows [19],

$$\begin{aligned} P^* &= \arg\min\{\textstyle\sum_{k=1}^{N} S_{e,k}\} \\ \text{s.t.} \qquad & \textstyle\sum_{k=1}^{N} P_k = P_l, \end{aligned} \tag{3.7}$$

where P^* is a vector of optimally allocated power on each subcarrier while maintaining total transmission power constraint, P_k is the power on each subcarrier, and P_l is the total adapted power for a CR l. As the constraint is a linear function, the formulation in (3.7) is a convex optimization problem, which can be solved using the Lagrange multipliers.

The corresponding Lagrangian function for (3.7) can be obtained as follows [23],

$$\Omega = \sum_{k=1}^{N} S_{e,k} + \lambda \sum_{k=1}^{N} (P_k - P_l), \tag{3.8}$$

where λ is the Lagrange multiplier. The corresponding constraint equations can be obtained by taking the derivatives of Lagrangian function and equating them to zero as follows,

$$\frac{\partial \Omega}{\partial P_k} = S^*_{e,k} - \lambda = 0, \qquad k = 1, 2, \ldots, N \tag{3.9}$$

and

$$\frac{\partial \Omega}{\partial \lambda} = \sum_{k=1}^{N} P_k - P_l = 0, \tag{3.10}$$

where $S^*_{e,k}$ denotes the derivative of SER with respect to P_k for each subcarrier and also indicates the optimal power allocation ($P_{o,k}$) under this constraint. When the total adapted power and optimal power allocation based on (3.7) is known to the remote receiver, the subcarrier power profile will be selected from a set of profiles using these information.

To decide which power profile should be selected, we follow an iterative search method to find the best one from a predefined set of profiles, provided that optimal power allocation is known. The proposed algorithm is described in the following steps:

Step 1: At first, we need to normalize the optimally allocated power and power profiles in the set to make any valid comparison; and this is given by

$$\tilde{P}_{o,k} = \frac{P_{o,k}}{\sum_{k=1}^{N} P_{o,k}}, \tag{3.11}$$

and

$$\tilde{P}_{m,k} = \frac{P_{m,k}}{\sum_{k=1}^{N} P_{m,k}}, \tag{3.12}$$

where $\tilde{P}_{m,k}$ denotes m-th normalized profile in the set.

Step 2: Then to select a profile that is best matched with the optimal power allocation, mean squared error (MSE) will be carried among the profiles as follows,

$$E_m(\hat{\rho}) = E\big[\{\sum_{k=1}^{N}(\tilde{P}_{m,k} - \tilde{P}_{o,k})\}^2\big], \tag{3.13}$$

where $E_m(\hat{\rho})$ is the MSE error for the m-th profile.

Step 3: The subcarrier power profile with the lowest MSE error will be selected and corresponding pseudo-random sequence will be chosen as the imaginary part of CP to send this information to local CR.

Clearly, subcarrier power profile selected using this proposed method can serve as suboptimal scheme as it is selected from a limited profile set by comparing with the optimal scheme using the MSE criteria. Then the total adapted power is multiplied with the selected profile to redistribute power to all the subcarriers.

3.5 Interference Analysis

In this section, we study the effect of transmitter power control on mutual interference for primary users in CR communication. For this purpose, the interference model presented in [24],[25] is adopted. We assume that CRs are capable of sensing the presence of primary users. So if any primary user is detected in the CR neighborhoods, no transmission is initiated from the CR premises. Regarding this, a distributed CR network where active communicating nodes follow a Poisson point process with a CR radio density λ_u and a probability of transmission p_u is considered. The set of

transmitting users then also follows the same distribution with density parameter $\lambda = \lambda_u p_u$ [25]. The following assumption are made for our interference analysis:

- The secondary users are intelligent enough to do spectrum sensing and measurements to detect the existence of any primary user.
- The secondary users can move anywhere but not allowed to transmit when a primary user is detected.
- At the time of deployment, each secondary user is assumed to be assigned equal transmission power before starting any communication process.
- Mutual interference among the secondary users is assumed minimal. So the power adjustment for each secondary user depends only on the QoS requirement and distance between the users.
- For the propagation environment, we have assumed a rich scattered environment where the path loss constant is assumed four.

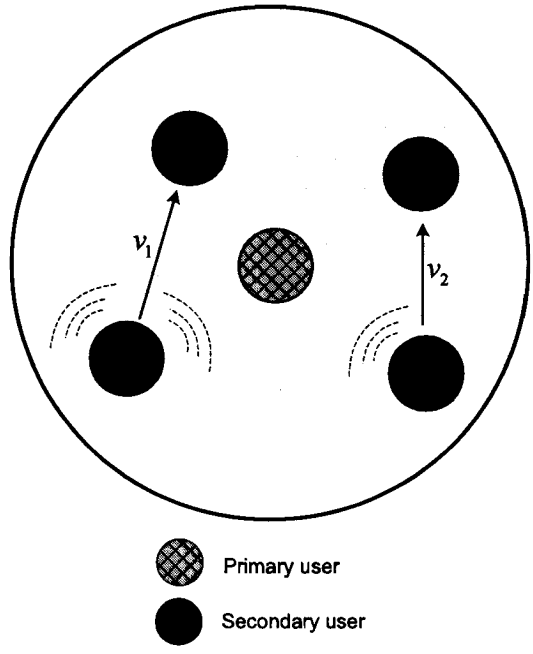

Figure 3.4: Mutual interference problem in CR communication.

Let us consider the power of the aggregated interference from the secondary users to a primary user is

$$\Gamma = \sum_{l=0}^{\infty} g(v_l)P_l, \tag{3.14}$$

where P_l is the adapted transmitting power and $g(v_l)$ be the path loss power gain at a distance v from the transmitter which follows $g(v) = 1/v^{\alpha}$ [25], for cognitive radio l. Let us take Γ_a be interference power received from active users in a radius of a and characteristics function Γ_a is given by,

$$\phi_{\Gamma_a} = E(e^{j\omega\Gamma_a}), \tag{3.15}$$

where E denotes the expectation operation. In addition, using conditional expectation (3.15) can be written as.

$$\begin{aligned}\phi_{\Gamma_a}(\omega) &= E(E(e^{j\omega\Gamma_a}|l)) \\ &= \frac{\sum_{l=0}^{\infty}(e^{-\lambda\pi a^2}(\lambda\pi a^2)^l)}{l!}E(e^{j\omega\Gamma_a}|l).\end{aligned} \tag{3.16}$$

According to the nature of Poisson distribution, within the area πa^2, the distance between the secondary users will follow uniform distribution as $\frac{2v}{a^2}$[25]. Then as discussed above, assuming that the CR is able to sense the environment at any location and hence without defining an interference region, after some manipulations the characteristics function for this modeling follows [24]

$$\phi_{\Gamma}(\omega) = \exp\Big(j\lambda\pi\omega\int_{p} pf_P(p)\int_{0}^{\infty}[g^{-1}(v)]^2 e^{j\omega vp}\mathrm{d}p\mathrm{d}v\Big). \tag{3.17}$$

As the power adaption information is unknown to other users, it is very difficult to decide the statistics of $f_P(p)$. To simplify this case, we assume that the interference among CR users is minimal. In order to maintain some guaranteed performance based

on this assumption, for any CR l it follows

$$\begin{aligned}\gamma_l &= \frac{P_l}{\sum_{k=1}^{N}\sigma_k^2} \\ &= \frac{P_T.g(v_l) \pm \Delta P_l}{\sum_{k=1}^{N}\sigma_k^2}.\end{aligned} \tag{3.18}$$

Using (3.4) and simplifying for 4QAM, P_T can be written as $P_T = \sum_{k=1}^{N} P_k = \sum_{k=1}^{N} 5\{Q^{-1}(S_{e,k}/1.5)\}^2\sigma_k^2$ and ΔP_l is the amount of power adjustment. Hence adapted power becomes a function of distance between CRs and QoS requirements which makes it easier to characterize.

For the chosen propagation model with a pathloss exponent of $\alpha = 4$, the characteristic function in (3.2) can be written as,

$$\phi_\Gamma(\omega) = \exp\Big(j\lambda\pi\omega \int_p p f_P(p) \int_0^\infty v^{-1/2} e^{j\omega v p} \mathrm{d}p\mathrm{d}v\Big). \tag{3.19}$$

Then the PDF of Γ becomes

$$\begin{aligned}f_\Gamma(\psi) &= \frac{1}{2\pi}\int_{-\infty}^{\infty} \phi_\Gamma(\omega) e^{-j\omega\psi}\mathrm{d}\omega \\ &= \frac{\pi}{2} z\psi^{-3/2} e^{-(\frac{\pi^3 z^2}{4\psi})},\end{aligned} \tag{3.20}$$

where $z = \zeta\lambda$ and $\zeta = \int_p \sqrt{p} f_P(p)\mathrm{d}p$ [24]. As discussed above, probabilistic distribution of the adapted power, $f_P(p)$ depends on the distance between users whereas the distance itself follows uniform distribution [25]. For simulation purpose, we have computed it numerically assuming the same CR network that is considered for interference analysis in Fig. 3.8. After decoding the power adaption information by local receiver, the local transmitter will adapt its power according to the signaling link information.

Again, total interference power in (3.14) can be written as,

$$\Gamma = \Gamma_T \pm \Delta\Gamma, \tag{3.21}$$

where Γ_T and $\Delta\Gamma$ are the interference due to the transmitter power before adjustment and interference due to the amount of power adjusted, respectively. Again, to analyze the overall interference in a network (3.14) can be re-written as

$$\Gamma = \sum_{l=1}^{R} g(v_l)(P_T \pm \Delta P_l), \tag{3.22}$$

where R denotes the total number of radios in CR network.

However, as discussed above, due to the limitation of PGC and step size chosen, it may not be possible to adjust the total power as required by the remote receiver. Therefore when the amount of power adjustment is very small or not exactly adjustable, the total perceived interference power follows,

$$\Gamma = \sum_{l=1}^{R} g(v_l)[P_T \pm \{(I \times F) \pm \delta P_l\}], \tag{3.23}$$

where I and F indicates the chosen step size and the number of full steps needed to adjust the required power (ΔP_l), respectively whereas δP_l indicates the adjustment error due to the chosen step size. Then the global interference Γ_G perceived at primary user is given by

$$\begin{aligned} \Gamma_G &= \Gamma + \delta\Gamma \\ &= \Gamma_T \pm \Delta\Gamma + \delta\Gamma, \end{aligned} \tag{3.24}$$

where $\delta\Gamma$ indicate the interference that is introduced due to δP_l. Note that in order to maintain guaranteed performance, remote CR receiver should always approach to the next integer step when precodes the power control information.

The other important aspect that should be mentioned here is that the profiles in the predefined set could be selected based on the channel forecasting for that particular region. As the profile set is sufficiently large, thus it would be able to accommodate a large varieties of channel characteristics.

Table 3.1: Brazil D channel model-Multipath 1

Channel parameters	**Channel taps**					
	1	**2**	**3**	**4**	**5**	**6**
Delay	0.15	0.63	2.22	3.05	5.86	5.93
Attenuation	0.1	3.8	2.6	1.3	0	2.8

Table 3.2: Brazil C channel model-Multipath 2

Channel parameters	**Channel taps**					
	1	**2**	**3**	**4**	**5**	**6**
Delay	0	0.089	0.419	1.506	2.322	2.799
Attenuation	2.8	0	3.8	0.1	2.5	1.3

3.6 Simulations Results and Discussions

To evaluate the performance of the proposed scheme, numerical simulations have been carried out. An OFDM system with a FFT size of 256, having a CP length of almost 1/4 of the symbol duration (63 samples for Kasami sequence degree of 6) is considered. 4QAM is chosen as the modulation scheme. For the channel modeling, both AWGN channel and two multipath channels as shown in Table 3.2 (Multipath channel 1 - Brazil D) and Table 3.1 (Multipath channel 2 - Brazil C) [26] are considered to evaluate the system performance.

Fig. 3.5 and Fig. 3.6 indicate the performance of the power control and subcarrier power profile information signaling link, respectively. The performance of the signaling links is evaluated according to the optimal matched filtering approach as discussed in Chapter 1. Also, the demodulator that is discussed in the next chapter can be used for this purpose. It is seen from Fig. 3.5 that performance of the power control signaling link is better than that of the subcarrier power profile link, specially in AWGN channel. As only few sequences are needed to indicate the necessary change in the transmission power adaptation process, the performance of total power adaptation signaling is more robust in comparison to that of the subcarrier power profile signaling link.

To characterize and simulate the interference in CR network, a network having uniformly distributed secondary users with different number of active communicating pairs at any given time is assumed. Since it is assumed that interference among the

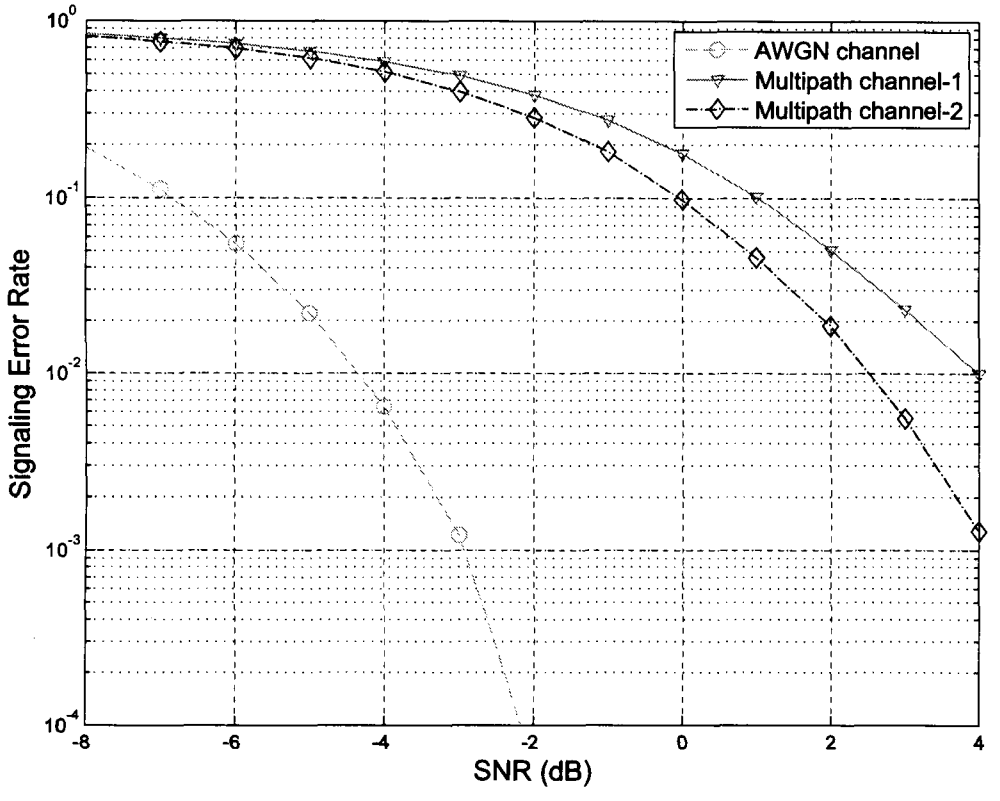

Figure 3.5: Error rate performance for transmission power control signaling link.

secondary users are at minimal level and in order to maintain target performance, power adaption is then becomes a function of distance between the communicating pairs. From this assumption, the parameter related with power adaptation (ζ) is calculated numerically to simulate the PDF using eqn. (3.20). At the same time, total amount of interference power perceived to a primary user is also calculated based on analysis presented in Section 3.5.

Fig. 3.7 shows the PDF of mutual interference power, with and without power adaption to the secondary users, while varying user density λ. Here solid and dashed line indicate the PDF of interference power, with and without power adaptation, respectively. The amount of reduced interference experienced by a primary user due to power adaption of CRs can be characterized using this PDF. It is seen that when power control is applied, the tail of the PDF is greatly reduced indicating more

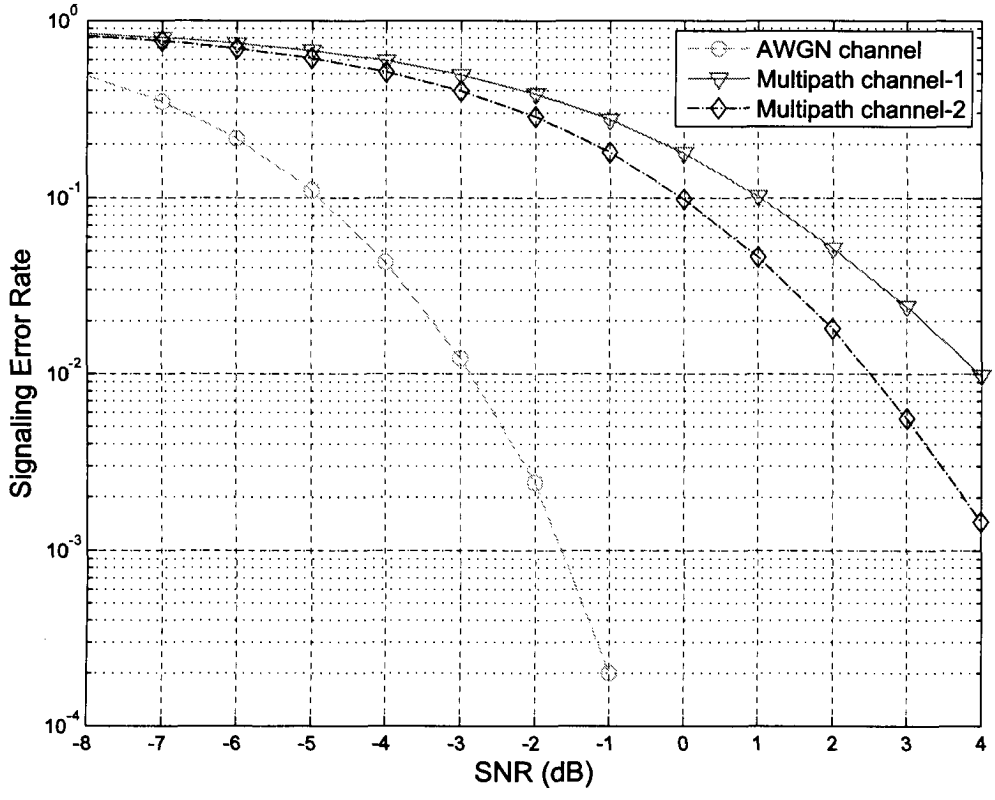

Figure 3.6: Error rate performance for subcarrier power profile signaling link.

controlled interference which is highly desirable for CR networks.

Fig. 3.8 shows the interference minimization to the primary users using proposed power control mechanism. In this simulation, we have assumed the same CR network discussed above. Adaptive power control is applied to the distributed nodes to maintain a target performance and resultant interference is found using eqn. (3.14) while varying the total number of active users in the network. It is seen that this power control mechanism can effectively minimize mutual interference to the primary users and the amount of interference minimization increases with the increased number of active users in the network. As the overall interference is minimized, more users can be deployed in the network while maintaining same required performance. Note that this technique can also be applied to a secondary network itself to minimize the overall average interference perceived among the secondary users.

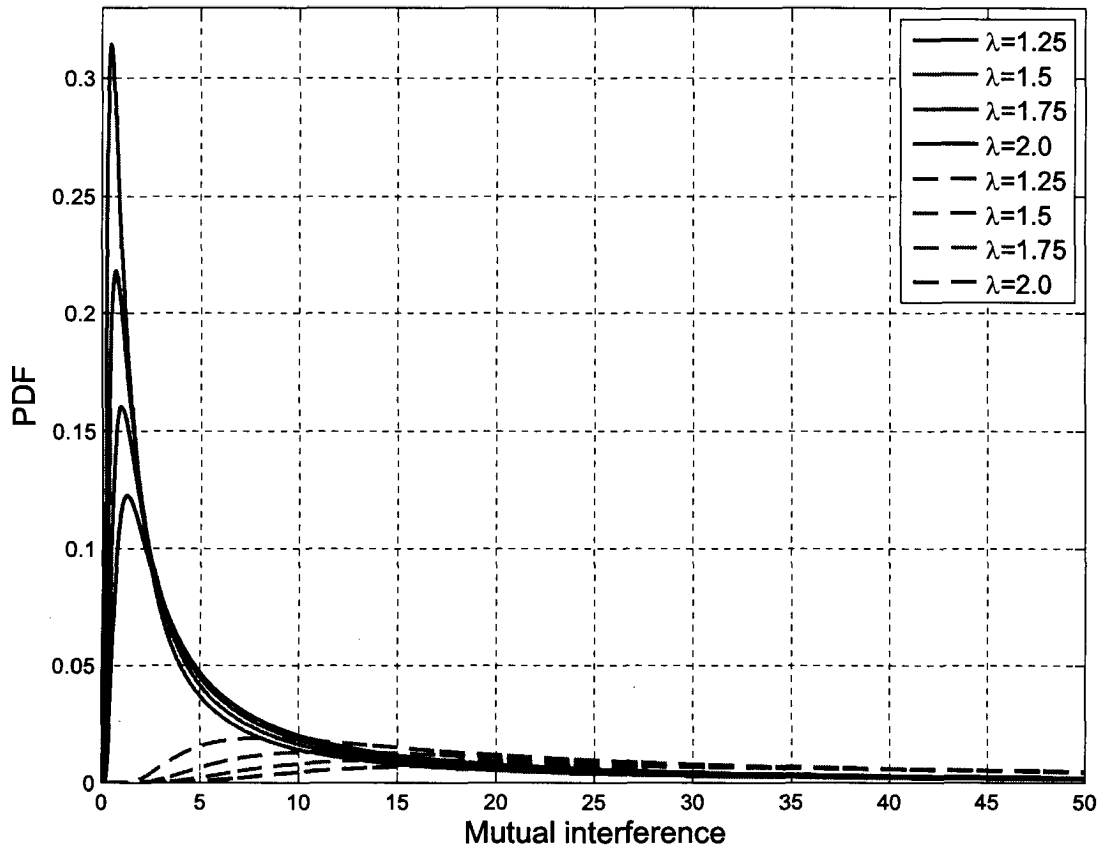

Figure 3.7: Mutual interference power PDF variation with user density λ.

3.7 Chapter Summary

An OFDM system with PCP for carrying transmitter power control and subcarrier power allocation information in CR environment is investigated in this chapter. With the PCP enabled signaling link, a transmission power negotiation is established between the neighbor CRs. As a result, mutual interference to the primary and other secondary users can be effectively minimized. Beside this, subcarrier power profile selection algorithm is presented which can also serve as a suboptimal solution. Control information can be sent at the same time without incurring additional spectrum and extra delay to the network which is very important in cognitive radio environment. Simulation results show the robustness of the signaling link in different channel sce-

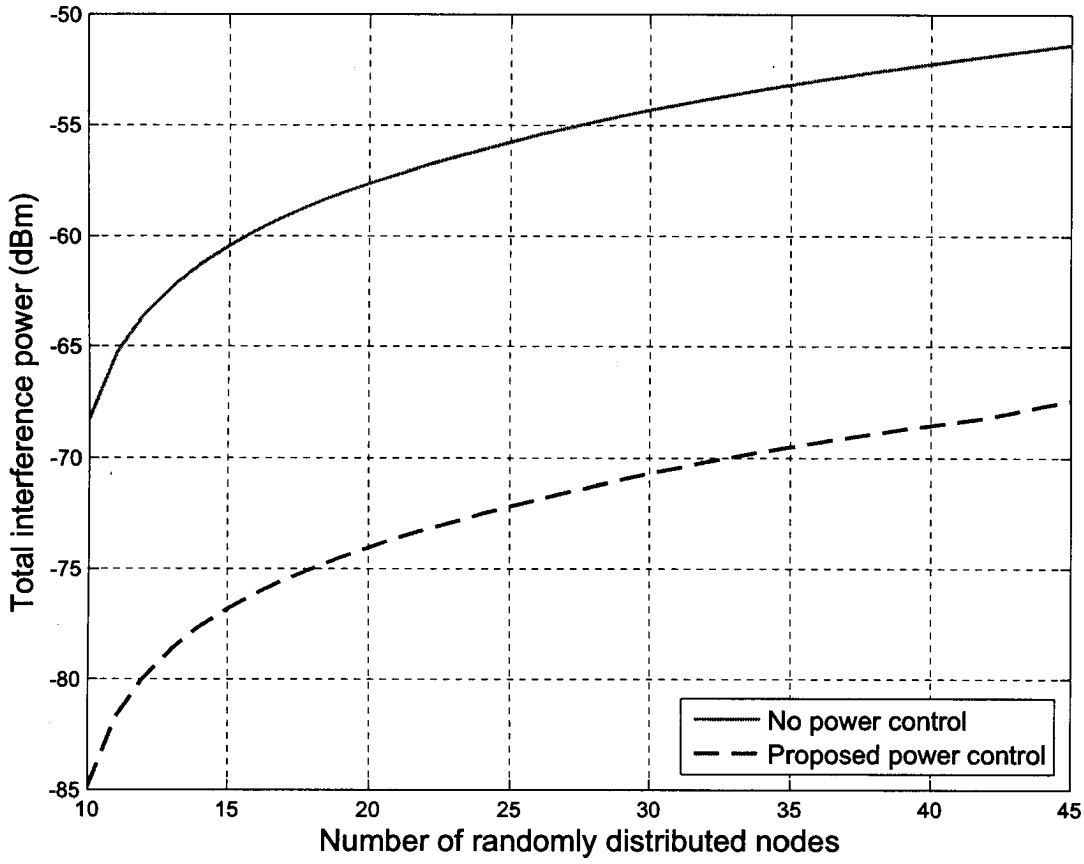

Figure 3.8: Interference minimization for the primary users using PCP signaling.

narios including multipath channels. In addition, interference minimization algorithm is validated through the observation of PDF for mutual interference with reduced tail. Therefore it is obvious that with this interference minimization technique, interference to primary users can be kept at minimal level and as a result more CR users can be deployed which will increase the overall capacity of the CR network.

Chapter 4
Demodulation of PCP Signaling

4.1 Introduction

In cognitive radio (CR) networks, it is very difficult to set up a dedicated control channel to exchange system transmission parameters among CRs where the communication environment changes very fast. To deal with this problem, precoded cyclic prefix (PCP)-OFDM system provides a flexible and efficient technique, specifically designed for cognitive radio communications to carry time-varying signaling parameters, which clearly meets the need for a dedicated control channel and makes the overall communication spectrum efficient. Note that as discussed in Chapter 3, PCP is combined from two Kasami sequences as its real and imaginary parts, providing efficient technique of sending system control parameters among CRs. In order to make use of these signaling parameters, a reliable and efficient PCP demodulator is required for low implementation complexity and processing delay. The conventional approach of PCP demodulation is to correlate the incoming PCP signal with all the possible local reference sequences available in the library based on exhaustive search method or optimal matched filtering approach as discussed in Chapter 2 [14]. According to this approach, a separate correlator is needed for each sequence in the library and therefore the implementation complexity is very high. Due to its high implementation complexity, conventional optimal matched filter is not suitable for practical implementation.

In [13, 27], a three-stage approach is proposed for demodulating PCP sequence which has substantially reduced implementation complexity in terms of number of correlators and multipliers but still the practical implementation is too complex. On the other hand, as it is a signaling link, the demodulator for this purpose must be robust such that signaling information is demodulated with high accuracy. In

this chapter, a low complexity PCP signaling demodulator is proposed which can substantially reduce the implementation complexity compared to other demodulators discussed above while providing the same performance. The idea is to partition the demodulation technique according to the generation of PCP i.e., Kasami sequence which comes with substantially reduced complexity.

The rest of the chapter is organized as follows. Conventional demodulation approach is discussed in more details in section 4.2. The principle and architecture of the proposed demodulator are presented in Section 4.3. In Section 4.4, multipath combining algorithm for the proposed demodulator is discussed. PCP detection error is analyzed in Section 4.5. Simulation results for validating and assessing the performance of the proposed techniques are presented in Section 4.6 and the chapter is summarized in Section 4.7.

4.2 Conventional Demodulation Approach

In conventional PCP-OFDM system receiver, as the PCP code set size is increased, the corresponding hardware implementation of PCP signaling demodulator becomes unprecedentedly complex. The best available demodulator for demodulating PCP sequence is optimal matched filter, which is a bank of correlators and each one is corresponding to one of the sequences in a code set as shown in Fig. 2.8. The signaling information is then demodulated based on the largest correlation peak between the received PCP segment and correlator banks. Obviously, it suffers the disadvantages due to the fact that the implementation complexity increases linearly with the increase of the code set size. More specifically, when the code set size is M, the number of correlators requires is in the order of M, i.e., $O(M)$.

On the other hand, for a code set size of M and sequence length L, hardware complexity in terms of multipliers is given by,

$$\Gamma_{OMF} = M \times L. \tag{4.1}$$

Again in [27], where the demodulation is partitioned into three stages, offers a much lower complexity than the optimal matched filter. For this demodulator, the required number of correlators is $O(M^{1/3})$ and corresponding number of multipliers

is given by

$$\Gamma_{TSD} = L + S_p L + S_p(3L - 1). \tag{4.2}$$

where S_p denotes the required number of correlators and equals to $2^{n/2}$. It is obvious that three-stage approach outperforms optimal matched filter but the complexity is still very high.

4.3 Proposed Demodulator

As discussed above, conventional optimal matched filter suffers the disadvantage due to the implementation complexity which increases linearly with the increase of the corresponding degree of Kasami sequence i.e., PCP. Therefore finding an efficient identification scheme is an important issue for PCP-OFDM system and it should be able to provide the same performance as the optimal matched filter with a reduced implementation complexity. To do this, we propose to use an identification scheme as shown in Fig. 4.1. The detection approach provides the same performance as the conventional optimal matched filtering approach at a significantly reduced implementation complexity. In addition, a multipath combiner is also included to enhance the performance in multipath channel condition as shown in Fig. 4.4. In paper [27], implementation complexity of that identifier is still higher and there was no combining technique introduced to enhance the performance under multipath condition.

To understand the proposed demodulator, the generation of large set Kasami sequence is first discussed very briefly, as it would give us the necessary intuition to understand the proposed identification scheme. It is discussed in Chapter 2 that large set Kasami sequence is the exclusive-OR outcome of the three elementary code sequences [12]. Let us define these three sequences as u, u', and u'', where u and u' form a preferred pair of binary m-sequence and $V(u')$ and $C(u'')$ can be constructed as follows

$$\begin{aligned} V(u') &\equiv \{0_L, u', Du', D^2u', ..., D^{L-1}u'\} \\ &\equiv v_d\{d = 0, ..., L\}, \end{aligned} \tag{4.3}$$

and

$$C(u'') \equiv 0_L \cup D^{j-1}c \equiv \{c_j, j = 0, ..., L_1\}, \tag{4.4}$$

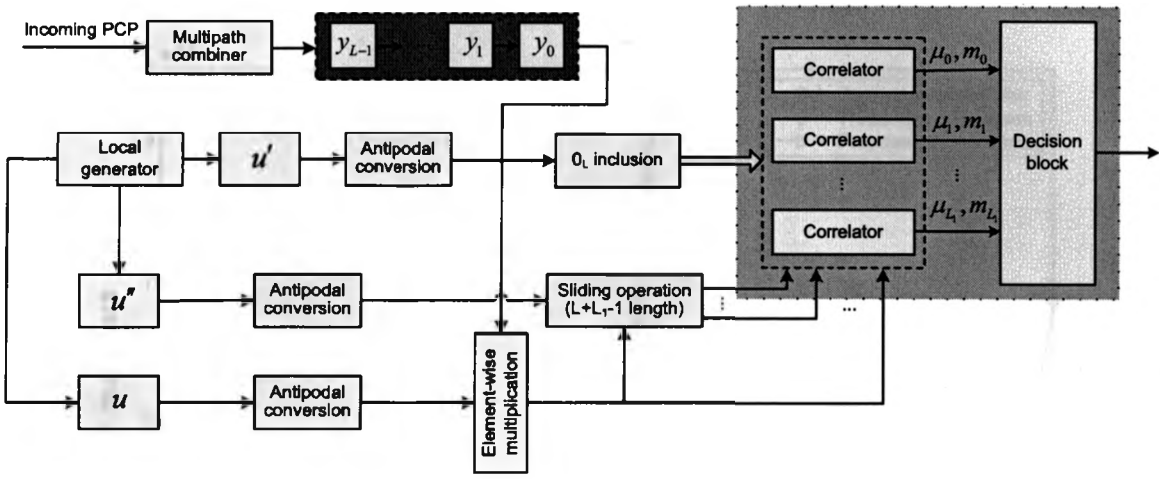

Figure 4.1: Proposed signaling demodulator for PCP-OFDM system.

where 0_L is an all-zero sequence with length $L = 2^n - 1$; $\bigcup$ denotes the union of sets and u'' has a period of $L_1 = 2^{n/2} - 1$. u is the initial sequence with no variant.

To determine the transmitted PCP sequence, except u which is unique, we need to find out the corresponding elements of $V(u')$ and $C(u'')$ in the received signal before we are able to decide which sequence has been transmitted. Thus in the proposed identification scheme, these three code sequences are correlated with the received PCP segment sequentially to determine those elements of $V(u')$ and $C(u'')$. In this approach, we have first taken into account the elementary code sequence u which is unique, then u'' and finally u'. Note that this order of sequence is optimal since the number of correlators in this case is determined by the set of sequences obtained from u'' which is much smaller than u' as in (4.3) and (4.4). On the other hand, set of sequences obtained from u' is a shifted version of the original decimated sequence and hence we can do a sliding operation over a length of $2L - 1$ to correlate with all sequences in this set.

Let $y = [y_0, y_1, ..., y_{L-1}]$ denotes the received PCP sequence segment, which contains interference from the OFDM signal, channel impact and also noise. Then the proposed demodulation scheme can be described by the following steps,

At first, the received sequence segment y is multiplied by the antipodal version of the basic sequence, $\chi(u)$ and the corresponding output sequence is given by

$$\lambda_i = y_i \times \chi(u_i), i = 0, ..., L - 1. \tag{4.5}$$

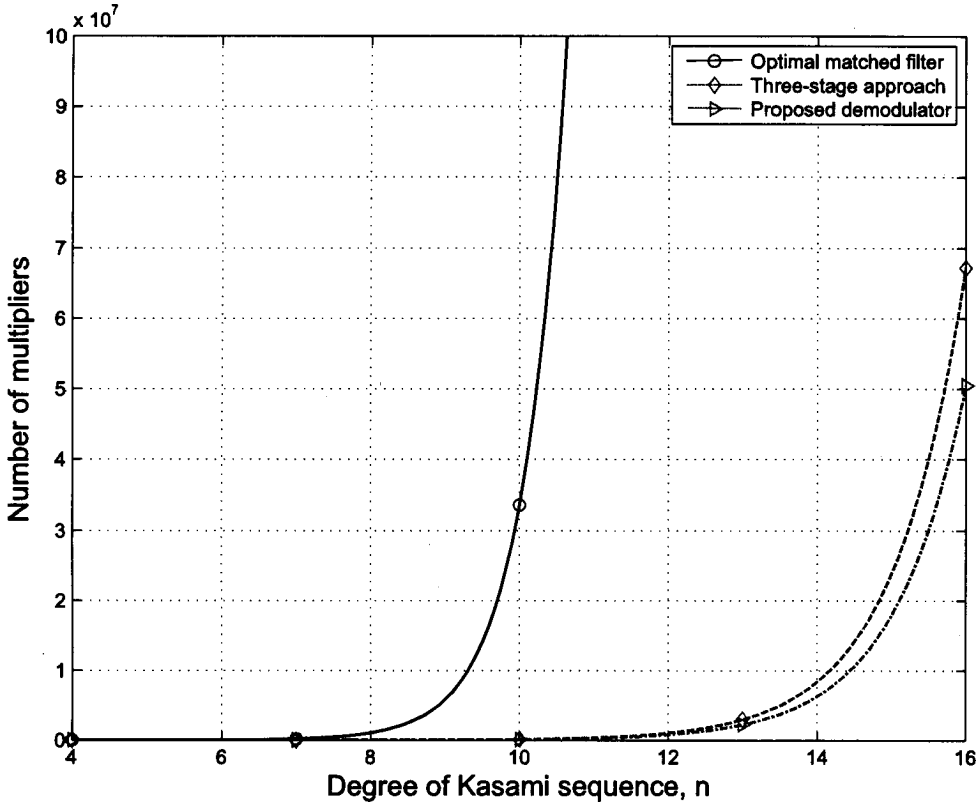

Figure 4.2: Comparison of number of multipliers for the proposed PCP demodulator (logarithmic scale).

The vector λ is then passed through a correlator of length $L + L_1 - 1$, composed of a repeated version of the third code sequence u''. This operation is equivalent to pass λ through different shifted versions of the third code sequence given as follows

$$z_j = \prod_{j=1}^{L_1} \lfloor c_j \rfloor_L \times \lambda. \tag{4.6}$$

In the next step, correlation is carried out between these outcomes, z_j and second decimated sequence u'. Here the number of correlators required is given by $\zeta_C = L_1 + 1$ and each correlator corresponds to an elementary code sequence of $C(u'')$. Therefore z_j is passed through a correlator of length $2L - 1$ corresponding

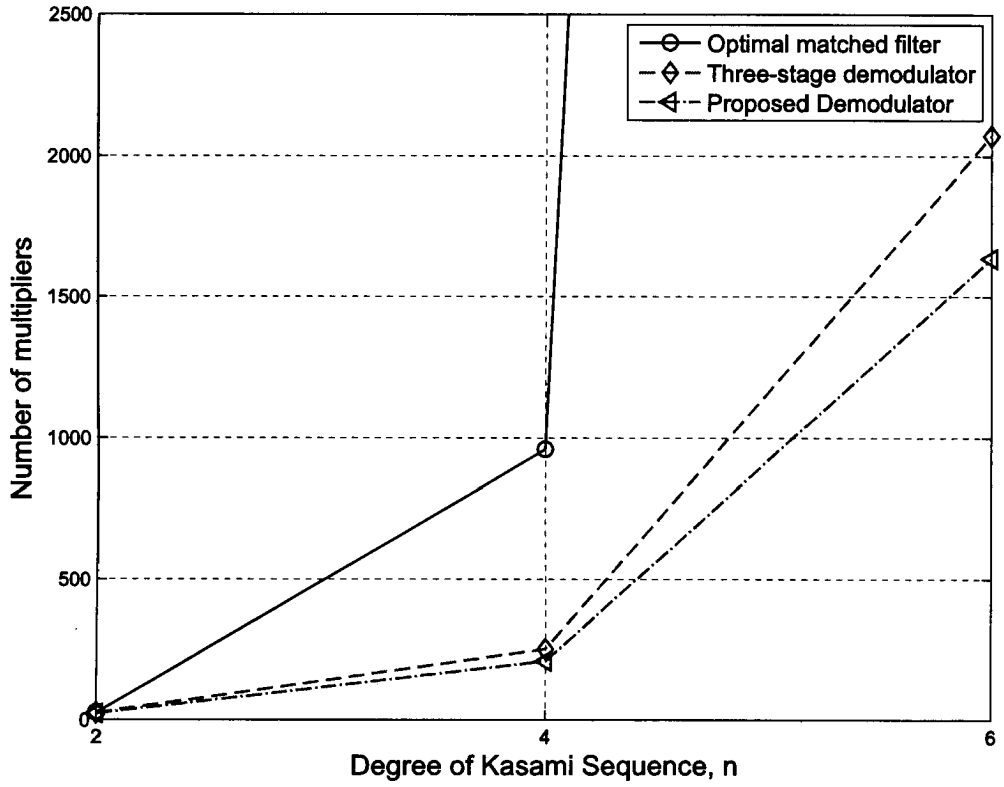

Figure 4.3: Comparison of number of multipliers for the proposed PCP demodulator (expanded view in linear scale).

to u' to evaluate the correlations between each element of z_j and $\chi(v_d), d = 0, ..., L$. The correlation can be done as follows

$$\mu_{j,d}(q) = \sum_{q=1}^{L+1} V(q)_L z_j(d-q). \tag{4.7}$$

Further, each correlator selects the local maximum among the peaks $\mu_{j,d}$, $d = 0, ..., L$ and then passes μ_j parameters and the related argument d_j to next stage.

Then the global maximum among $\mu_j, j = 0, ..., L_1$, is determined. The identification sequence is determined according to the argument j and the related d_j using corresponding exclusive-OR operation, $u \oplus c_j \oplus v_d$.

From the above discussions it is manifested that with this proposed identifi-

cation scheme, it is possible to identify PCP sequence with a significantly reduced implementation complexity. As discussed above, the complexity in terms of correlators for conventional optimal matched filter is in the order of M whereas proposed scheme requires only $2^{n/2}+1 = M^{1/3}$ correlators. For example, for Kasami sequence degree $n = 6$ and considering a complete set, conventional optimal matched filter for PCP-OFDM system requires 512 matched filters, whereas proposed scheme will require only $S_p = 2^{n/2} = 8$ correlators to identify the same PCP sequence. However, the number of correlators required for the proposed demodulator and the demodulator discussed in [13, 27] is same.

Again, hardware complexity i.e., multipliers required for the proposed demodulator is given by,

$$\Gamma_{Pro} = 2L + L_1 - 1 + S_p(3L - 1). \tag{4.8}$$

Fig. 4.2 shows the comparison of complexity in terms of multipliers in log scale for proposed scheme and other demodulators. Fig. 4.3 shows an expanded view in linear scale to better realize the difference in complexities for different schemes. It is seen that number of multipliers required for proposed demodulator is significantly less than that of other demodulators.

4.3.1 Proof of Optimal Performance

As discussed , Kasami sequence is the exclusive-OR operation of the three code sequences u, u' and u''. In order to proof that the performance of the proposed demodulator is also optimal, we need to essentially prove that in the process of identification of one sequence, this demodulator also compares all the sequences available in the code set, which is a clear indication of optimality.

Let us consider the multiplication of the incoming signal with sequence u is given by $r_l(n) = r(l).u(l)$ where $l = 1, 2, \ldots, L$. The output of the next stage i.e., multiplication with the third code sequence c_j is given by $r_2(l) = r_1(l).c_j(l)$. At the

last stage, this outcome $r_2(l)$ is correlated with v_d as follows,

$$\begin{aligned} R_c &= \frac{1}{L}\sum_{l=1}^{L} r_2(n)v_d(n-l) \\ &= \frac{1}{L}\sum_{l=1}^{L}\{r_1(n).c_j(n)\}v_d(n-l) \\ &= \frac{1}{L}\sum_{l=1}^{L}[\{r(n).u(n)\}.c_j(n)]v_d(n-l) \\ &= \frac{1}{L}\sum_{l=1}^{L}[r(n)\{u(n)\oplus c_j(n)\}]v_d(n-l) \\ &= \frac{1}{L}\sum_{l=1}^{L}[r(n)\{u(n)\oplus c_j(n)\oplus v_d(n-l)\}] \\ &= \frac{1}{L}\sum_{l=1}^{L} r(n)K_m(n-l), \end{aligned} \tag{4.9}$$

where m indicates a sequence in the set and $m\varepsilon M$. Eqn. (4.9) is the equivalent operation of the optimal matched filtering operation which indicates this demodulator also provides optimal performance i.e., it also correlates with all the available sequences in the process of identifying one sequence.

4.4 Multipath Combining Algorithm

When the amplitudes for the multipath signals are close in magnitude and there is no line of sight (LOS) component, combining multipath could significantly improve the performance of the proposed demodulator. Again, sometimes because of the sparse nature of the channel and long duration of the PCP sequence, it is not efficient to compute the correlation functions over the whole channel duration. Therefore applying combining algorithm where only selected paths are included to make the decision can significantly improve the performance. The flow diagram for the proposed combining technique is shown in Fig. 4.4.

Let us consider a multipath channel $h = [h_0, h_1, \ldots, h_{P-1}]^{\mathrm{T}}$ with P taps. A straightforward way for detecting a sequence is to use correlation peak corresponding

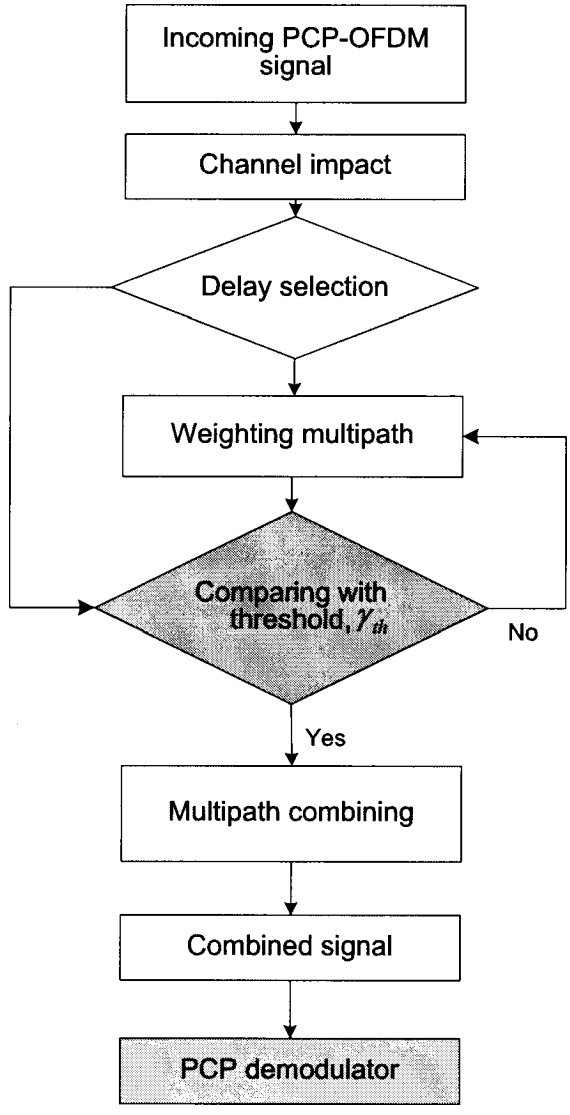

Figure 4.4: Multipath combining algorithm for PCP-OFDM system.

to the strongest path. Since the signal components from other multipaths will be interference to the detection process, therefore the variance of noise component for the m-th path becomes

$$\begin{aligned}\sigma_{n,m}^2 &= \sigma_m^2 + \sigma_s'^2 \\ &= \frac{P}{2}\left(\sigma_{m,r}^2 + \sigma_s^2 \sum_{p=0,p\neq m}^{P-1} |h_p|^2\right) \\ &= \frac{P}{2}\left(\sigma_{m,r}^2 + \sigma_s^2\right), \end{aligned} \tag{4.10}$$

where $\sigma_{m,r}^2$ and σ_s^2 is the variance of AWGN (real part) and the OFDM signal, respectively.

In the proposed combining algorithm, multipath signals are combined using a modified version of maximum ratio combining (MRC) technique. To implement the optimal combining, the SNR for each path has to be estimated. SNR and the variance of AWGN in the received PCP segment are evaluated using simple SNR estimation method [28]. Note the difference in the traditional MRC antenna combining is that the variance of noise component for each antenna input is roughly the same, while the noise component in eqn. (4.10) can be substantially different for each multipath signal.

In order to choose the multipath signals to be included in the combining process, an iterative search is studied. The combining process starts with the single strongest path. Additional multipaths are weighted and combined with the strongest path one by one in the order of its SNR. Every time when a new path is included, the SNR in the combined signal will be evaluated. However, if SNR threshold (γ_{th}) is set for a particular channel condition, the SNR in each signal should satisfy eqn. (4.11) to be included in the combining process:

$$\gamma_l \geq \gamma_{th}, \tag{4.11}$$

where $l \in p$. There may be some weak paths, by including which the SNR of the combined signal may not be significantly increased and this threshold setting avoids the inclusion of such paths. This approach follows the selection combining process. It should be noted here that the performance of the combining largely depends on the

channel condition at any particular instant. However, this threshold may be changed depending on the channel conditions and identification error performance required for any particular communication system.

4.5 Identification Error Rate Analysis

In order to analyze the identification error rate (IER), at first analysis will be carried out with the assumption of an AWGN channel. Then the identification error performance in the presence of multipath channel along with multipath combining mechanism will be considered.

Let us consider the correlation peak is denoted as $A + n_a$, where A is the autocorrelation peak of a PCP sequence and n_a is the associated interference for that autocorrelation function at first sample instant. When a PCP sequence of L samples is used, ideally the autocorrelation peak will be L. If there is a total of M PCP sequences, for the rest of $M-1$ cross-correlation functions at first sample instant, $B_c + n_c$ will take values centered on five discrete levels given as follows [12]

$$\{-t(n),\ -s(n),\ -1,\ s(n)-2,\ t(n)-2\}, \tag{4.12}$$

where $t(n) = 1 + 2^{\frac{n+2}{2}}$, $s(n) = \frac{1}{2}[t(n)+1]$ and n_c is the interference for the cross-correlation function at first sample instant. Both n_a and n_c are considered Gaussian distributed since they are summations of sufficiently long interference samples as a result of the autocorrelation and cross-correlations. However, the correct detection of the PCP sequence in the presence of one cross-correlation function with a peak of $B_c + n_c$ should meet the criteria $A - B_c > n_a + n_c$. Hence we can obtain the probability density function (PDF) of this random variable $Y > n_a + n_c$ as follows

$$\begin{aligned} f_Y(y) &= \int_{-\infty}^{\infty} f_{N_1}(n_1) f_{N_2}(y - n_1) dn_1 \\ &= \int_{-\infty}^{\infty} \frac{1}{\sigma_n\sqrt{2\pi}} e^{-\frac{n_1^2}{2\sigma_n^2}} \frac{1}{\sigma_n\sqrt{2\pi}} e^{-\frac{(y-n_1)^2}{2\sigma_n^2}} dn_1 \end{aligned}$$

$$= \frac{1}{\sigma_n\sqrt{2\pi}} e^{-\frac{y^2}{2\sigma_n^2}} \int_{-\infty}^{\infty} \frac{1}{\sigma_n\sqrt{2\pi}} e^{-\frac{2(n_1-y/2)^2-y^2/2}{2\sigma_n^2}} dn_1$$

$$= \frac{1}{2\sigma_n\sqrt{\pi}} e^{-\frac{y^2}{4\sigma_n^2}}, \tag{4.13}$$

where σ_n is the standard deviation of AWGN. Thus the probability of getting an erroneous decision for one correlation is given as follows,

$$\begin{aligned} P_{e,c}(n_a + n_c > A - B_c) &= \int_{A-B_c}^{\infty} \frac{1}{2\sigma_n\sqrt{\pi}} e^{-\frac{y^2}{4\sigma_n^2}} dy \\ &= \sqrt{2}\sigma_n \int_{\frac{A-B_c}{\sqrt{2}\sigma_n}}^{\infty} \frac{1}{2\sigma_n\sqrt{\pi}} e^{-\frac{f^2}{2}} df \\ &= Q\left(\frac{A - B_c}{\sqrt{2}\sigma_n}\right), \end{aligned} \tag{4.14}$$

where $f = \frac{y}{\sqrt{2}\sigma_n}$. As the total number of sequences is large, it is almost impossible to find out the exact occurrence probabilities of different cross-correlation peaks analytically. Therefore, in our analysis, we assume that the occurrence probabilities for five different cross-correlation peaks are equal. So, the average probability that the decision is erroneous in presence of one correlation is given by,

$$P_e = \frac{1}{5}\sum_{c=1}^{5} P_{e,c}(n_a + n_c > A - B_c). \tag{4.15}$$

The corresponding probability of getting a correct decision can be written as

$$\overline{P}_e = 1 - P_e. \tag{4.16}$$

Therefore, probability of making false detection in presence of the rest of the $M - 1$ sequences is given by,

$$P_t = [1 - (1 - P_e)^{M-1}]. \tag{4.17}$$

On the other hand when the multipath combining is applied at the beginning of the demodulator, both the autocorrelation and cross-correlation peak will be increased but the SNR in the combined peak will be higher than the case without combining which results in an improvement of performance in terms of identification error rate. After applying the weight for each multipath signal $x_1, x_2, ..., x_p$, the combined signal is given by

$$x = a_1x_1 + a_2x_2 + ... + a_px_p, \tag{4.18}$$

where $a_1, a_2, ..., a_p$ denote the weight factor for each multipath and given by $a_p = \frac{h_p}{N_p}$ [[29], App. A]. As signals are co-phased and added together coherently, the combined signal will have the same characteristics to those of individual multipath components. As it is a linear combination of the multipath signals, noise in the combined signal will follow Gaussian distribution as well.

Let us consider that P paths are added together, so the ideal autocorrelation peak would be P times that of a single autocorrelation peak i.e.,PA. However due to the presence of noise, actual autocorrelation peak would be $PA + n'_a$ where noise component n'_a is given by

$$n'_a = \frac{h_1}{N_1}n_1 + \frac{h_2}{N_2}n_2 + ... + \frac{h_p}{N_p}n_p. \tag{4.19}$$

As n'_a is a linear combination of Gaussian distributed noise $n_1, n_2, ..., n_p$, clearly it will also follow Gaussian distribution.

Again, cross-correlation peak for this combined signal would be $PB_c+n'_c$, where n'_c denotes the resultant noise in the cross-correlation peaks which will follow Gaussian distribution. Therefore condition for getting a correct decision after multipath combining follows

$$\begin{aligned} &PA + n'_a - PB_c + n'_c > 0 \\ \Rightarrow &PA - PB_c > n'_a + n'_c. \end{aligned} \tag{4.20}$$

Following similar approach as in (3.20), the PDF of the variable $Y' > n'_a + n'_c$ for making a correct decision is

$$f_{Y'}(y') = \frac{1}{2\sigma'_n\sqrt{\pi}}e^{-\frac{y'^2}{4\sigma'^2_n}}, \tag{4.21}$$

Therefore probability of getting an erroneous decision for one correlation after combining multipaths is given by,

$$P_{e,c}\{n'_a + n'_c > P(A - B_c)\} = \int_{P(A-B_c)}^{\infty} \frac{1}{2\sigma'_n\sqrt{\pi}} e^{-\frac{y'^2}{4\sigma'^2_n}} dy' = Q\left\{\frac{P(A - B_c)}{\sqrt{2}\sigma'_n}\right\}. \tag{4.22}$$

Therefore probability of getting a correct decision is given by,

$$\overline{P}'_e = 1 - P'_e, \tag{4.23}$$

where P'_e indicates the average probability of getting an erroneous decision over five cross-correlation peaks. So the overall probability of making a false detection for the rest of $M - 1$ sequences in presence of a multipath channel with combining follows

$$P'_t = [1 - (1 - P'_e)^{M-1}]. \tag{4.24}$$

However, in order to evaluate the performance of the overall system, the impact of the PCP signaling link failure also needs to be determined. It should be noted here that the error probability for the OFDM symbol is dependent on the probability of error for PCP signaling link. Even if the demodulation of PCP signaling link is successful, there will be error for the OFDM symbol as usual. Considering these two situations, the overall error probability for OFDM symbol is given as follows,

$$\begin{aligned} P_o &= P_{t,\kappa} \times P'_{ser} + (1 - P_{t,\kappa}) \times P_{ser} \\ &= \frac{1}{M-1} \sum_{\kappa=1}^{M-1} \left[\left\{1 - (1 - P_{e,\kappa})^{M-1}\right\} \times P'_{ser} \right. \\ &\quad \left. + \left\{(1 - P_{e,\kappa})^{M-1} \times P_{ser}\right\}\right], \end{aligned} \tag{4.25}$$

where P_{ser} and P'_{ser} is the symbol error probability (SER) for OFDM data carrying signal when PCP detection is correct and incorrect, respectively. It is seen from (4.25) that if the identification error is low enough, total system error probability becomes as low as the conventional CP-OFDM system.

However, in order to get a reliable signaling performance, a hold-and-demodulation scheme can be followed. If the demodulated PCP signaling carries different information from the present system parameters, demodulation can be hold and wait for the demodulation of next PCP for confirmation purpose. If it finds that next demodulated PCP gives the same information as the previous one, it may accept and trust the information carried by the demodulated PCP. But if the next demodulated PCP carries different information than the previous one, it should wait for another PCP demodulation. Based on the next demodulation and if it matches with the previous one, it can make the decision for the adjustment of system parameters. It should be noted that total decision time should be justified with the channel coherence time.

4.6 Simulation Results and Discussions

To simulate the proposed scheme, as in Chapter 3 one OFDM symbol having 256 subcarriers is considered and for the PCP design with $n = 6$, corresponding PCP duration is $L = 2^n - 1 = 63$, which is almost one-fourth of an OFDM symbol.

For the channel modeling, we have considered one multipath channel as in Table 3.2 shown in Chapter 3, in addition to AWGN channel, while the channel length is smaller than the PCP duration to avoid ISI.

The performance of the proposed demodulator is evaluated in the above mentioned channel scenarios in terms of identification error rate (IER). It is seen from Fig. 4.5 that proposed PCP demodulation scheme provides the same performance as the optimal matched filter irrespective of channel scenarios. For this simulation, we have considered all the sequences available in the set for Kasami sequence degree $n = 6$ i.e., 512 sequences but in an efficient way so that the implementation complexity is significantly reduced. Also, theoretical and simulation results are almost matched. In the theoretical analysis, in addition to the assumption that cross-correlation peaks occur with equal probabilities, the impact of OFDM data carrying signal, specially ISI on PCP is not considered. These reasons may cause the performance gap between the theoretical and simulation results.

Fig. 4.6 shows the comparison of the performance for the proposed demodulator while different number of sequences available in the code set. In this case, we have assumed three different scenarios for $n = 6$ i.e., when 512 (full code set), 256, and 128 sequences are available in the family. As expected, with the lesser number of

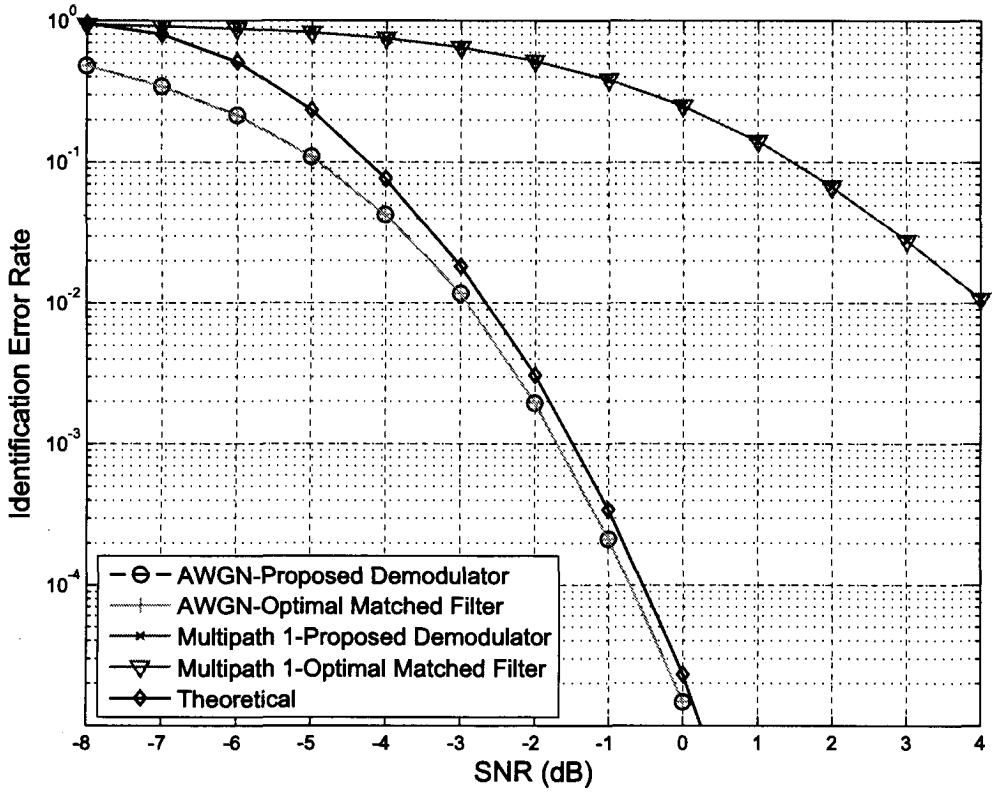

Figure 4.5: Identification error rate performance for the proposed demodulator (PCP length L=63).

the sequences in the family, there is lesser probability of error. However, in any case, the demodulator provides the same performance as the optimal matched filtering approach. It should be mentioned here that for larger PCP length, IER performance will be improved for the same SNR level due to the availability of larger decision peak, although the code set size is increased.

To further improve the performance of the proposed demodulator in multipath scenario, we have used a technique to combine the multipath signals that can make the decision process much robust in real communication scenario as in multipath cases. Depending on the nonzero components in the multipath channel, we will have different received versions for the same received signal. Therefore instead of selecting the strongest multipath among all the received versions for the same transmitted PCP, few stronger multipaths are combined with optimum weights coefficient according

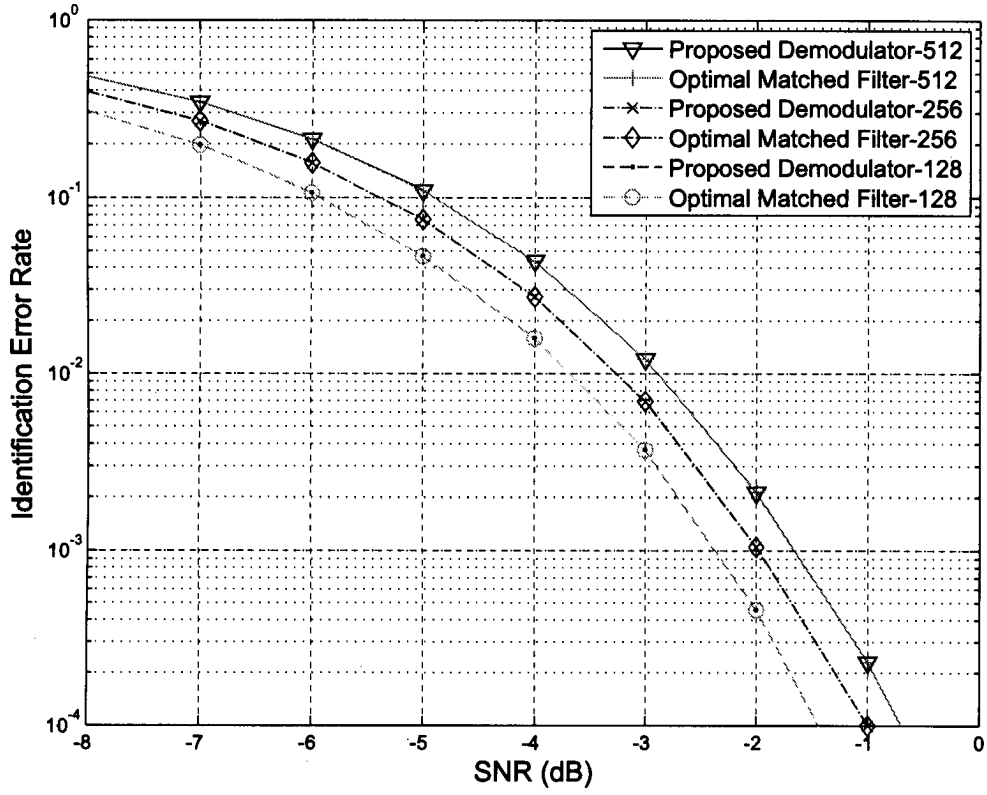

Figure 4.6: Comparison of IER performance with different code set sizes.

to maximum ratio combining with unequal noise components in each branch. This approach improves the performance of the proposed demodulator to a great extent indicating the robustness of this demodulator in real communication system. However, it is found that after combining the first few strongest paths, the performance is not that much improved because in that case the combined path becomes much stronger than other paths from the multipath channel. It is seen from Fig. 4.7 that performance is significantly improved when two most strongest paths are combined, comparing to that of the no peak combining case. But the improvement in performance when three most strongest paths are combined is not that significant when comparing to the case of combining two most strongest paths. As seen from figure, this observation is more pronounced for the case of combining three and four paths. It should be also noted that the performance improvement depends on the relative

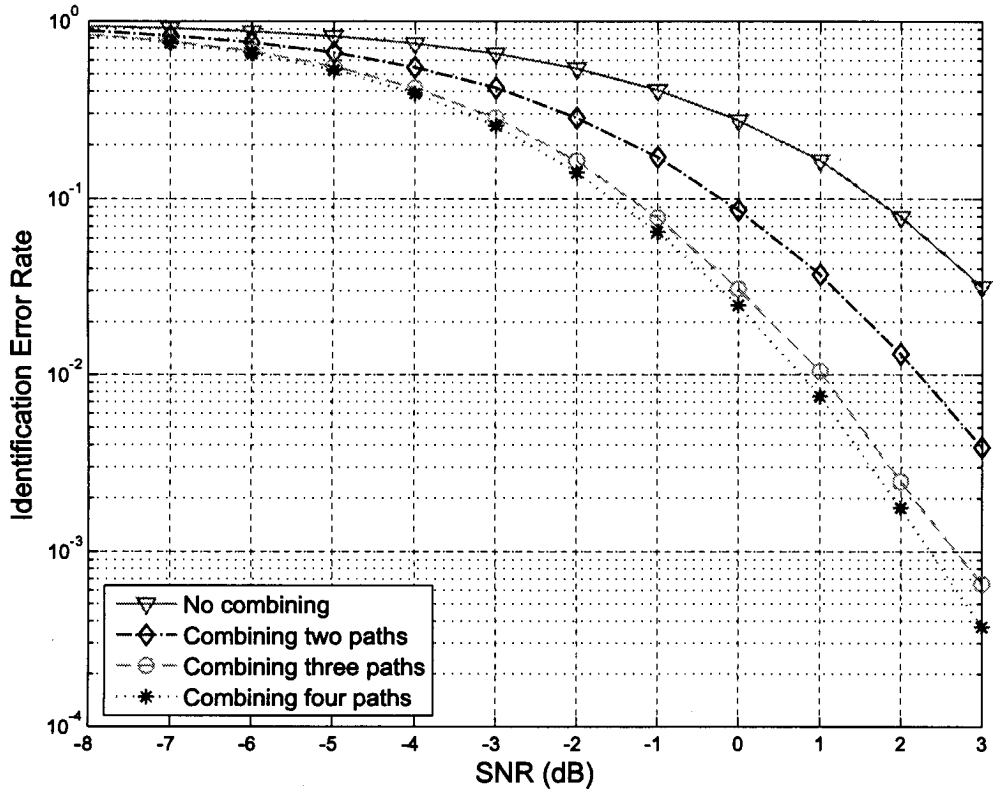

Figure 4.7: Performance improvement using peak combining technique.

attenuation among the multipath components.

4.7 Chapter Summary

Efficient design of PCP demodulator with low implementation complexity is very important for flexible spectrum sharing in cognitive radio communication. This chapter presents an improved PCP demodulator which provides reduced implementation complexity, while providing the same performance as the optimal matched filter and that of three-stage approach. The identification error rate for this demodulator is simulated. It is observed that theoretical and simulation results are almost matched. With different number of available code sequences in the set, it is found that the identification error rate is relatively lower when few sequences are compared. It is

also presented that performance of this proposed demodulator can be significantly improved in multipath channel scenarios using multipath combining technique. On the other hand, impact of PCP link failure on the system performance is analyzed and the average error probability is also derived.

Chapter 5
Robust Data Transmission using DTV Watermark Signal

5.1 Introduction

In the last few decades, the world has seen more disastrous situations than ever caused by various environmental, social and political movements, and even man-made. In the recent history, September 11 attacks in the United States of America (2001), devastating Tsunami in Asia-Pacific (2004), Hurricane Katrina in the United States of America (2005), and cyclone Nargis in Myanmar (2008), only few of many others, remind us the outmost necessity of reliable emergency communication system to lessen the sheer magnitude of the disaster the world has seen. The situation is even worse in remote areas which are not covered by modern communication systems such as land or cellular communications. Therefore, it is extremely important to have an effective emergency communication system to make mass people aware in the advent and during national emergencies, including people living in distant rural areas.

Several ad-hoc based emergency networks such as enhanced communication scheme combining centralized and ad-hoc networks (ECCA) [30], sensor network based emergency communication system [31], integrated cellular and ad-hoc relaying system [32] etc., have been investigated in literature. The key advantages of these ad-hoc based emergency networks are self-organized and fast reconfigurable. However, on top of conventional power constraint and delay problem, due to limited coverage, a large number of communicating nodes are required and hence reliability is a major problem in these networks.

On the other hand, infrastructure based emergency networks consist public switched telephone network (PSTN) access network, cellular networks, satellite networks and other broadband communication systems. For example, TErrestrial Trunked

RAdio (TETRA) [33], integration of IEEE 802.11 and 3G networks [34], HUGHES broadband satellite communication [35] etc. are able to provide emergency communication during disastrous situations. However, the crucial problem for the infrastructure based emergency communication system is the requirement of a great deal of interoperability among existing communication systems. Although to solve interoperability issue, different measures have been taken through the development of IEEE 802.21 standard body, they are still under evaluation [36]. However, all the major concerns such as interoperability and reliability are co-related and driven by the limited coverage of existing emergency communication systems.

In this chapter, we propose to use modulated TxID watermark signals as a technique to send alerting message to the people during emergency situations. It is found that data transmission based on modulated TxID watermark signals are much more robust than the 8-VSB modulated ATSC DTV broadcasting, providing us the opportunity to have a robust data distribution technique with extended coverage. As we are almost at the verge of a fully-fledged DTV broadcasting, this extended coverage ensures that even the people living at the rural distant areas would be able to receive the emergency alerting message before and/or during the disastrous situations. In addition, as the interoperability is still a far-reach issue and with this proposed technique a greater coverage area is obtained, it obviates the interoperability issue along with the higher reliability of the overall communication network.

The rest of this chapter is organized as follows. The overview of this emergency communication model is presented in Section 5.2. The TxID watermark data insertion procedure is discussed in Section 5.3. Synchronization technique for the proper reception of TxID watermark is briefly analyzed in Section 5.4. The demodulation of TxID watermark signal and error performance analysis for emergency data is presented in Section 5.5 and 5.6, respectively. Section 5.7 describes the signal propagation model for the coverage prediction and analysis for this communication technique is carried out in Section 5.8. Overall reliability of the emergency communication network with comparison to some other existing systems is studied in Section 5.9 and finally, the chapter is summarized in Section 5.10.

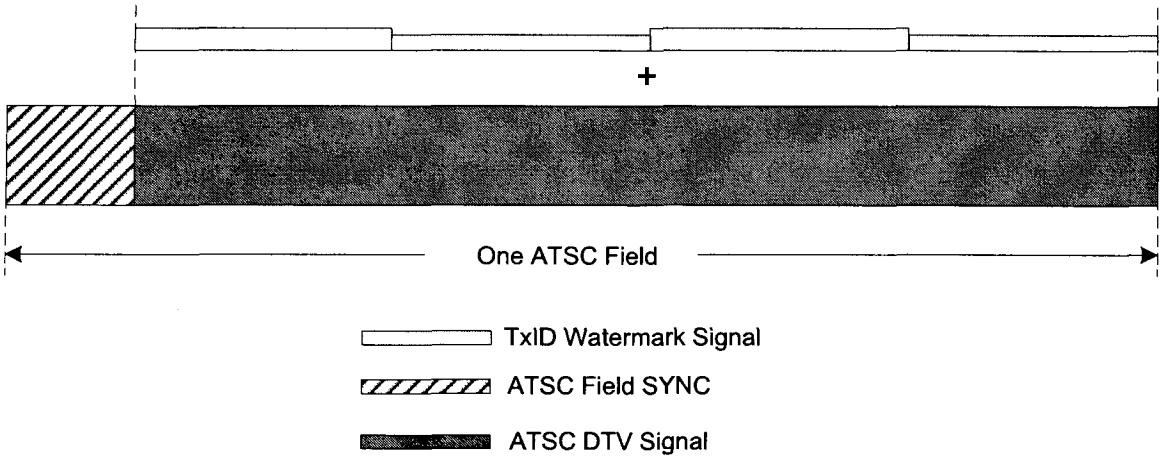

Figure 5.1: ATSC DTV signal with modulated TxID watermark.

5.2 Emergency Communication System Model

DTV broadcasting has gained immense popularity over the last few years. Following this way, the U.S. TV broadcast industry already made an all-digital transmission and that in Canada by August 31, 2011. At the end of 2011, North America will have an all-digital DTV broadcasting opportunity and few other countries such as The Netherlands, Finland have already made the transition.

The Advanced Television System Committee (ATSC) DTV standards are entirely different from the conventional analog TV signals and have many new features e.g., allowing higher-quality images, sound, and more programming choices etc. [21]. One interesting feature of the ATSC system is that a unique pseudo-random sequence will be assigned for each DTV transmitter as a RF watermark. Since the identification sequence is embedded into original DTV signal as a watermark as shown in Fig. 5.1 and the strength is very low compared to the original DTV signal, the pseudo-random sequences must be long enough so that the peaks obtained from the correlations associated with background DTV noise can be detected.

The emergency communication system in this chapter is enabled by this newly introduced feature of transmitter identification watermark to DTV broadcasting systems. According to our proposal, modulated TxID watermark signals will be encoded to send the emergency alerting message to the people during disastrous situations. The corresponding transmitter and receiver structure are shown in Fig. 5.2 and Fig.

5.3, respectively. The sequence can be detected based on matched filtering approach discussed in [14] or the demodulator presented in Chapter 4. Once the watermark signal is decoded, the terminal user will be able to get the emergency messages sent from either the government or private authorities. As a result, we can use existing DTV infrastructure which clearly obviates the need for new infrastructure and thus cost-effective than most other emergency communication systems currently available.

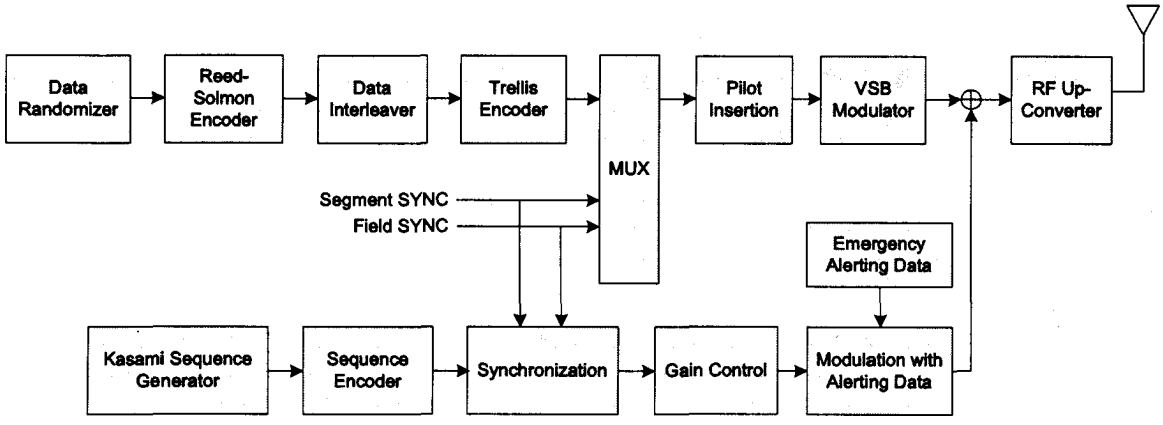

Figure 5.2: TxID enabled emergency communication system transmitter.

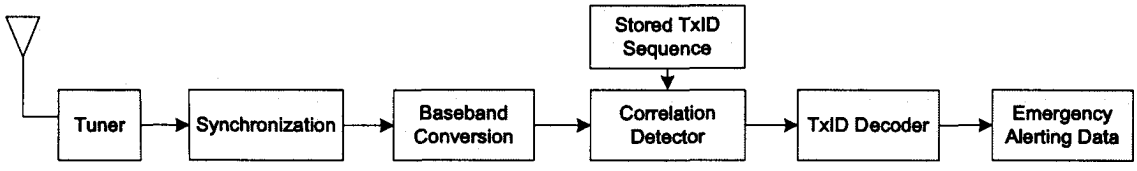

Figure 5.3: TxID enabled emergency communication system receiver.

5.3 TxID Watermark Emergency Data Insertion

In this section, TxID watermark emergency data insertion into DTV signal and corresponding detection algorithm will be discussed. Let us take DTV signal from i-th transmitter before and after the injection of the pseudo-random sequence (large set Kasami sequence of degree 16) $x_i(n)$ is $d_i(n)$ and $d_i'(n)$, respectively. Note that each

DTV transmitter would have a unique TxID sequence x_i, thus it is always recognizable even within the coverage of other stations. The injection of the transmitter identification sequence into DTV signal being modulated by the emergency alerting data a_d, results

$$d_i'(n) = d_i(n) + \rho x_i(n) a_d(i), \tag{5.1}$$

where ρ is a gain coefficient to control the injection level. The injection level of the TxID watermark signal can be different from transmitter to transmitter. It will be convenient for the emergency data demodulation process if the gain is set to the same level for all the transmitters [3]. The insertion ratio (IR) can be defined as follows

$$\text{IR} = 10 \log_{10} \left(\frac{\rho^2 . E\{x_i^2(n)\}}{E\{d_i^2(n)\}} \right). \tag{5.2}$$

However, 8-VSB DTV signal energy is $E\{d_i^2(n)\} = 21$. Again, BPSK modulated watermark signal energy is $E\{x_i^2(n)\} = 1$. Hence for a given IR, injection level can be determined as

$$\rho = \sqrt{\frac{21}{10^{-IR/10}}}. \tag{5.3}$$

After passing through channel h_i, the received signal from the i-th transmitter, r_i is

$$r_i(n) = d_i'(n) \otimes h_i + n_i(n), \tag{5.4}$$

where $n_i(n)$ is the noise at the input of the i-th receiver. The overall received signal, $r(n)$ is then given by,

$$r(n) = \sum_{i=1}^{T} \left[d_i'(n) \otimes h_i + n_i(n) \right], \tag{5.5}$$

where T is the total number of DTV transmitters in the broadcasting area.

5.4 Synchronization of TxID Watermark Signal

Synchronization is very important for proper demodulation of the alerting message, due to its low signal strength and long duration. For this purpose, one PN-511 SYNC field is reserved in each field of ATSC signal shown in Fig. 2.12. Traditionally, a time

domain sliding correlation approach is used to achieve synchronization which is equal to the length of PN-511 (511 samples) shown in Fig. 5.4. However, in presence of frequency offset and sampling clock error, the time domain synchronization becomes very difficult to achieve in low SNR condition. Alternatively, PN-511 in the frequency domain can be used to achieve synchronization. The obvious advantage of using frequency domain synchronization is that just taking the magnitude of the correlation peak, these frequency and sampling clock offsets can be alleviated.

5.4.1 PN-511 Based Time Domain Approach

In this simple process, correlation will be carried out between PN-511 signal of first and the second incoming ATSC field. As the subsequent adjacent signal will have the same amount of time offset, this process is able to identify the starting point of the incoming signal. Let us consider that the received signal segment with PN-511 is given by r which consists of l data frames. The correlation which is N samples apart (length of one complete ATSC data frame) is carried out as follows,

$$R_t(n) = \sum_{n=1}^{511} r(n)r(N+n). \tag{5.6}$$

In this case correlation is carried out along with the adjacent frames. And synchronization is decided based on the maximum correlation value. Fig. 5.5 and 5.6 show the time domain and its squared correlations samples.

5.4.2 PN-511 Based Frequency Domain Approach

In frequency domain approach, correlation will be carried out in the frequency domain between the PN-511 of first incoming single and the adjacent one. As the subsequent adjacent signal will have the same frequency and sampling clock offsets, only taking the magnitude of the correlation value will help to alleviate these offsets. Following the similar approach as in time domain, the correlation between adjacent PN-511 is carried out as follows,

$$R'_f(n) = \sum_{n=1}^{511} F^{-1}\{r(n)\}.F^{-1}\{r(N+n)\}. \tag{5.7}$$

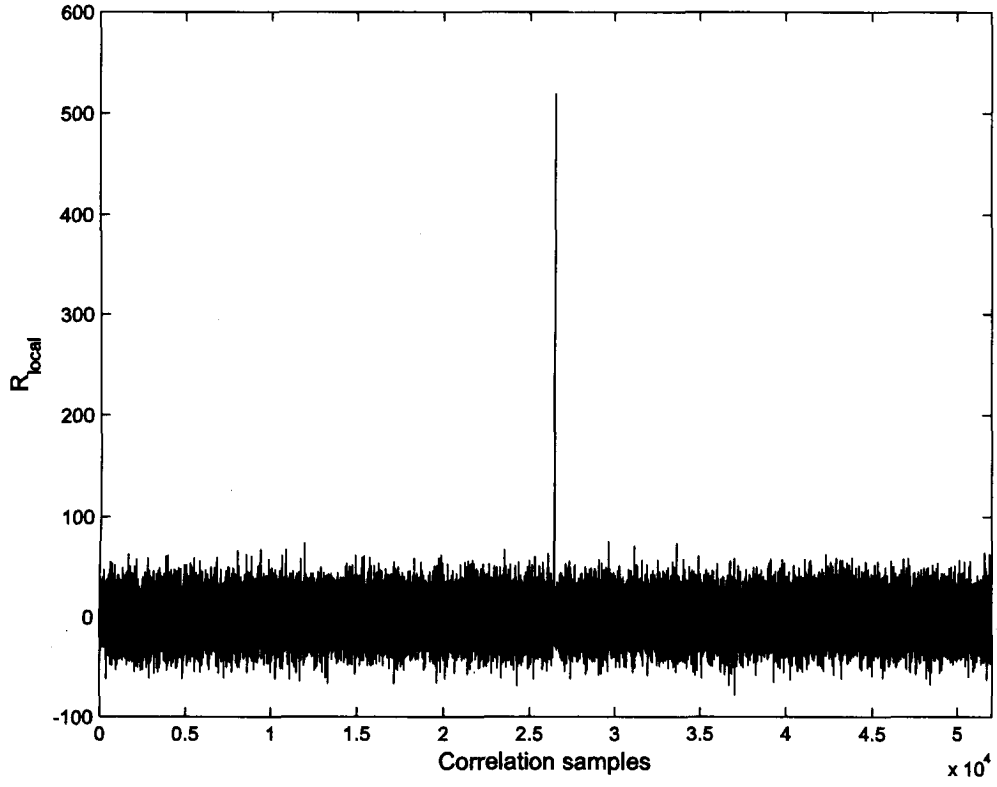

Figure 5.4: Time domain correlation peaks for local PN-511 (local reference).

The correlation value obtained in this case is a complex number. However, by taking the conjugate of the correlation value and multiplying, we can have real correlation value as

$$R_f = R'_f R'^*_f. \tag{5.8}$$

Similarly decision is taken based on the maximum correlation value but frequency and sampling clock offset is now removed. Fig. 5.7 and 5.8 show the frequency domain and its squared correlations samples for synchronization purpose.

Therefore synchronized reception can be achieved using the frequency domain approach where synchronization performance is kept the same because of the sharp correlation peak as shown in Fig. 5.8 (even stronger than time domain squared peak)

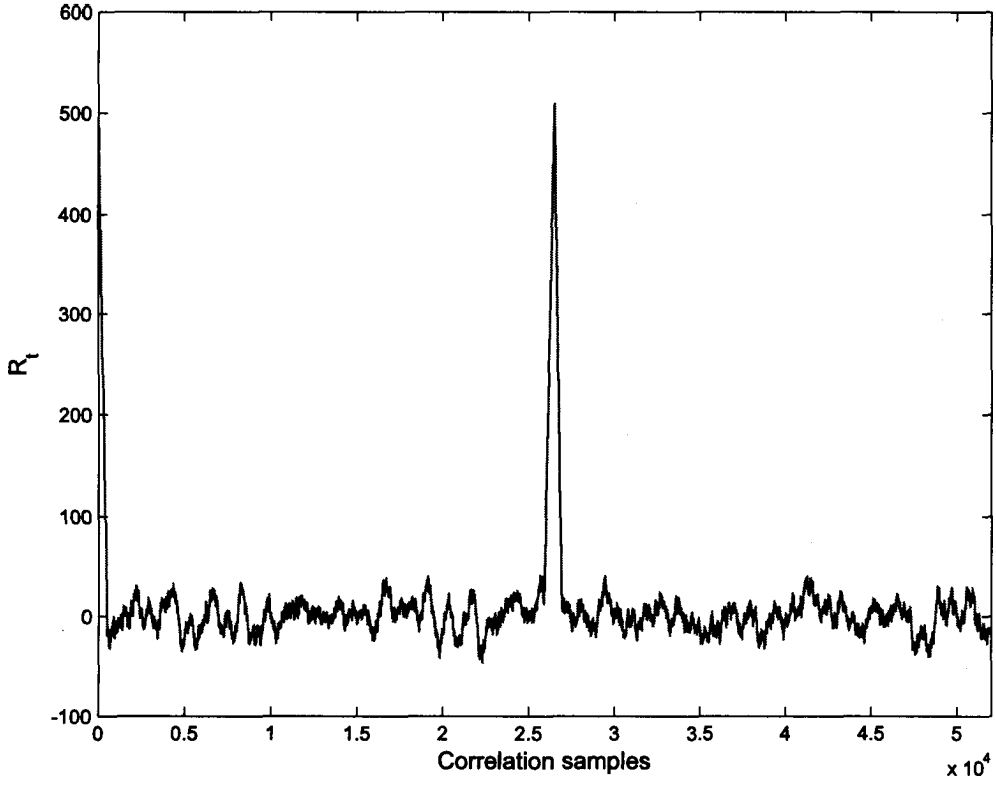

Figure 5.5: Time domain correlation peaks using PN-511.

and at the same time we can alleviate the frequency and sampling clock offsets by taking only magnitude of the squared correlation peak.

5.5 TxID Watermark Emergency Data Detection

The TxID watermark signal i.e., the emergency data will be demodulated based on the correlation process. Using this approach, cross-correlation between $r(n)$ and $x_j(n)$ will be evaluated at the receiver side to find out the emergency data from the j-th

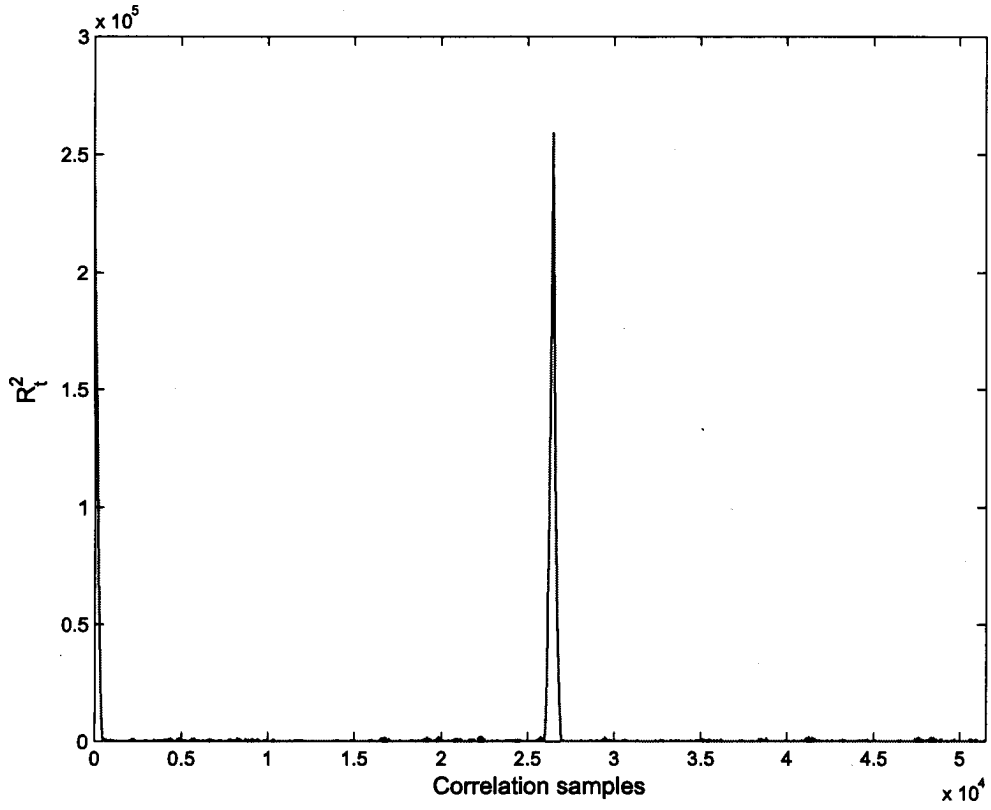

Figure 5.6: Time domain squared correlation peaks using PN-511.

transmitter as follows,

$$
\begin{aligned}
R_{rx_j}(m) &= \sum_{n=0}^{N-1} r(n)x_j(n-m) \\
&= \sum_{n=0}^{N-1}\left\{\sum_{i=1}^{T} d_i'(n) \otimes h_i + n_i(n)\right\} x_j(n-m) \\
&= \sum_{n=0}^{N-1}\left[\sum_{i=1}^{T} \{d_i(n) + \rho x_i(n) a_d(i)\} \otimes h_i + n_i(n)\right] x_j(n-m)
\end{aligned}
$$

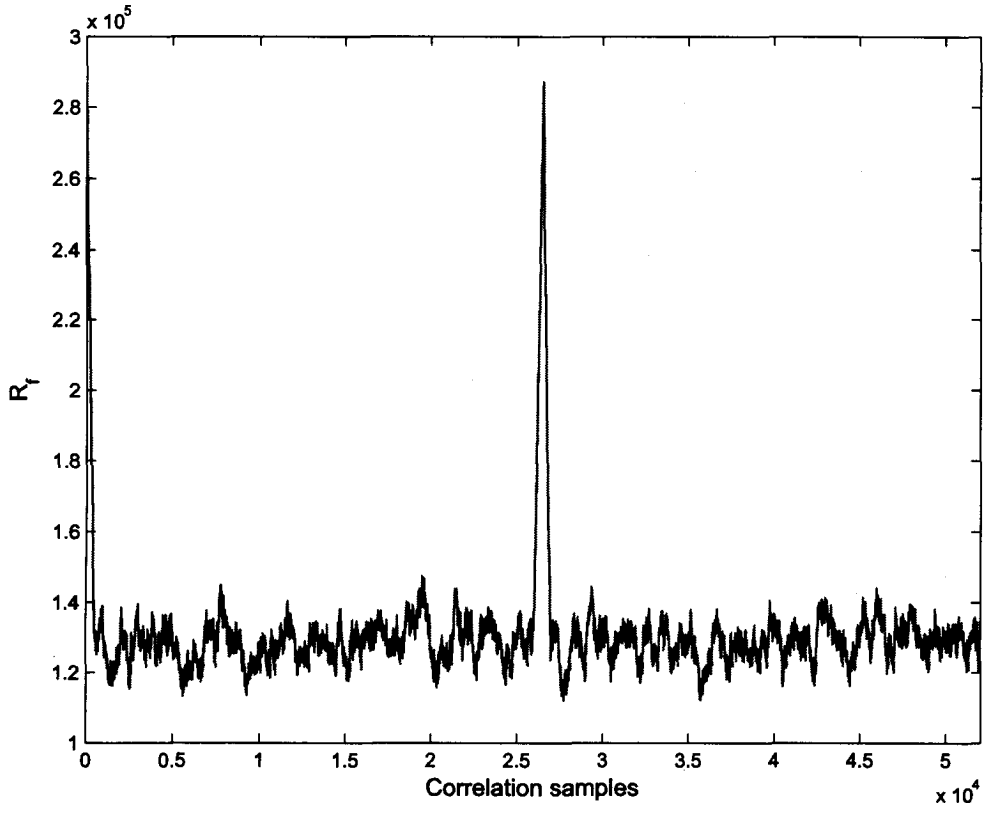

Figure 5.7: Frequency domain correlation peaks using PN-511.

$$= \rho a_d R_{x_j x_j} \otimes h_j + \sum_{i=1, i\neq j}^{T} \rho R_{x_i x_j} \otimes h_i + \sum_{n=0}^{N-1} \sum_{i=1}^{T} [d_i(n) \otimes h_i + n_i(n)]\, x_j(n-m), \tag{5.9}$$

where N is the length of the pseudo random sequence $x_j(n)$ which is used as TxID watermark signal. With the orthogonal property of the selected pseudo-random sequence, $R_{x_j x_j}$ can be approximated as a delta function. The second and third terms in the above equation are only noise-like sequences from the in-band DTV signals of the same transmitter and other neighboring transmitters. Therefore, the received channel response h_j from the j-th transmitter can be approximated from R_{rx_j} and

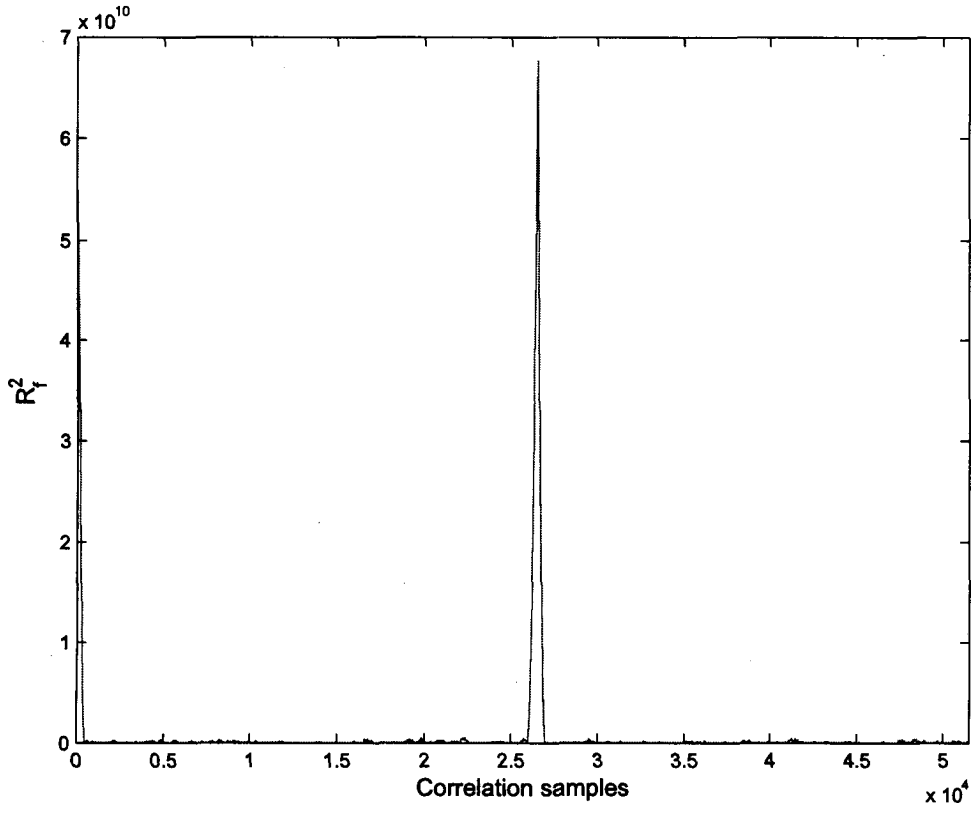

Figure 5.8: Frequency domain squared correlation peaks using PN-511.

is given by

$$\begin{aligned} R_{rx_j}(m) &= Aa_d h_j + \text{noise} \\ &= A^{'} h_j + \text{noise}, \end{aligned} \tag{5.10}$$

where A is a constant determined by $R_{x_j x_j}$ and the gain coefficient ρ. The received channel response h_j from the j-th transmitter can be determined as $R_{x_j x_j}$ and ρ is also known. Then the decision about a particular TxID enabled emergency signal, a_d can be determined based on the correlation output obtained in (5.10). However, the demodulator discussed in Chapter 4 can be beneficial to use for the demodulation of the emergency data due to its low implementation complexity.

In the subsequent sections, the analysis will be carried out with the assumption

of an AWGN channel. As the TxID watermark signal is long enough and most of the times DTV antenna stature will be higher than that of the average terrain or obstacle height, it is reasonably a valid assumption.

5.6 Error Rate Analysis for Emergency Data

The error rate analysis presented in this section is similar to the analysis carried out in Section 4.5 but it is in the light of TxID watermark signal. Let us consider, the correlation peak is denoted as $A+n_1$, where A is the auto-correlation peak of a TxID emergency sequence and n_1 is the associated interference for that autocorrelation function at first sample instant. When a TxID emergency sequence of N samples is used, ideally the autocorrelation peak will be N. If TxID has a total of M watermark signals, for the rest of $M-1$ cross-correlation functions at first sample instant, B_c+n_2 will take values centered on the following discrete levels

$$\{-t(n),\ -s(n),\ -1,\ s(n)-2,\ t(n)-2\},$$

where $t(n) = 1+2^{\frac{n+2}{2}}$, and $s(n) = \frac{1}{2}[t(n)+1]$. n_2 is the interference for the cross-correlation function at first sample instant. Both n_1 and n_2 are considered Gaussian distributed since they are the summations of sufficiently long interference samples as a result of the autocorrelation and cross-correlations. However, the correct demodulation of the TxID encoded emergency data sequence in the presence of one cross-correlation function with a peak of B_c+n_2 should meet the criteria $A-B_c > n_1+n_2$. Considering the probability density function of a new random variable $Y > n_1+n_2$, for the evaluation of probability of making false detection and following similar analysis in Chapter 4 gives us

$$\begin{aligned} f_Y(y) &= \int_{-\infty}^{\infty} f_{N_1}(n_1) f_{N_2}(y-n_1) dn_1 \\ &= \int_{-\infty}^{\infty} \frac{1}{\sigma_n\sqrt{2\pi}} e^{-\frac{n_1^2}{2\sigma_n^2}} \frac{1}{\sigma_n\sqrt{2\pi}} e^{-\frac{(y-n_1)^2}{2\sigma_n^2}} dn_1 \\ &= \frac{1}{2\sigma_n\sqrt{\pi}} e^{-\frac{y^2}{4\sigma_n^2}}, \end{aligned} \tag{5.11}$$

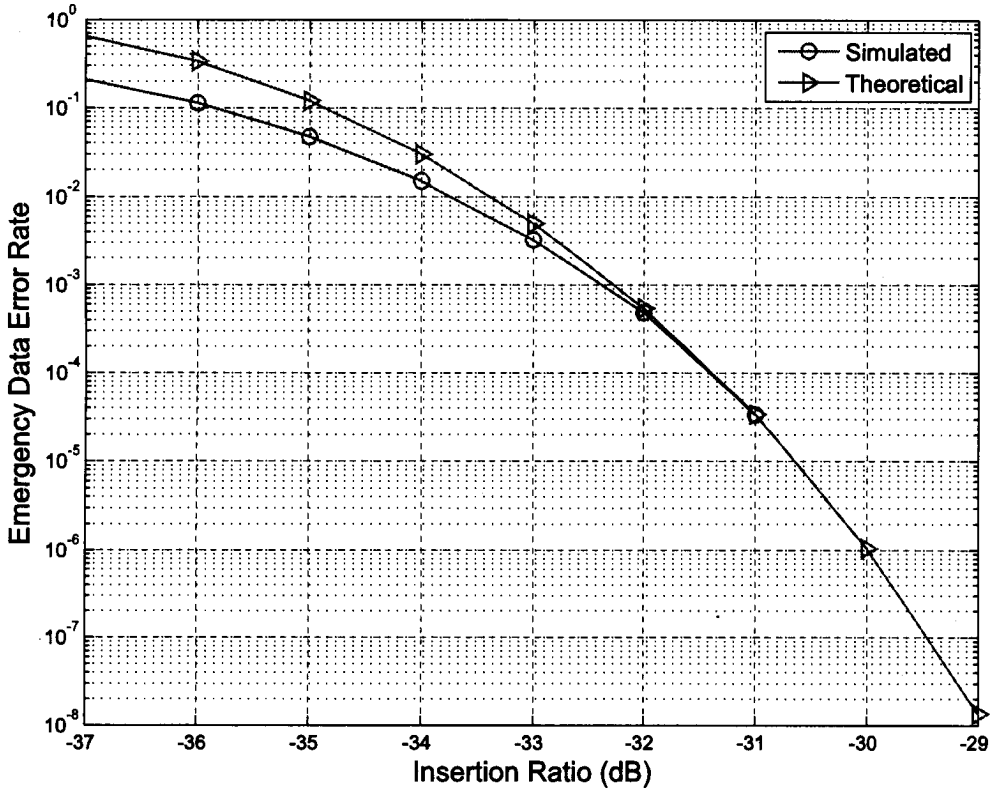

Figure 5.9: Comparisn of theoretical and simulated error rate for emergency alerting data.

where σ_n is the standard deviation of the noise from dominant in-band DTV signal and AWGN, given by

$$\sigma_n^2 = N(\sigma_{DTV}^2 + \sigma_{AWGN}^2). \tag{5.12}$$

Similarly the probability of getting an erroneous decision in presence of one correlation is given as follows,

$$P_{e,c}(n_1 + n_2 > A - B_c) = Q\left(\frac{A - B_c}{\sqrt{2}\sigma_n}\right). \tag{5.13}$$

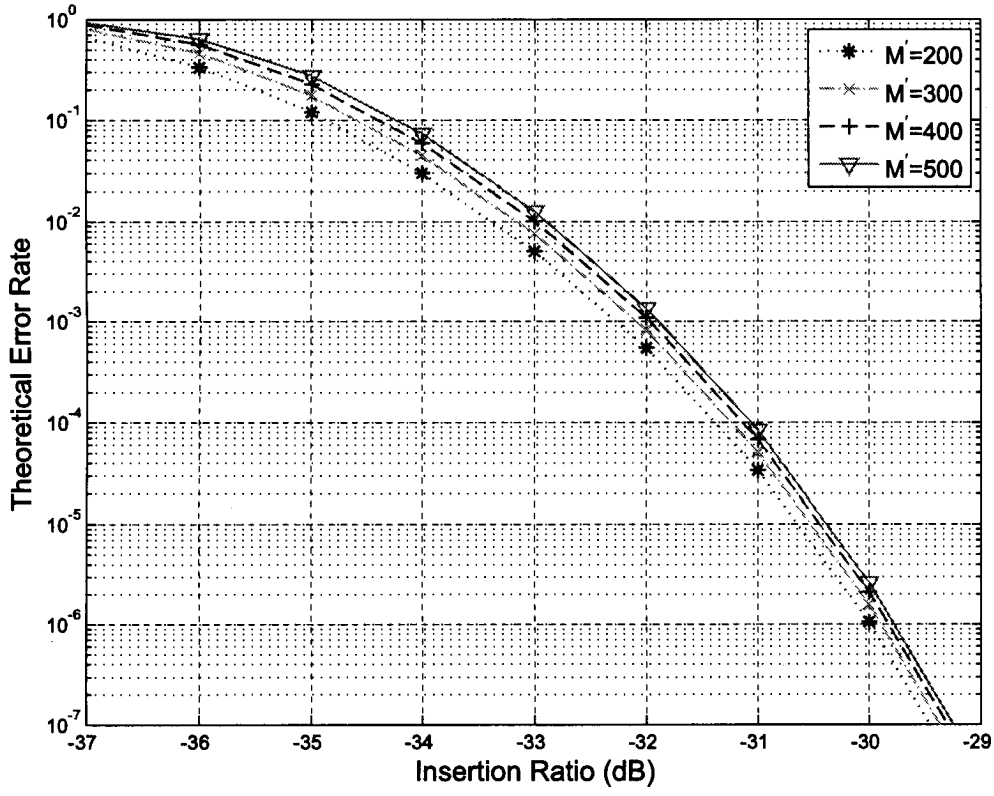

Figure 5.10: Theoretical error rate for emergency alerting data with different number of sequences in the correlation process.

Letting $\beta = (\frac{A-B_c}{\sqrt{2}\sigma_n})$, (5.13) can be further simplified as

$$\begin{aligned} P_{e,c}(n_1 + n_2 > A - B_c) &= Q(\beta) \\ &= \frac{1}{2} - \frac{1}{2}erf(\frac{\beta}{\sqrt{2}}). \end{aligned} \tag{5.14}$$

As the sequence length is very long, it is quite impossible to find out the exact occurrence of different cross-correlation peaks. Therefore, in our analysis, we assume that the occurrence probabilities for five different cross-correlation peaks are equal. So, the average probability that the decision is false in presence of one correlation is

given by,

$$P_e = \frac{1}{5}\sum_{c=1}^{5} P_{e,c}(n_1 + n_2 > A - B_c). \tag{5.15}$$

The corresponding probability of getting a correct decision can be written as

$$\overline{P}_e = 1 - P_e. \tag{5.16}$$

Therefore, probability of making false detection in presence of the rest $M^{'} - 1$ sequences is given by,

$$\begin{aligned} P_{et} &= [1 - \overline{P}_e^{M^{'}-1}] \\ &= [1 - (1 - P_e)^{M^{'}-1}], \end{aligned} \tag{5.17}$$

where M' is the number of sequences compared in the demodulation procedure which is generally less than the complete set of sequences, M. Fig. 5.9 shows the theoretical and simulated error rate for emergency alerting data for a sequence set of 200, those are compared in the correlation process. The performance gap between theoretical and simulation results may come from the fact that in the theoretical analysis, it is assumed the occurrence probabilities for each cross-correlation peak is equal. In simulation it is found that each cross-correlation peak occurs with different probabilities. However, at the higher insertion ratio (IR), the theoretical and simulated results are matched due to the fact that the autocorrelation peak for watermark signal is much stronger than the corresponding cross-correlation peaks, making the decision less erroneous. The emergency data error rate performance indicates that very low error rate i.e., robust data communication can be achieved using the TxID watermark signal, which is crucial for emergency situations.

Fig. 5.10 shows the theoretical error rate for emergency data while varying the number of sequence comparing in the correlation process. It is seen that as the number of sequences compared in the demodulation process is increased, the error rate is also increased, but the increase is not linear. Thus it is expected that when larger number of sequences will be compared, the increase in error rate will be insignificant.

5.6.1 Performance Evaluation Criteria

According to the ATSC DTV standard, the reliable reception of DTV signal at the terminal user requires a carrier to noise (C/N) ratio of 15dB [37] at the threshold of visibility (TOV) which is assumed as BER $= 3 \times 10^{-6}$. However, in our comparison with other systems, we have considered signal to noise ratio (SNR) as the reference parameter. It is well known that in DTV transmission a pilot is added at 310KHz frequency to facilitate the synchronization issue [21]. Thus to find the equivalent SNR of that C/N ratio, we need to determine the power carried by the pilot.

If we take R_s as the symbol rate for DTV transmission, then the average signal power in a 8-VSB system is $21R_s$ [21]. Thus energy for a single pulse is $E_s = 21$. A DC offset, $a = 1.25$V is added to the 8-VSB signal to generate the pilot tone. Therefore, the ratio of pilot power to the average signal power is $r = \frac{a^2}{E_s} \approx 7.44\%$. Hence, the SNR for 8-VSB signal can be written as,

$$\begin{aligned} \text{SNR} &= C/N - 10\log a^2 \\ &= 13.061 \text{ dB}. \end{aligned} \tag{5.18}$$

According to standard, one complete ATSC DTV field contains 259584 symbols. Hence if the TxID watermark is embedded 30dB below the DTV signal, the equivalent signal to interference ratio (SIR) is then $10\log(259584) - 30 = 24.14$dB and for a BPSK modulated system this corresponds to a BER $\approx 10^{-68}$. But the requirement for TOV is much less than that, only BER $= 3 \times 10^{-6}$. In other words, for BER at TOV, it can be found from Fig. 5.10 that TxID watermark is almost 30dB more robust than the DTV signal, giving the insight that TxID data can be received in a much larger area than that of DTV coverage. However in case of multipath channel, if we consider a loss of around 3dB, still TxID is 27dB stronger than the DTV signal. In this chapter, we have made use of this key concept of using TxID watermark signal to enable emergency communication.

5.7 Coverage Prediction

The next step is to analyze the coverage for the proposed emergency communication technique. To predict the coverage for the proposed technique, Hata-Davidson model is considered which is an extension of Okumura-Hata model [38] with some flexibilities

in the range of propagation distance, antenna height at the base station with a broader frequency range [39]. The range of input parameters for Hata-Davidson model are shown in Table 5.1.

Table 5.1: Range of input parameters for Hata-Davidson model

Frequency range, f_{MHz}	30-1500MHz
Base station antenna height, h_1	20-2500m
Receiving station antenna height, h_2	1-10m
Propagation distance, d_{km}	1-300km

Table 5.2: Area dependent parameters for Hata-Davidson model

Type of area	$l(h_2)$	k
Open		$4.78(\log f_{MHz})^2 - 18.33 \log f_{MHz} + 40.94$
Suburban	$(1.1 \log f_{MHz} - 0.7)h_2 - (1.56 \log f_{MHz} - 0.8)$	$2[\log(f_{MHz/28})]^2 + 5.4$
Medium-small city		0

Table 5.3: Propagation distance dependent parameters for Hata-Davidson model

Distance	$L(h_2, d_{km})$	$S_1(d_{km})$
$d_{km} < 20$	0	0
$20 \leq d_{km} < 64.38$	$0.62137(d_{km} - 20)[0.5 + 0.15 \log(h_1/121.92)]$	0
$64.38 \leq d_{km} < 300$	$0.62137(d_{km} - 20)[0.5 + 0.15 \log(h_1/121.92)]$	$0.174(d_{km} - 64.38)$

According to the Hata propagation model, the loss in dB scale is given by

$$\begin{aligned} L_{Hata} =& 69.55 + 26.16 \log f_{MHz} - 13.82 h_1 - l(h_2) \\ &+ (44.9 - 6.55 \log h_1) \log d_{km} - K, \end{aligned} \tag{5.19}$$

where the parameters $l(h_2)$ and K depends on type of areas tabulated in Table 5.2.

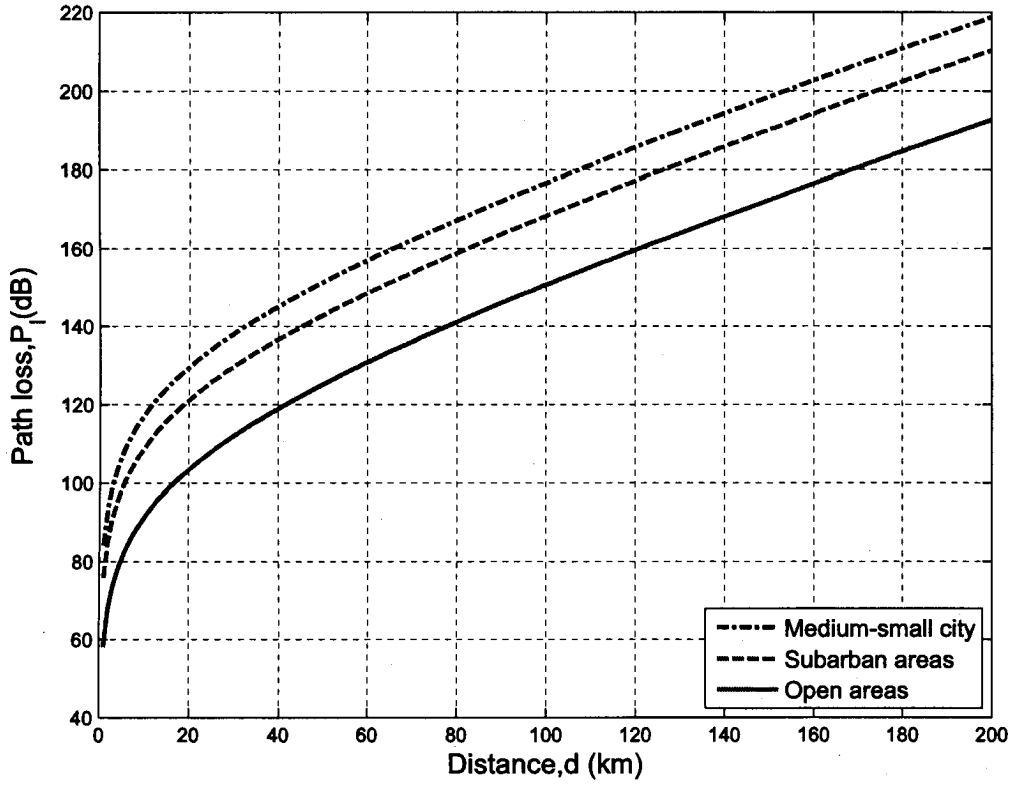

Figure 5.11: Propagation path loss using Hata-Davidson model in different type of areas.

Then the Hata-Davidson propagation loss follows [39]

$$\begin{aligned} L_{HD} =& L_{Hata} + L(h_1, d_{km}) - S_1(d_{km}) - S_2(h_1, d_{km}) \\ & - S_3(f_{MHz}) - S_4(f_{MHz}, d_{km}), \end{aligned} \tag{5.20}$$

where L and S_1 are distance correction factors extending the range to 300km and are shown in Table 5.3.

The other factors such as $S_2(h_1, d_{km})$ is the base station antenna height correction factor, $S_3(f_{MHz})$ and $S_4(f_{MHz}, d_{km})$ are frequency correction factors which are not used in our analysis. The path loss, according to Hata-Davidson model for different types of areas is shown in Fig. 5.11.

To analyze the coverage, a DTV station in South Huron (near London), ON, Canada area is considered and the parameters are obtained from DTV allotment

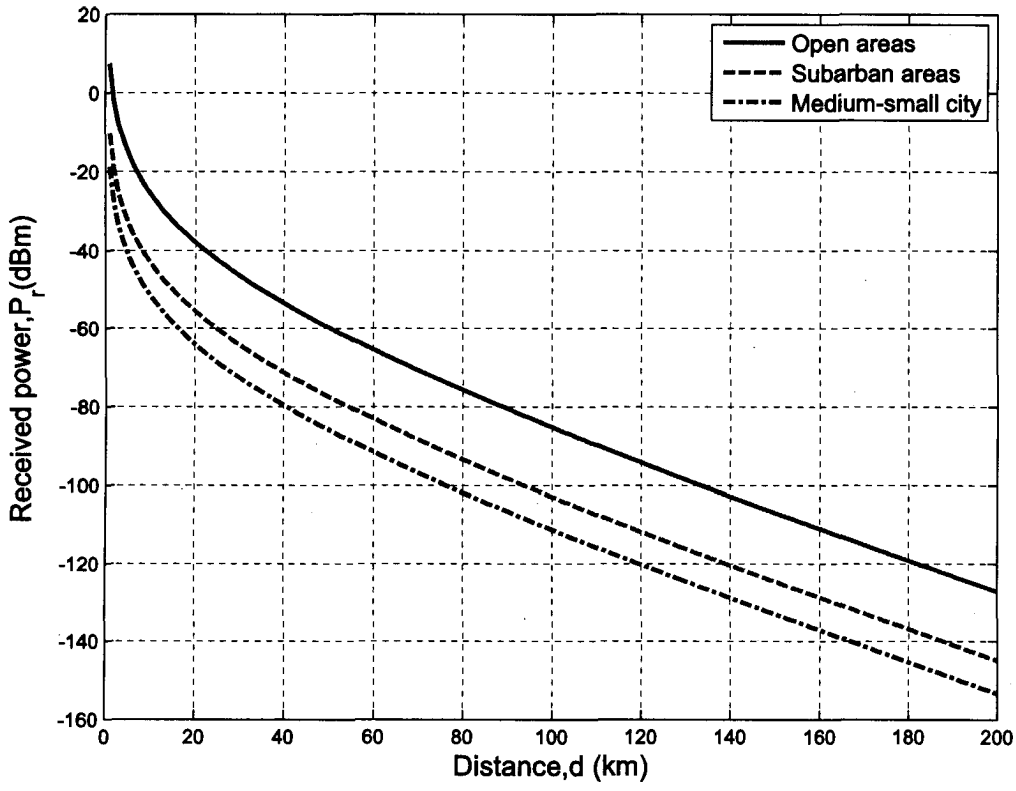

Figure 5.12: Received power for a DTV station at South Huron area near London, ON, Canada with a transmitter power of 3.5kw.

table provided by Industry Canada and shown in Table 5.4 [40]. Please note that as the suburban areas in Tokyo (as experiment for Hata-Davidson model was conducted in this area) generally reflects the propagation characteristics of North American typical urban areas [38], in coverage analysis South Huron, Canada is considered as a suburban area for this propagation loss modeling.

Once the path loss is known, the received power is determined by

$$P_r(\text{dBm}) = P_T(\text{dBm}) - L_{HD}(\text{dB}). \tag{5.21}$$

The loss of received power with the propagation distance is shown in Fig. 5.12 for the DTV station mentioned above.

As the analysis is based on the SNR of received signal and to obtain the variation

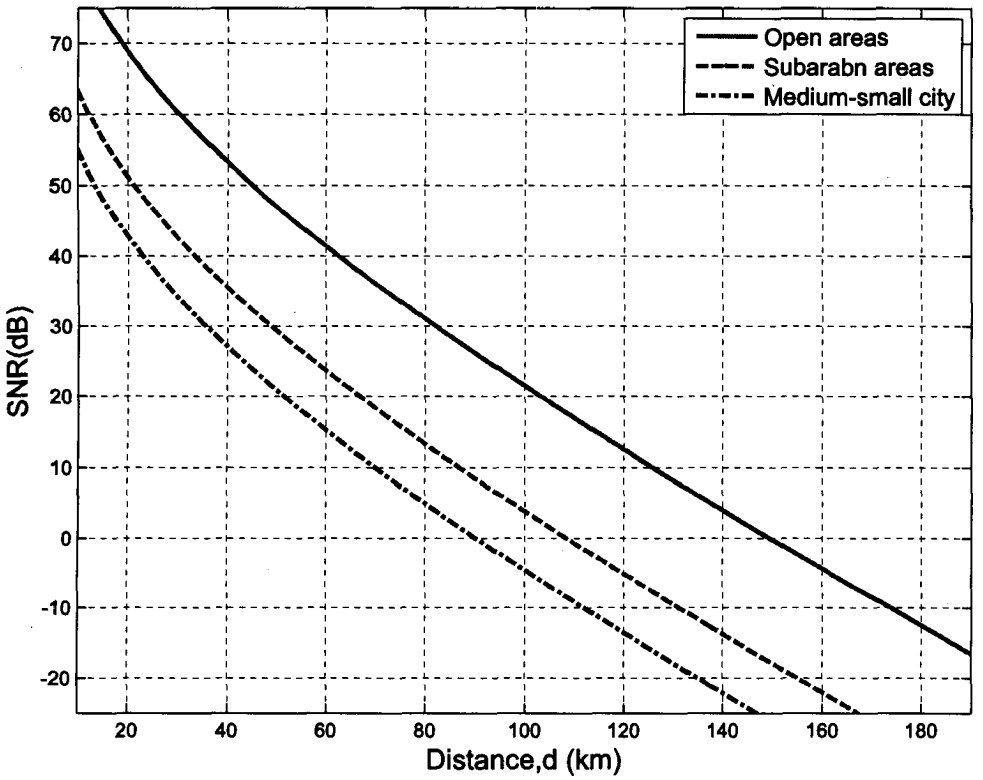

Figure 5.13: Variation of SNR with the propagation distance for a DTV station at South Huron area.

of SNR with distance, we need to know the corresponding noise power. The well-known noise model to determine the noise in the TV bandwidth is given by [21],

$$N = -174 + 10\log(\Delta f), \tag{5.22}$$

where N is the noise power and Δf is the effective TV bandwidth which equals 5.38MHz and hence noise power becomes -106.7dBm. The corresponding variation of noise with respect to distance for that DTV station in South Huron area is shown in Fig. 5.13.

The coverage is then predicted based on the SNR requirement for the system as discussed in subsection 5.6.1. It is seen from Fig. 5.13 that for the DTV station at South Huron, the 8-VSB DTV coverage at 13.061dB maintaining TOV is approx-

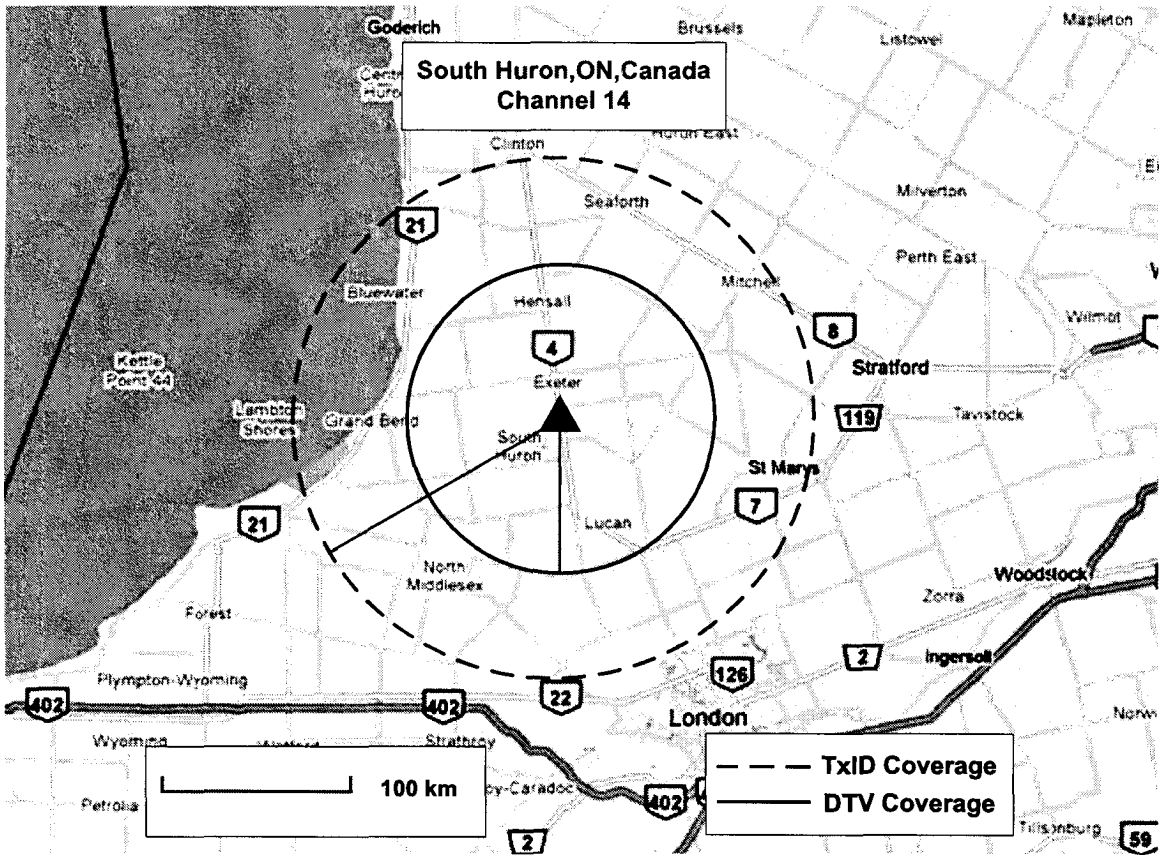

Figure 5.14: Extended emergency coverage obtained using modulated TxID watermark signal at South Huron area.

imately 81km. On the other hand, as the TxID is found to be at least 27dB more robust than the DTV signal i.e. requirement of SNR for maintaining TOV is now about -13.94dB, it could be reached at approximately 141km, providing the extended coverage for emergency communications.

5.8 Coverage Analysis

By the virtue of TxID watermark signal enabled emergency communication, basically we have obtained two fold advantages. The first advantage is that it can provide extended coverage as discussed in previous section. Next it is found that the proposed system can also provide overlapped coverage with other stations without bringing any extra cost. The eventual advantage obtained by the overlapped coverage is that even

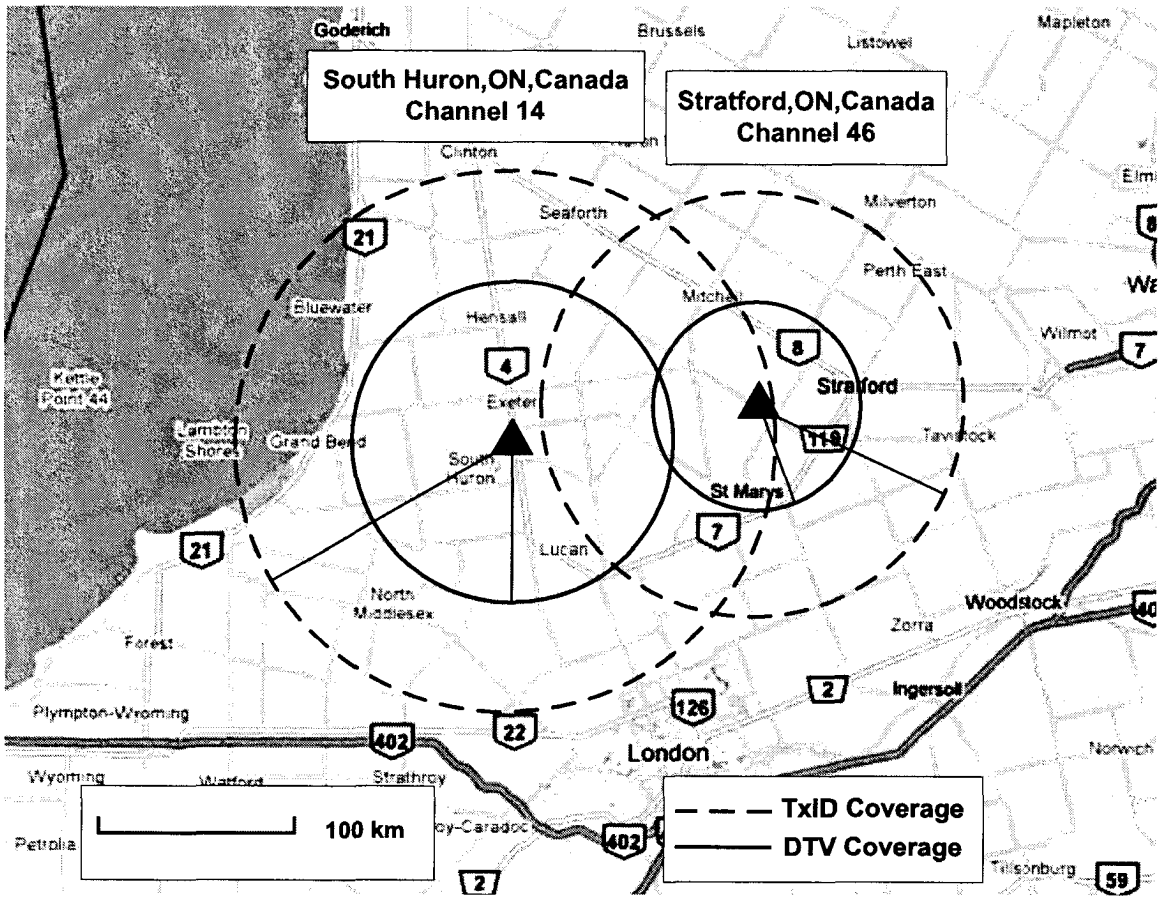

Figure 5.15: Overlapped emergency coverage obtained using modulated TxID watermark signal at South Huron and Stratford area.

if one station fails during disastrous situations, the nearby station will be able to provide emergency service to a considerable coverage of that failed station which is indeed very important in emergency situations.

Fig. 5.14 shows the extended coverage obtained by this proposed emergency communication technique with respect to DTV coverage at South Huron near London city, Ontario. It is also obvious from this map that an appreciable extended coverage, approximately 60km is obtained using TxID watermark signal.

Next another region is considered, namely Stratford area nearby London city to show the overlapped coverage with that station. The parameters for this DTV station is shown in Table 5.5 [40]. Similarly, it is found that maintaining TOV at the required SNR, the DTV coverage is approximately 44km whereas that of TxID

Table 5.4: Parameters for DTV station at South Huron area

Channel	14
Frequency, f_{MHz}	473MHz
DTV station antenna height, h_1	197.6m
TV antenna height, h_2 (assumed)	9.2m
DTV transmitter power, P_T	3.5kw

Table 5.5: Parameters for DTV station at Stratford area

Channel	46
Frequency, f_{MHz}	665MHz
DTV station antenna height, h_1	100m
TV antenna height, h_2 (assumed)	9.2m
DTV transmitter power, P_T	0.3kw

emergency coverage is approximately 99km. From Fig. 5.15 it is obvious that with the assigned transmission power they marginally overlap each other in terms of DTV coverage but largely overlap each other when the TxID coverage is considered.

According to the report published by United Nations, currently more than three billion people are living in rural areas [41]. On the other hand, the quality of services offered by existing communication systems in rural areas, characterized by low densities of populations, is well below than that offered by operators in urban and suburban areas [42, 43]. In those cases, TxID enabled extended coverage can provide emergency alerting services to rural people which is not generally available from other existing systems due to cost of radio coverage and trunking.

5.9 Network Reliability

In this section, the network reliability along with some other relevant advantages obtained by the proposed emergency communication technique is mainly discussed. The first and foremost advantage is the extended coverage than other existing homogenous and/or heterogenous emergency communication technique. As it will be using existing DTV infrastructure, the inherent advantages obtained by this technique is the cost-effectiveness. At the same time, other existing systems will require a large number of stations to have the same TxID watermark enabled emergency coverage.

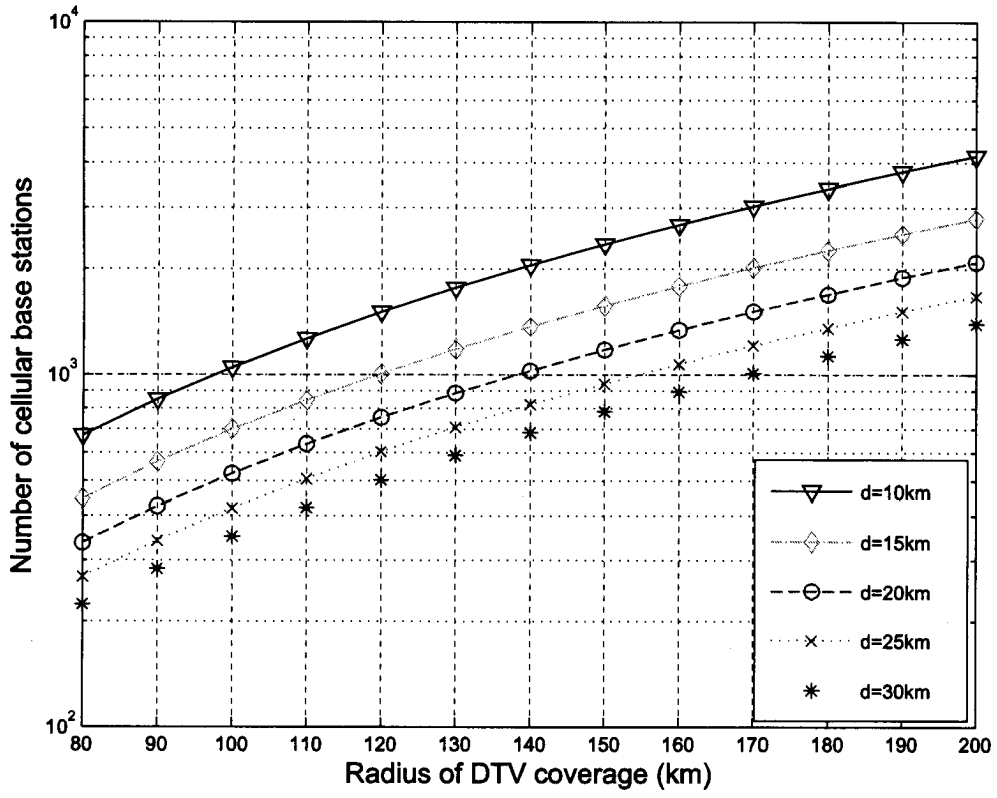

Figure 5.16: Number of cellular stations required for typical TxID equivalent emergency coverage.

Fig. 5.16 shows the number of cellular stations required to have typical TxID emergency coverage. It is observed that a large number of cellular stations are required to have TxID equivalent coverage, which ultimately brings the concern of network reliability.

To make viable, reliability of any communication network needs to be considered with proper attention. By definition, reliability is the ability of a network to perform a designated set of functions under certain conditions for a specified period of time [44] and it also depends on the total number of units performing in a communication system. As for the other system to have the same TxID enabled emergency coverage, the required number of nodes/stations in the network would be much larger and therefore weakness in the network infrastructure is inevitable. For the purpose of analysis, a wireless ad-hoc based emergency communication system is considered.

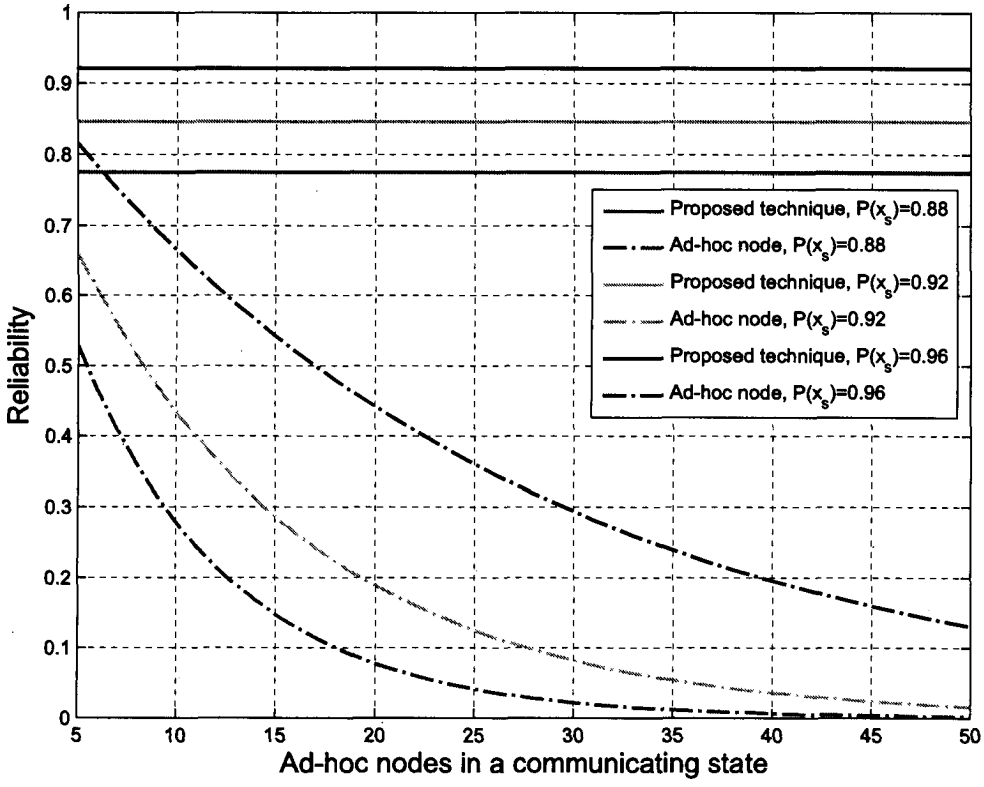

Figure 5.17: Comparison of reliability between wireless ad-hoc based and proposed emergency communication technique.

Let T be a random variable representing lifetime of a communication node, then for any specified time t, reliability $R(t)$ and unreliability $F(t)$ can be defined as

$$R(t) = P(T > t), \quad t \geq 0, \tag{5.23}$$

and

$$F(t) = P(T \leq t) = 1 - R(t), \quad t \geq 0, \tag{5.24}$$

where $P(T > t)$ denotes the probability that communicating node performs the designated task for the specified time t. To have the same coverage as the proposed TxID enabled communication technique, total number of ad-hoc nodes can be determined using Fig. 5.16. However, not all the nodes are connected in a particular communi-

cation process. A few of them are active to send the collected data to the destination while the others are inactive.

Let us take there are S nodes involved in a certain communication state q and $P(x_s)$ denotes the probability of successful communication between nodes. If the nodes are randomly distributed, the reliability for this state is given by [45],

$$\begin{aligned} R_q &= P(x_1, x_2, \ldots, x_S) \\ &= P(x_1)P(x_2|x_1)\ldots P(x_S|x_1, x_2, \ldots, x_{S-1}). \end{aligned} \tag{5.25}$$

However, if the nodes are independent of each other, then the reliability for state q is as follows,

$$R_q = P(x_1)P(x_2)\ldots P(x_S). \tag{5.26}$$

Again, if there are a total of Q states within the specified time, the overall network reliability is

$$R = \prod_{q=1}^{Q} R_q. \tag{5.27}$$

But for TxID enabled emergency communication system, most of the times very few, one or two stations are involved. Hence even with the same probability of success, the reliability of the proposed emergency communication system would be much higher than that of the ad-hoc based emergency network.

Fig. 5.23 shows the comparison of radiabilities between proposed technique and wireless ad-hoc based emergency communication system. Here, $P(x_s)$ indicates the probability of successful communication, which is assumed equal for both ad-hoc nodes and DTV station. We have assumed that two DTV stations are involved in the emergency communication. Similarly, comparison of reliability with other communication system such as IEEE 802.16 wireless mesh network considering fading model can be assessed using similar approach in [46]. However, network reliability also depends on the physical strength of the telecommunication tower [47]. As the DTV transmitter uses a much stronger tower, it will be less vulnerable to disastrous situations than most other existing techniques which makes the system more viable in emergency situations.

5.10 Chapter Summary

In a nutshell, in this chapter a DTV TxID watermark signal enabled robust communication technique which is suitable for national emergency situations is proposed. The corresponding emergency alerting transmitter and receiver structure is developed. It is observed from the analysis that this technique can provide a much larger coverage than other existing emergency communication systems. With the extended coverage, it is now possible to send the emergency alerting data to the people living in outskirts, even in rural areas. Again, due to the overlapped coverage among DTV stations, the coverage area of any failed station can be provided emergency service by nearby stations. Beside these, corresponding theoretical error rate analysis for emergency data is carried out and compared with the simulations. Finally, performance of the proposed technique is evaluated in terms of communicating station requirement, network reliability and shown to have better suitability than other existing emergency communication systems.

Chapter 6
Conclusion

In this thesis, the first attempt has been made to enhance the flexibility and efficiency of cognitive radio communication in hostile environment. Using PCP-OFDM system, it is possible to send system transmission parameters such as transmission power control and subcarrier power allocation information concurrently. Therefore mutual interference from CR network to primary users is controlled effectively while maintaining the required system performance. In addition, an efficient signaling demodulator is also investigated to retrieve the PCP signaling information. The latter part of the thesis proposes a robust communication technique based on DTV broadcasting technology, which is suitable for national emergency situations. Major contributions of this thesis are summarized as follows.

- Precoded CP or PCP enabled signaling link provides an effective and spectrum efficient technique to carry system transmission parameters for CR communication. It helps to maintain smooth operation of the cognitive communication where system parameters are changed more frequently and adjusted according to change in the environment. An iterative demodulation technique for OFDM data demodulation can be followed where the effect of PCP can be taken out and therefore performance of OFDM data demodulation remains same.

- An effective technique to control transmission power is proposed where the adjustment is constrained on required system performance for other users in the network. Therefore, unnecessary transmission power is controlled while the performance is still maintained. Following this technique, the overall mutual interference to the primary users can also be minimized. In addition, more users can be accommodated which will certainly increase the overall capacity of the CR network.

- An subcarrier power allocation scheme is investigated which can provide suboptimal solution and this information can be sent without requiring any dedicated signaling link. As this adjustment is done at purely physical layer and therefore higher layer access is not necessary, this technique can provide sufficiently fast adjustment of subcarrier power allocation which is highly desirable for CR environment.

- A low complexity PCP signaling demodulator is proposed which can substantially reduce the overall implementation complexity. The proposed demodulator provides the same performance as the optimal matched filter but with reduced implementation complexity, keeping the overall complexity of the PCP-OFDM receiver minimal. With the use of a multipath combining technique, further performance improvement is achieved.

- Watermark signal which is embedded into original DTV signal is found to be much more robust than 8-VSB data carrying signal and therefore can be reached over a wider coverage. This key concept of DTV broadcasting technology is used to propose a robust communication system which is suitable for national emergency situations.

- Due to the increased coverage of DTV watermark enabled communication technique, number of stations required to provide similar emergency coverage is significantly less than other emergency communication systems such as wireless ad-hoc networks. As less number of stations are required and more robust communication network is used than conventional emergency communication systems, the proposed emergency communication system provides significantly increased reliability.

6.1 Future Works

These are several interesting areas which are worthwhile for future studies:

- In this thesis it is assumed that channel is known through estimation and multipath combining technique is also based on this assumption. Therefore it is meaningful to evaluate the multipath combining technique as well as performance of signaling demodulation with improper channel estimation.

- Another important research topic is to find out the position of multipath channel taps. As only the paths with SNR higher than certain threshold will be included, knowing the channel taps will greatly reduce the computational complexity for the multipath combining process.

- The complexity of PCP-OFDM receiver is a major concern comparing to conventional OFDM system. Therefore future effort would be given to reduce the complexity of the PCP signaling demodulator so that overall PCP-OFDM receiver complexity can be reduced further.

References

[1] S. Haykin, "Cognitive radio: Brain-empowered wireless communications," *IEEE J. Sel. Areas in Commun.*, vol. 23, pp. 201-220, Feb. 2005.

[2] H. Schulze and C. Lüders, *Theory and applications of OFDM and CDMA*, John Wiley & Sons Ltd., 2005.

[3] X. Wang, Y. Wu, and B. caron "Transmitter identification using embedded pseudo random sequences," *IEEE Trans. on Broadcasting*, vol. 50, no. 3, Sep. 2004.

[4] L. M. Gavrilovska and V. M. Atanasovski, "Enabling communications in emergency scenarios," in *Proc. Int. Conf. on Telecommun. in Modern Satellite, Cable and Broadcasting Services*, Sep. 2007.

[5] K. D. Stepahn, "We've got to talk: Emergency communications and engineering ethics," *IEEE Tech. and Society Magazine*, vol. 26, no. 3, Fall 2007.

[6] E. Dahlman et. al., "The 3G Long-Term Evolution - Radio interface concepts and performance Evaluation," in *Proc. IEEE VTC'06*, vol. 50, no. 13, pp. 137-141, May 2006.

[7] X. Wang, Y. Wu, and H.-C. Wu, "A new adaptive OFDM system with precoded cyclic prefix for cognitive radio," in *Proc. IEEE ICC'08*, pp. 3642-3646, May 2008.

[8] I. F. Akyildiz, W.-Y. Lee, M. C. Vuran, and S. Mohanty, "Next generation/dynamic spectrum access/cognitive radio wireless networks: A survey," *Computer Networks (Elsevier)*, vol. 50, no. 13, pp. 2127-2159, Sept. 2006.

[9] Q. Zhao and B. M. Sadler, "A survey of dynamic spectrum access," *IEEE Signal Processing Magazine*, vol. 24, no. 3, pp. 79-89, May 2007.

[10] Federal Communications Commission (FCC) ET Docket 03-108, "Facilitating opportunities for flexible, efficient, and reliable spectrum use employing cognitive radio technologies," 2003.

[11] W. Hu, D. Willkomm, M. Abusubaih, J. Gross, G. Vlantis, M. Gerla, and A. Wolisz, "Cognitive radios for dynamic spectrum access - Dynamic frequency hopping communities for efficient IEEE 802.22 operation," *IEEE Commun. Magazine*, vol. 45, no. 5, pp. 80-87-79, May 2007.

[12] D. V. Sarwate and M. B. Pursley, "Cross correlation properties of pseudorandom and pelated sequences," in *Proc. IEEE*, vol. 68, no. 5, pp. 593-619, May 1980.

[13] Yuh-Ren Tsai and Xiu-sheng Li, "Kasami code-shift-keying modulation for ultra-wideband communication systems," *IEEE Trans. Commun.*, vol. 55, no. 6, pp. 1242-1252, June 2007.

[14] A. G. Burr, "Capacity improvement of CDMA system using M-ary code shift keying," in *Proc. IEEE sixth Int. Conf. on Mobile Radio and Personal Commun.*, Dec. 1991.

[15] X. Wang, Y. Wu, G. Gangon, J-Y. Chouinard, B. Tian, and K. Yi, "On the computational complexity of the MSE-OFDM system using pseudo random sequemce," in *Proc. Can. Workshop on Info. Theory*, pp. 29-32, June 2007.

[16] G. Bansal, M. J. hossain, and V. K. Bhargava, "Adaptive power loading for OFDM-based cognitive radio," in *Proc. IEEE ICC'07*, pp. 5137-5142, June 2007.

[17] P. Wang, M. Zhao, L. Xiao, S. Zhou, and J. Wang, "Power allocation in OFDM-based cognitive radio systems," in *Proc. IEEE GLOBECOM'07*, pp. 4061-4065, Nov. 2007.

[18] C. Zhao, M. Zou, B. Shen, and K. Kwak, "Power allocation in OFDM-based cognitive networks with interference," in *Proc. Int. Conf. on Convergence and Hybrid Infor. Tech.*, pp. 797-800, 2008.

[19] Y. M. Tsang and R. S. Cheng, "Optimal resource allocation in SDMA/multi-input-multi-output/OFDM systems under QoS and power constraints", in *Proc. IEEE WCNC'04*, vol. 3, pp. 1595-1600, Mar. 2004.

[20] Federal Communication Commission (FCC), URL: http://www.fcc.gov

[21] J. Arnold, M. Frater, and M. Pickering, "Digital television: Technology and satndard," *John Wiley & Sons.*, 2007.

[22] J. G. Proakis, *Digital Communications*, 3rd Edition, McGraw-Hill, 2001.

[23] D. P. Bertsekas, *Nonlinear programing*, 2nd Edition, Athena Scientific, 1999.

[24] X. Hong, C. Wang, and J. Thompson, "Interference modelling of cognitive radio networks," in *Proc. IEEE VTC'08*, pp. 1851-1855, May 2008.

[25] E. S. Sousa and J. A. Silvester, "Optimum transmission ranges in a direct-sequence spread-spectrum multihop packet radio network," *IEEE J. Sel. Areas in Commun.*, vol. 8, no. 5, pp. 762-771, June 1990.

[26] Mackenzie, ABERT, and SET, "General description of laboratory tests," Field Test Report in Brazil, July 2000.

[27] X. Wang, M. J. Rahman, and H.-C. Wu, "Design and performance evlauation of signaling link demodulator for PCP-OFDM system," Accepted, *IEEE VTC Fall'09* .

[28] D. R. Pauluzzi and N. C. Beaulieu, "A comparison of SNR estimation techniques for the AWGN channel," *IEEE Trans. Commun.*, vol. 48, no. 10, pp. 1681-1691, Oct. 2000.

[29] B. Holter and G. E. Øien, "The optimal weights of a maximum ratio combiner using an eigenfilter approach," in *Proc. 5th IEEE Nordic Signal Processing Symposium*, Oct. 2002.

[30] T. Fujiwara, N. Iida, and T. Watanbe, "An ad-hoc routing protocol in hybrid wireless networks for emergency communications," in *Proc. 24th Int. Conf. on Distributed Computing Systems*, Mar. 2004.

[31] T. Fujiwara, H. Makie, and T. Watanbe, "A framework for data collection system with sensor netwoks in disaster communications," in *Proc. Int. workshop on Wireless Ad-Hoc Networks*, 2004.

[32] H. Wu, C. Quiao, and O. Tonguz, "Integrated cellular and ad-hoc relaying system: iCAR," *IEEE Journal on Selected Areas in Commun.*, vol. 19, no. 10, Oct. 2001.

[33] Terrestrial Trunked Radio-TETRA, URL: http://www.tetramou.com.

[34] M. Buddhikot, G. Chrandramenon, S. Han, Y. W. Lee, S. Miller, and L. Salgarelli, "Integration of 802.11 and third-genration wireless data networks," in *Proc. IEEE INFOCOM*, 2003.

[35] HUGHES Network Systems, "The new age of satellite communications: Meeting the 21st century business needs of the government with satellite broadband solutions," *white paper*, Oct. 2003.

[36] IEEE 802.21: Media Independent Handover, URL: http://www.ieee802.org/21

[37] O. Bendov, J. F. Browne, C. Rhodes, and Y. Wu, "DTV coverage and service prediction, measurement and performance indices," *IEEE Trans. on Broadcasting*, vol. 47, no. 3, Sep. 2001.

[38] G. L. Stüber, "Principles of mobile communication," 2nd Edition, Kluwer Academic Publisher, 2001.

[39] Telecommunication Industry association (TIA), URL: http://www.antd.nist.gov/wctg/manet/docs/TIAWG88_20.pdf

[40] SMBR-005-08-FCC to IC letter at Dec. 2008, Letter of understanding between FCC and Industry Canada (IC), URL: http://www.ic.gc.ca/eic/site/smt-gst.nsf/vwapj/SMBR-005-08-FCC_to_IC_letter_Dec08_e.pdf

[41] Dept. of Economics and Social Affairs, United Nations, "World urbinization prospects: The 2005 revision," Oct. 2006. URL: http://www.un.org/esa/population/publications

[42] I. Güvenc, U. C. Kozat, M.-R. Jeong, F. Watanbe, and C.-C. Chong, "Reliable multicast and broadcast services in relay-based emergency communications," *IEEE Journal on Wireless Commun.*, vol. 15, no. 3, June 2008.

[43] M. Pipattanasomporn and S. Rahman, "Information and communication technology infrastructure and its distributed generation solutions in remote areas," in *Proc. Int. Conf. on Elec. and Com. Engg. (ICECE)*, Dec. 2002.

[44] A. P. Snow, U. Varshney, and A. D. Malloy, "Reliabilty and survivabilty of wireless and mobile networks," *IEEE Computer*, vol. 33, no. 7, June 2000.

[45] M. G. H. Bell and Y. Iida, "Network reliability: Experiments with a symbolic algebra environment," *Pergamon Press*, 2003.

[46] S. Dominick, N. Bayer, J. Habermann, V. Rakocevic, and B. Xu, "Reliabilty analysis of IEEE 802.16 meah networks," in *Proc. IEEE/IFIP Int. Broadband Convergence Networks*, pp. 1-12, May 2007.

[47] K. El-Fashny, L. E. Chouinard Bayer, and G. McClure, "Reliabilty analysis of a telecommunicatior tower," *Can. J. of Civil Engg.*, vol. 26, no. 1, pp. 1-12, 1999.

Appendix A
Derivation of weight factors for optimal multipath combining

Let us consider that average power for each multipath signal is P_{avg}. Weighting each multipath with a weight coefficient of $a_1, a_2, ..., a_p$ and for P branches having unequal noise component $N_1, N_2, \ldots, N_p$, total SNR is given by,

$$\gamma_t = P_{avg} \frac{(a_1 h_1 + a_2 h_2 + \ldots + a_p h_p)^2}{a_1^2 N_1 + a_2^2 N_2 + \ldots + a_p^2 N_p}. \tag{A.1}$$

Now taking partial derivative of the total SNR with respect to weight coefficients $a_1, a_2, \ldots, a_p$ follows

$$\begin{aligned}
\frac{\partial^p(\gamma_t)}{\partial a_1 \partial a_2 \ldots \partial a_p} &= \frac{\partial^p(\gamma_t)}{\partial a_1 \partial a_2 \ldots \partial a_p} \left\{ P_{avg} \frac{(a_1 h_1 + a_2 h_2 + \ldots + a_p h_p)^2}{a_1^2 N_1 + a_2^2 N_2 + \ldots + a_p^2 N_p} \right\} \\
&= P_{avg} \frac{\partial}{\partial a_1} \left\{ \frac{(a_1 h_1 + a_2 h_2 + \ldots + a_p h_p)^2}{a_1^2 N_1 + a_2^2 N_2 + \ldots + a_p^2 N_p} \right\} + \ldots \\
&\quad P_{avg} \frac{\partial}{\partial a_p} \left\{ \frac{(a_1 h_1 + a_2 h_2 + \ldots + a_p h_p)^2}{a_1^2 N_1 + a_2^2 N_2 + \ldots + a_p^2 N_p} \right\} \\
&= P_{avg} \left\{ \frac{(a_1^2 N_1 + a_2^2 N_2 + \ldots + a_p^2 N_p)(a_1 h_1 + a_2 h_2 + a_p h_p) 2 h_1}{(a_1^2 N_1 + a_2^2 N_2 + \ldots + a_p^2 N_p)^2} \right. \\
&\quad \left. - \frac{(a_1 h_1 + a_2 h_2 + \ldots + a_p h_p)^2 . 2 a_1 N_1}{(a_1^2 N_1 + a_2^2 N_2 + \ldots + a_p^2 N_p)^2} \right\} + \ldots \\
&\quad + P_{avg} \left\{ \frac{(a_1^2 N_1 + a_2^2 N_2 + \ldots + a_i^2 N_i)(a_1 h_1 + a_2 h_2 + a_p h_p) 2 h_p}{(a_1^2 N_1 + a_2^2 N_2 + \ldots + a_p^2 N_p)^2} \right. \\
&\quad \left. - \frac{(a_1 h_1 + a_2 h_2 + \ldots + a_p h_p)^2 . 2 a_p N_p}{(a_1^2 N_1 + a_2^2 N_2 + \ldots + a_p^2 N_p)^2} \right\}.
\end{aligned} \tag{A.2}$$

Again, in order to achieve maximum SNR, numerators of above equation (A2) need to be zero separately. Hence by letting numerator of first part to be zero and after some simple re-arrangement, we get

$$\begin{aligned}
&P_{avg}\{(a_1^2N_1 + a_2^2N_2 + \ldots + a_p^2N_p)(a_1h_1 + a_2h_2 + a_ph_p)2h_1 \\
&- (a_1h_1 + a_2h_2 + \ldots + a_ph_p)^2.2a_1N_1\} = 0 \\
&\Rightarrow a_1^2N_1 + a_2^2N_2 + \ldots + a_p^2N_p)2h_1 \\
&= (a_1h_1 + a_2h_2 + \ldots + a_ph_p).2a_1N_1. \qquad \text{(A.3)}
\end{aligned}$$

Putting $a_1 = \frac{h_1}{N_1}, a_2 = \frac{h_2}{N_2}, \ldots, a_p = \frac{h_p}{N_p}$ in the above equation we get,

$$\begin{aligned}
&(\frac{h_1}{N_1})^2N_1 + (\frac{h_2}{N_2})^2N_2 + \ldots + (\frac{h_p}{N_p})^2N_p\}.2h_1 \\
&= \{(\frac{h_1}{N_1})h_1 + (\frac{h_2}{N_2})h_2 + \ldots + (\frac{h_p}{N_p})h_p\}.2(\frac{h_1}{N_1})N_1. \qquad \text{(A.4)}
\end{aligned}$$

Resulting from (A.4), each term in the numerator of (A.2) becomes zero. Therefore, the right hand side of (A.2) is zero as well which indicates that the total SNR in the combined signal is maximum for these chosen weight factors. Thus $a_1 = \frac{h_1}{N_1}, a_2 = \frac{h_2}{N_2}, \ldots, a_p = \frac{h_p}{N_p}$ are the optimal weight coefficients for MRC with p branches having unequal noise components $N_1, N_2, \ldots, N_p$. In general, the optimal weight coefficients for branches with unequal noise powers are given by,

$$a_p = \frac{h_p}{N_p}. \qquad \text{(A.5)}$$